The 3rd Nuclear Physics School for Young Scientists

Fudan University, Shanghai

Aug 11 & 12 (6-13), 2023

Nuclear landscape in the 2020's

Takaharu Otsuka

This work was supported also by MEXT as "Program for Promoting Researches on the Supercomputer Fugaku" (Simulation for basic science: from fundamental laws of particles to creation of nuclei) and "Priority Issue on post-K computer" (Elucidation of the Fundamental Laws and Evolution of the Universe), and by JICFuS.

Some models of atomic nuclei in nuclear physics were conceived based on intuitions obtained in the 1950's. A good example is a liquid drop model and related works.

atomic nucleus as multi-nucleon system ⇨ liquid drop of uniform density

sphere

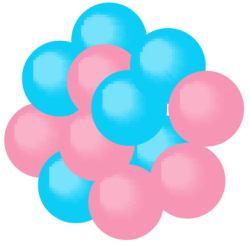

ellipsoid

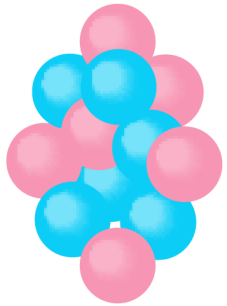

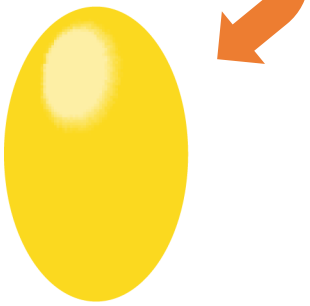

Many nuclei exhibit strong deformation
(long axis ~ 1.3 x short axis)

described by Bohr Hamiltonian
(Aage Bohr and B.R. Mottelson, 1952)

↳ *Nilsson model* (1955), *DFT models*, *Interacting Boson Model* (1975)

Those are excellent pieces of physics ideas. However, quantum many-body simulations with a variety of correlations due to realistic nuclear forces may provide us with different pictures.

➔ *The underlying motivation of this lecture*

Outline

1. Basics of traditional shell model and Monte Carlo Shell Model
2. Shell evolution: from an introduction to the current landscape of magic numbers
3. Type-II Shell evolution: shape coexistence (parabola or linear or …)
4. Ellipsoidal nuclear shapes: Aage Bohr vs. Davydov
5. Shapes and driplines: who limits isotopes
6. α-clustering and nuclear matter: who likes α-cluster

physics
Physics 2022, 4, 258–285.
https://doi.org/10.3390/physics4010018
MDPI

Review

Emerging Concepts in Nuclear Structure Based on the Shell Model

Takaharu Otsuka [1,2,3]

Special Issue "The Nuclear Shell Model 70 Years after Its Advent: Achievements and Prospects"
edited by A. Gargano, G. De Gregorio and S. M. Lenzi

Shell evolution due to the monopole interaction
Type II shell evolution and shape coexistence

Triaxiality dominance in heavy nuclei as a consequence of the self-organization due to the monopole-quadrupole interplay ← *a bit more progress*
←→ traditional prolate dominance picture

New neutron dripline mechanism due to the monopole-quadrupole interplay, exemplified for F, Ne, Na and Mg isotopes
besides the traditional mechanism with single-particle nature

Alpha-clustering is not included

In 1949, Maria Goeppert Mayer and Hans Jensen independently proposed magic numbers and shell structure of atomic nuclei (shell model) (Nobel prize in 1963).

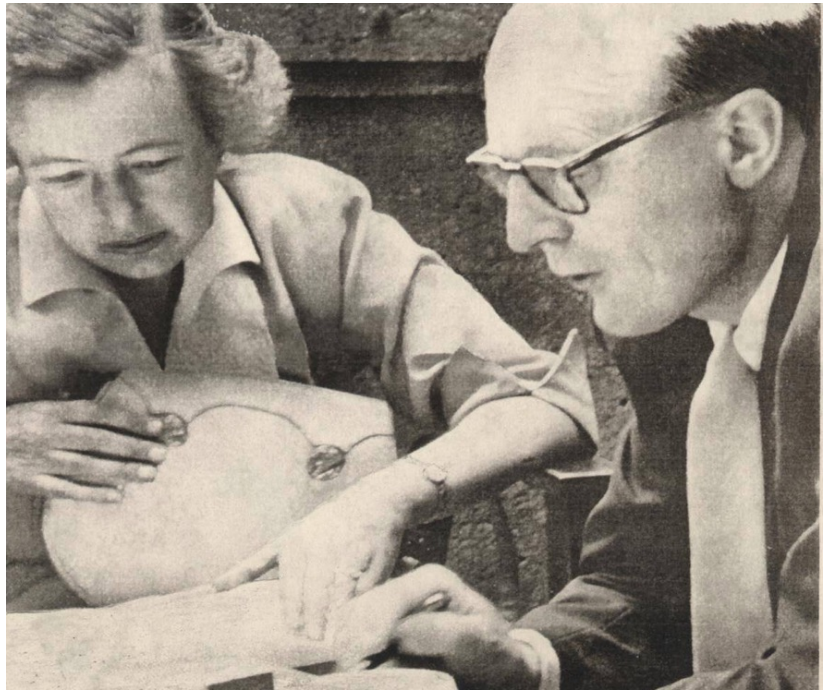

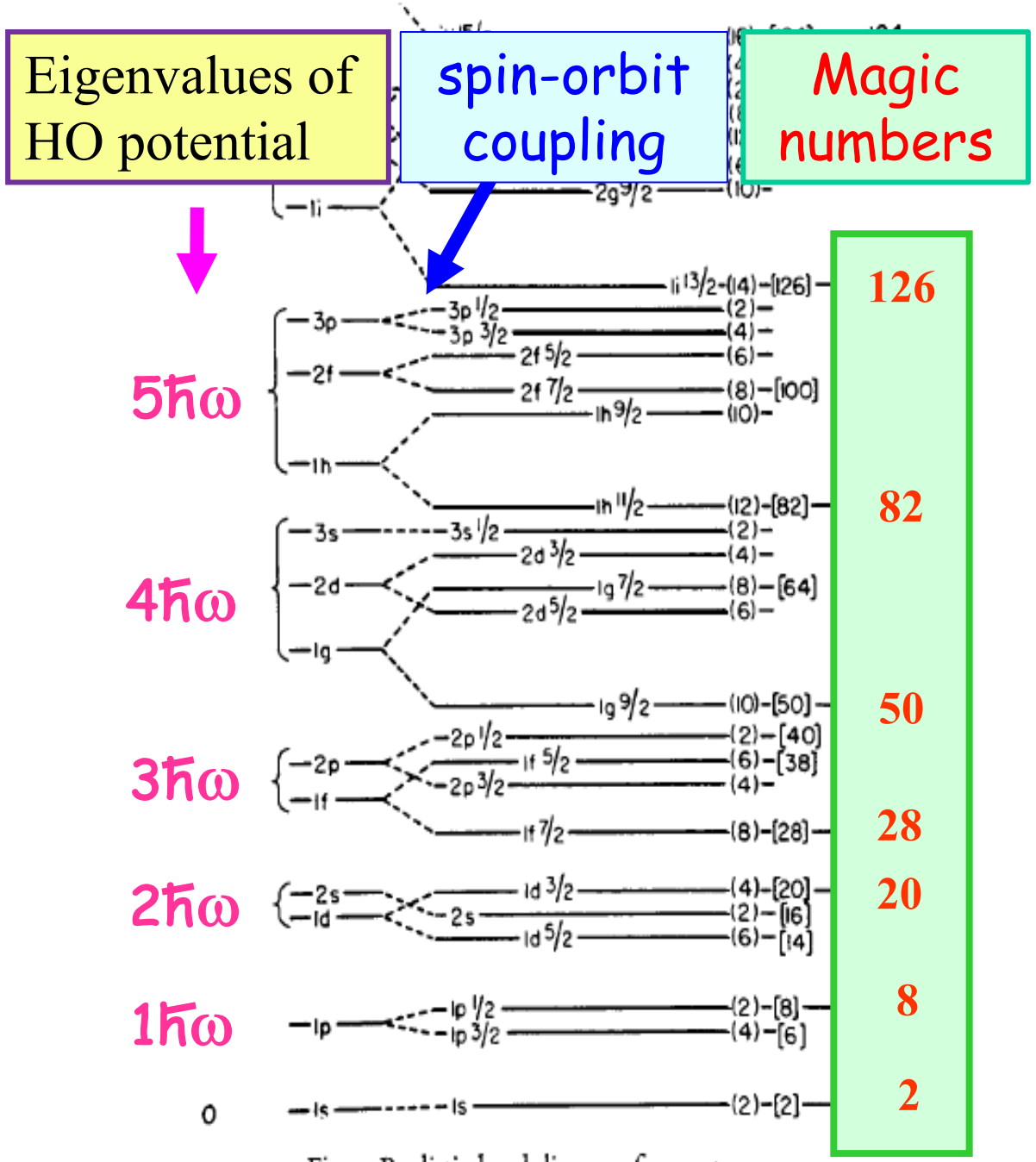

Fig. 7. Realistic level diagram for protons.

Methodology : CI (Configuration-Interaction) calculations with protons and neutrons

Protons and neutrons are orbiting in the mean potential → single-particle orbits

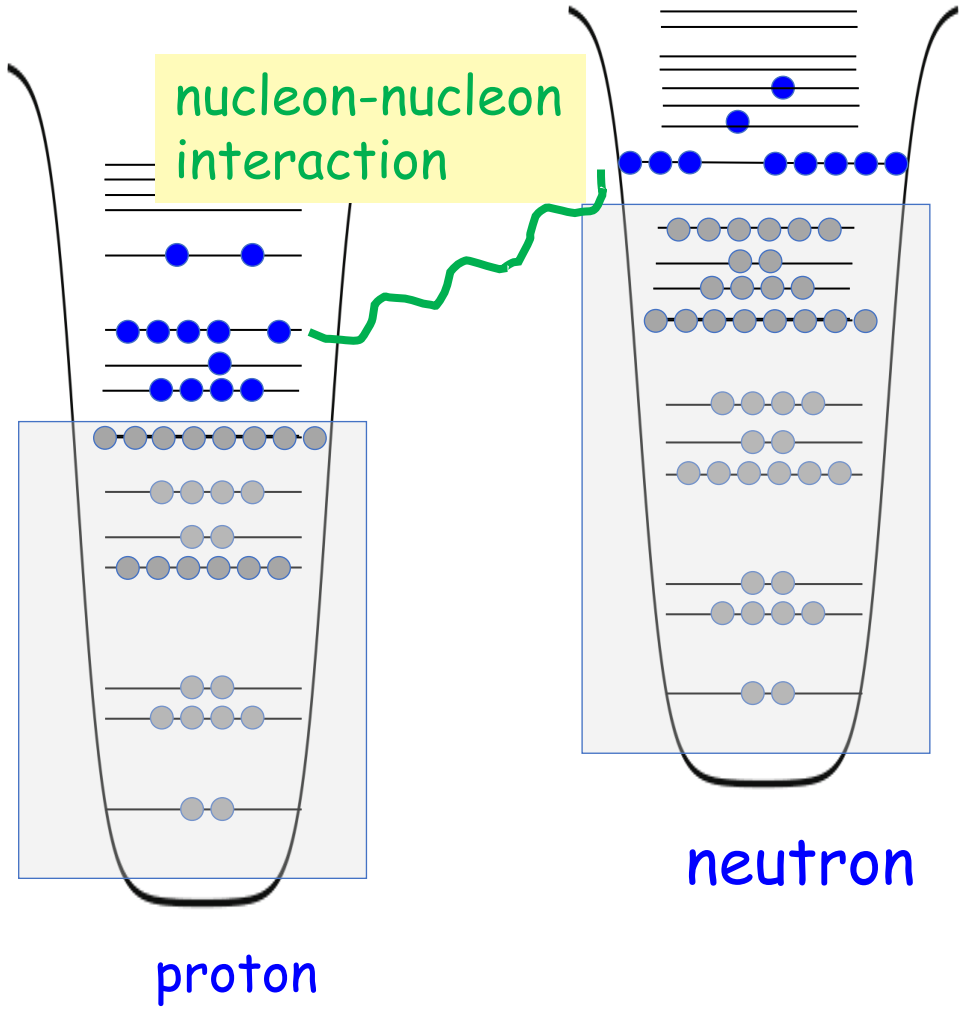

Upper orbits are only partially occupied
(valence orbits and valence nucleons).

Lower orbits form the inert core (or closed shell)
(*shaded parts in the figure*)

Valence nucleons are the major carriers of nuclear dynamics at low excitation energy, because the inert core is *frozen (implicitly taken into account in terms of effective interaction and operators)*.

Hamiltonian

$$H = \Sigma_i \epsilon_i n_i + \Sigma_{i,j,k,l} v_{ij,kl}\, a_i^\dagger\, a_j^\dagger\, a_l\, a_k$$

ε_i: Single Particle Energy (SPE) $v_{ij,kl}$: Two-Body Matrix Element (TBME)

i, j, k, l : single-particle states of valence orbits

Their values are given by ab initio calculations, phenomenological models, or something hybrid.

Schroedinger equation,

$$H\,\Phi = E\,\Phi$$

is solved for this *H*, by superposing various configurations. This can be fulfilled by the diagonalization of the Hamiltonian matrix.

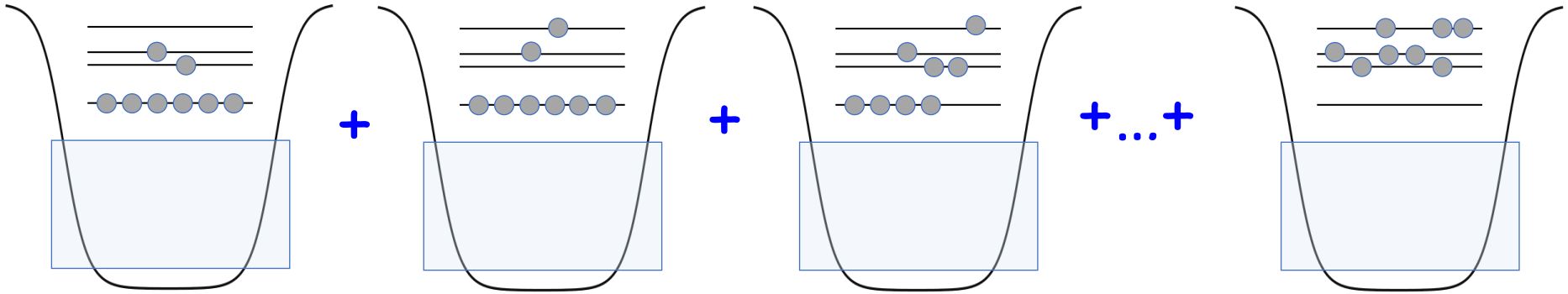

Step 1: Calculate matrix elements

$\langle \phi_1 | H | \phi_1 \rangle$, $\langle \phi_1 | H | \phi_2 \rangle$, $\langle \phi_1 | H | \phi_3 \rangle$, ...

where ϕ_1 , ϕ_2 , ϕ_3 are Slater determinants

In the second quantization,

inert core (closed shell)

$\phi_1 = a_\alpha^+ \, a_\beta^+ \, a_\gamma^+ \, ... | 0 \rangle$

$\phi_2 = a_\alpha,^+ \, a_\beta,^+ \, a_\gamma,^+ \, ... | 0 \rangle$

$\phi_3 = ...$

$$H = \Sigma_i \, \epsilon_i \, n_i + \Sigma_{i,j,k,l} \, v_{ij,kl} \, a_i^\dagger \, a_j^\dagger \, a_l \, a_k$$

Step 2 : Solve the eigenvalue problem : $\mathbf{H}\,\Psi = \mathbf{E}\,\Psi$

$$\begin{pmatrix} \langle \phi_1 |H| \phi_1 \rangle & \langle \phi_1 |H| \phi_2 \rangle & \cdots \\ \langle \phi_2 |H| \phi_1 \rangle & \langle \phi_2 |H| \phi_2 \rangle & \cdots \\ \langle \phi_3 |H| \phi_1 \rangle & \cdots & \cdots \\ \langle \phi_4 |H| \phi_1 \rangle & \cdots & \cdots \\ \cdots & \cdots & \cdots \end{pmatrix} \begin{pmatrix} c_1 \\ c_2 \\ c_3 \\ c_4 \\ \cdots \end{pmatrix} = E \begin{pmatrix} c_1 \\ c_2 \\ c_3 \\ c_4 \\ \cdots \end{pmatrix}$$

shell-model dimension

$$\Psi = c_1 \phi_1 + c_2 \phi_2 + c_3 \phi_3 + \ldots\ldots$$

c_i probability amplitudes

(Conventional) shell-model calculations

shell-model dim. <~ 10^{10}

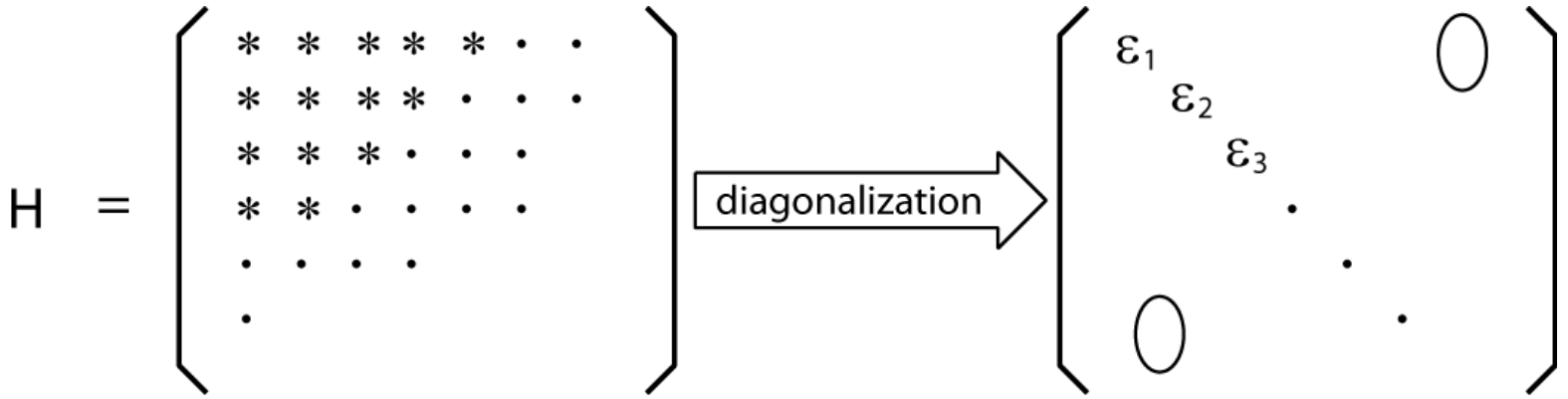

Conventional Shell Model

all Slater determinants

Direct diagonalization

Frequently used codes include

ANTOINE	Strasbourg
NEWSHEL	Michigan State
KSHELL	Tokyo – Tsukuba

where advanced computing technologies have been employed.

Shell-model Dimension as a function of the year

heavier nuclei

larger dimension

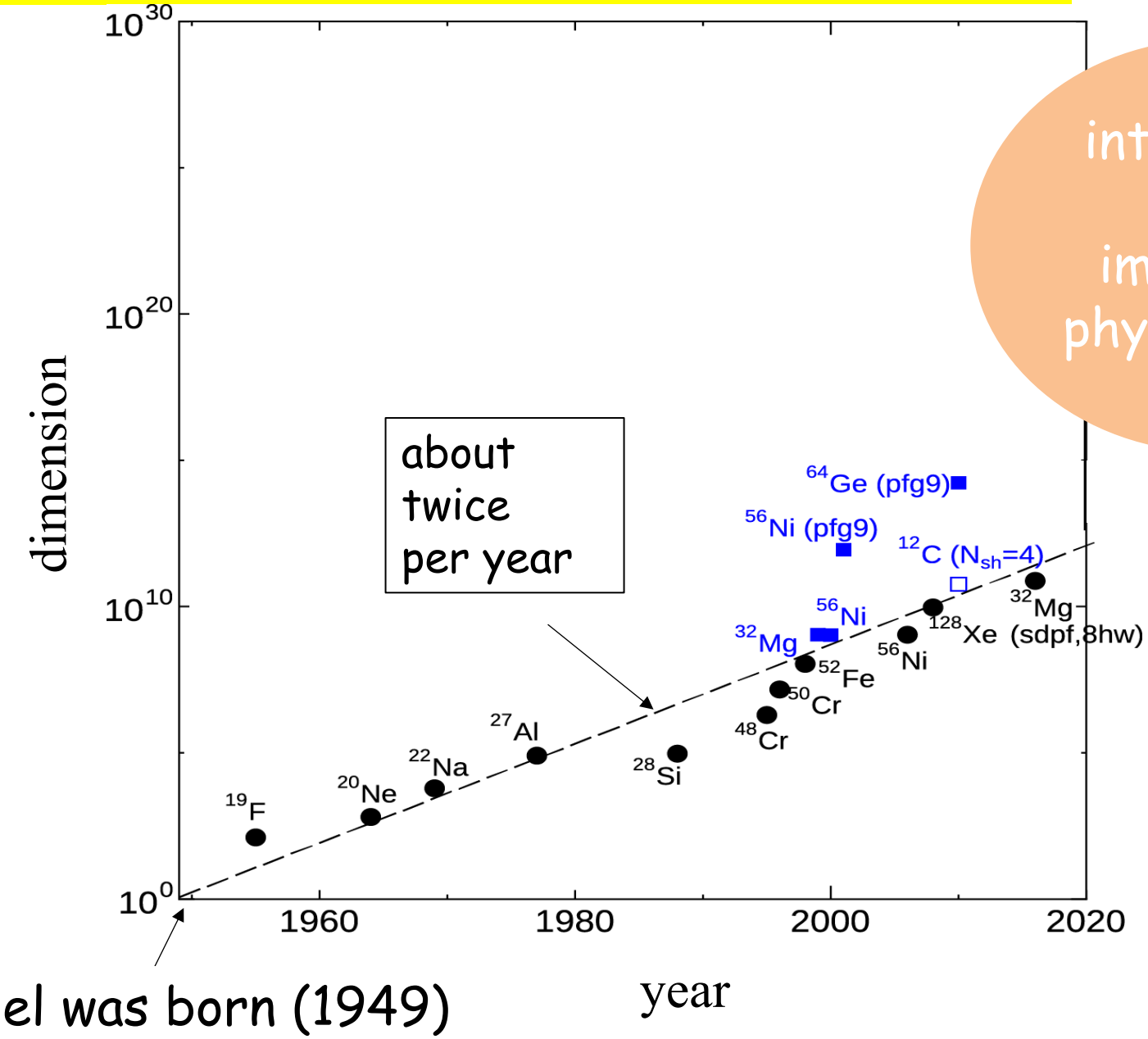

interesting and important physics cases

The shell model was born (1949)

Goal:

We must overcome the dimension problem, because of a huge variety of interesting and important physics cases beyond the limit of conventional methodology (matrix diagonalization).

Tip:

The basis vector does not have to be a naïve Slater determinant.

Strategy:

Let each basis vector carry a good fraction of correlations produced by the nucleon-nucleon interaction.

In other words, we use a kind of optimized basis vectors within the form of Slater determinant.

→ Monte Carlo Shell Model

Basic formulation of Monte Carlo Shell Model

eigenstate

N_B : number of basis vectors

$$|\Psi(D)\rangle = \sum_{n=1}^{N_B} c_i P^{J,\Pi} |\phi(D^{(n)})\rangle$$

amplitude

Projection op.

N_p : number of (active) particles

N_{sp} : number of single-particle states

$$|\phi(D^{(n)})\rangle = \prod_{\alpha=1}^{N_p} \left(\sum_{i=1}^{N_{sp}} a_i^\dagger D_{i\alpha}^{(n)} \right) |-\rangle$$

n-th basis vector (Slater determinant)

Superposition of original single-particle state

$$E(D) = \langle \Psi(D) | H | \Psi(D) \rangle$$

Minimize $E(D)$ with respect to D utilizing Quantum MC and variational methods

Step 1 : Shift randomly matrix matrix D. (The initial guess can be taken from Hartree-Fock.)
Select the one producing the lowest $E(D)$ (rate < 0.1 %)

Step 2 : Polish D by means of the conjugate gradient (CG) method variationally.

Dimension of the conventional and Monte-Carlo shell-model calculations

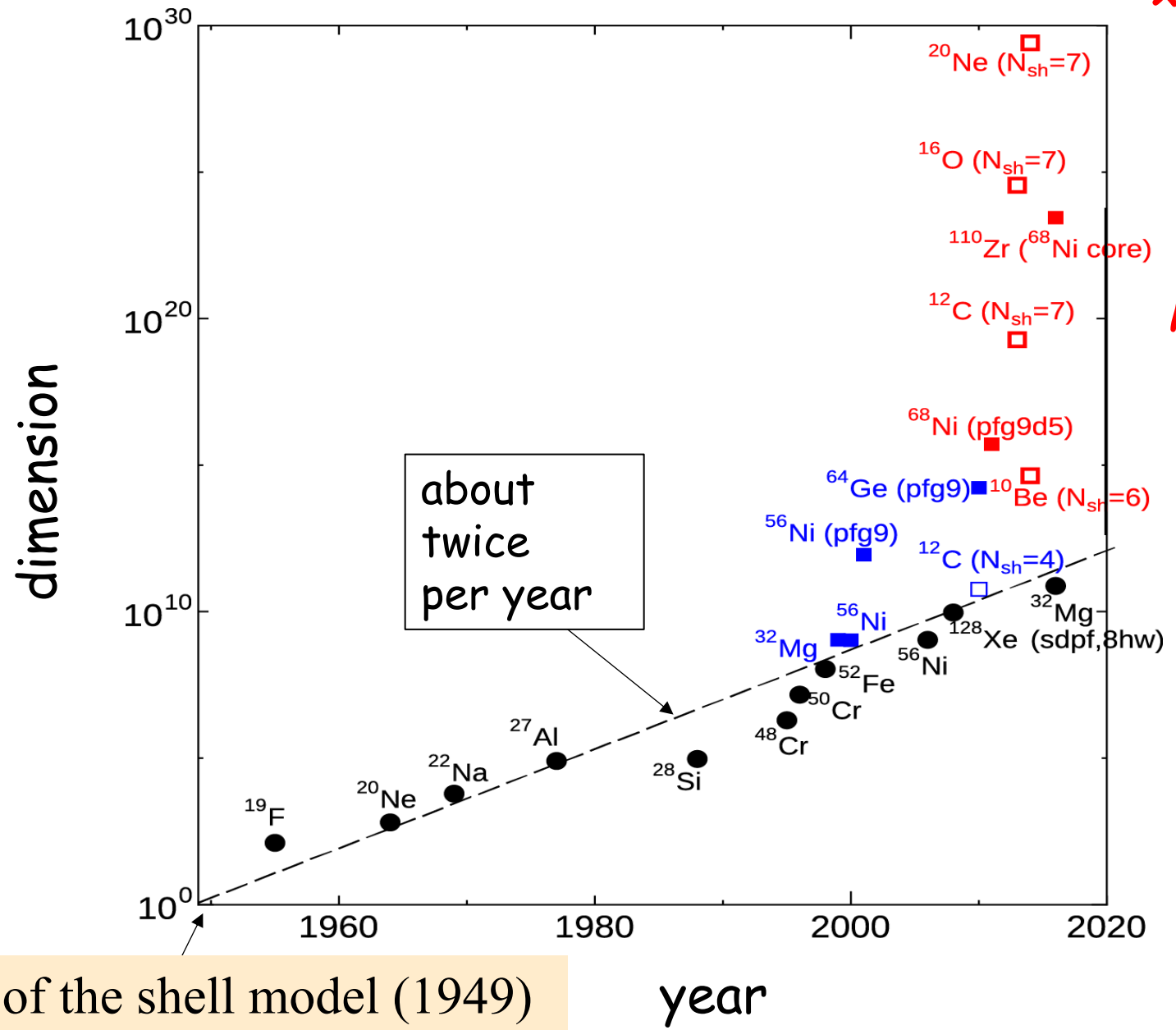

*^{166}Er (^{110}Zr core)

→ paradigm shift ?

Monte Carlo Shell Model
- a game changer -

Next year (2024) is the 75th anniversary of the nuclear shell model

By including more basis vectors, we can get closer to exact solutions.

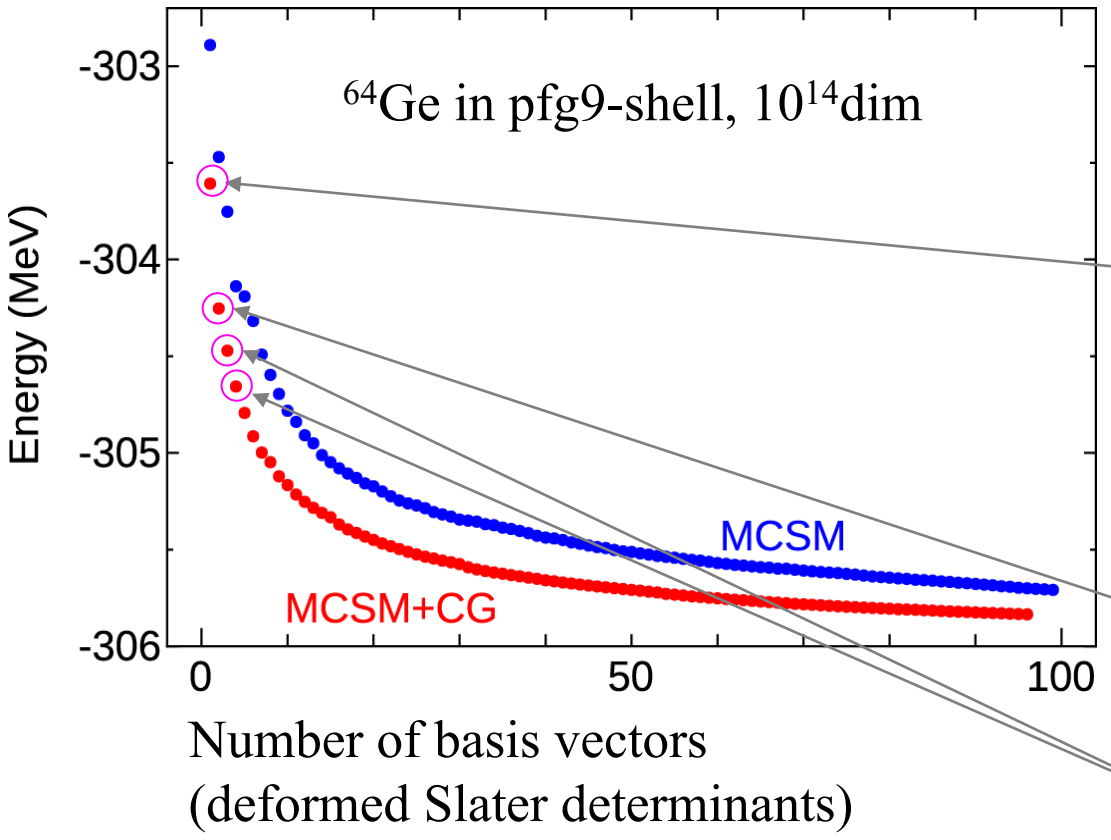

The MCSM calculation is carried out by successive search of basis vectors:

$$\left|\phi(D^{(n)})\right\rangle = \prod_{\alpha=1}^{N_p}\left(\sum_{i=1}^{N_{sp}} a_i^\dagger D_{i\alpha}^{(n)}\right)\left|-\right\rangle$$

The n=1 basis vector is fixed first by stochastic and variational searches for the most optimal $D^{(n=1)}$ matrix.
The initial guess for this search can be a mean-field solution, and we go beyond.

The n=2 basis vector is fixed next, under the presence of the n=1 basis vector.

The n=3, 4, … basis vectors are fixed likewise, driving the result closer to the exact solution.

Can we extrapolate to the exact solution ?

Magic recipe by Imada

Extrapolation by energy variance : $\langle \Delta H^2 \rangle = \langle H^2 \rangle - \langle H \rangle^2$ → 0 at the exact solution

For various subsets of the many-body Hilbert space

Hubbard model

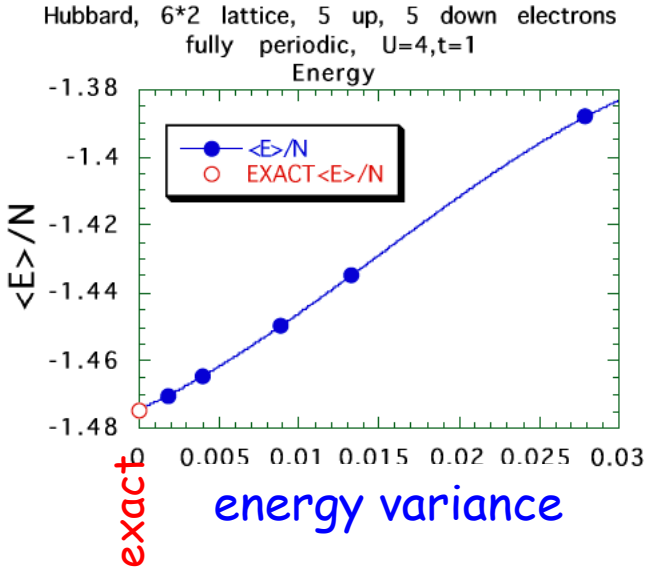

Fig. 1. The calculated energy of the Hubbard model at $t = 1$ and $U = 4$ as a function of the energy variance Δ_E for 5 up and 5 down electrons on the 6×2 lattice with the periodic boundary condition.

M. Imada and T. Kashima,
J. Phys. Soc. Jpn. 69, 2723 (2000)

Conventional Shell Model (different truncations)

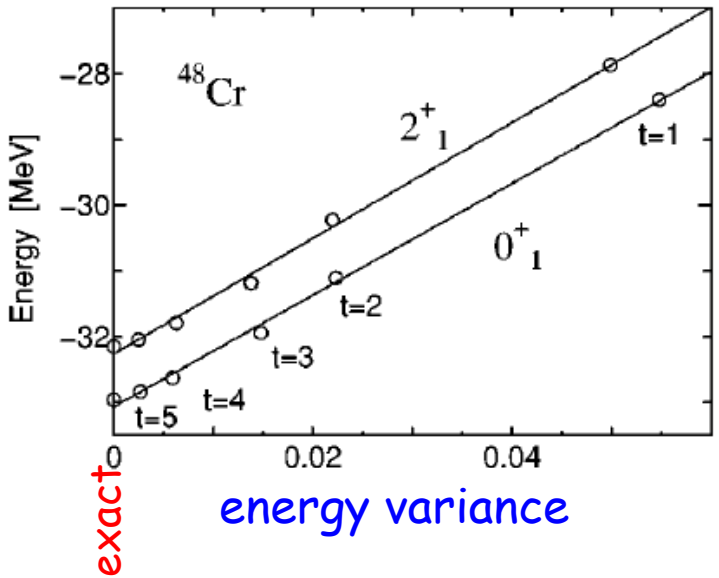

FIG. 2. Extrapolation of the energy to the zero energy variance for the 0_1^+ and 2_1^+ states of ^{48}Cr. The t values represent the truncation space.

T. Mizusaki and M. Imada,
Phys. Rev. C 65, 064319 (2002)

Monte Carlo Shell Model (more basis vectors)

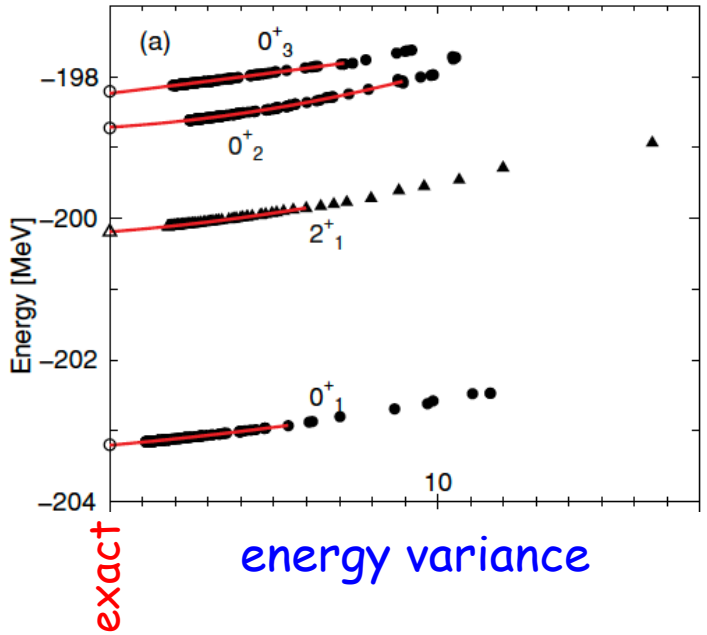

N. Shimizu *et al.*,
Phys. Rev. C 82, 061305 (2010)

Extrapolation by Energy Variance in the MCSM

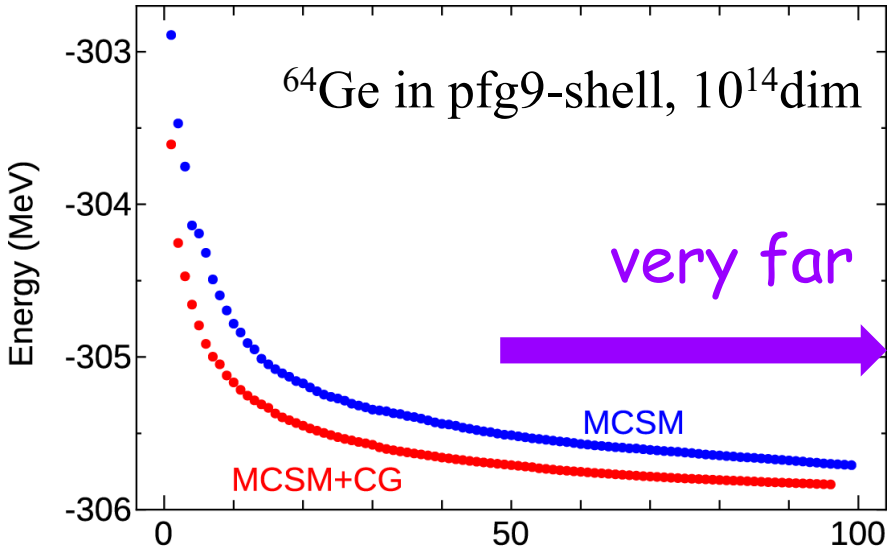

Number of basis vectors
(deformed Slater determinants)

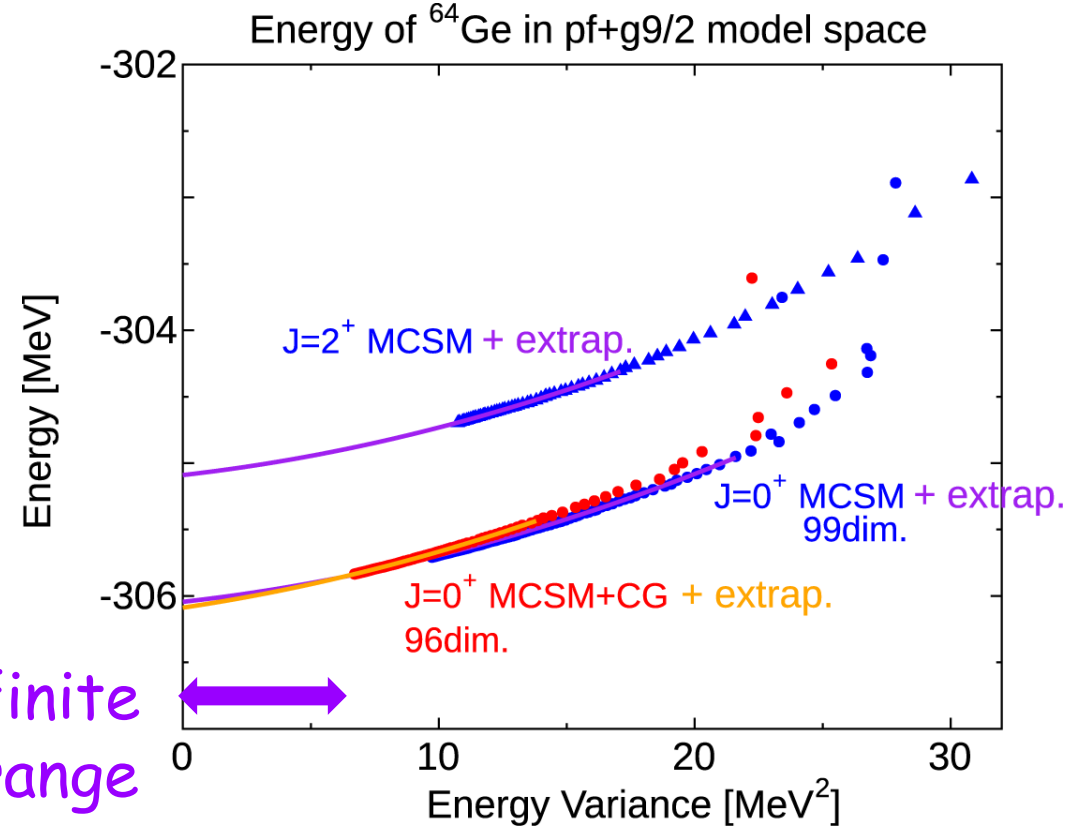

not easy but feasible

Variance : $\langle \Delta H^2 \rangle = \langle H^2 \rangle - \langle H \rangle^2$

$$\langle H \rangle = E_0 + a\langle \Delta H^2 \rangle + b\langle \Delta H^2 \rangle^2 + \ldots$$

N. Shimizu, et al.,
Phys. Rev. C **82,** 061305(R) (2010).

Summary : two types of shell-model calculations

dim. <~ 10^{10}

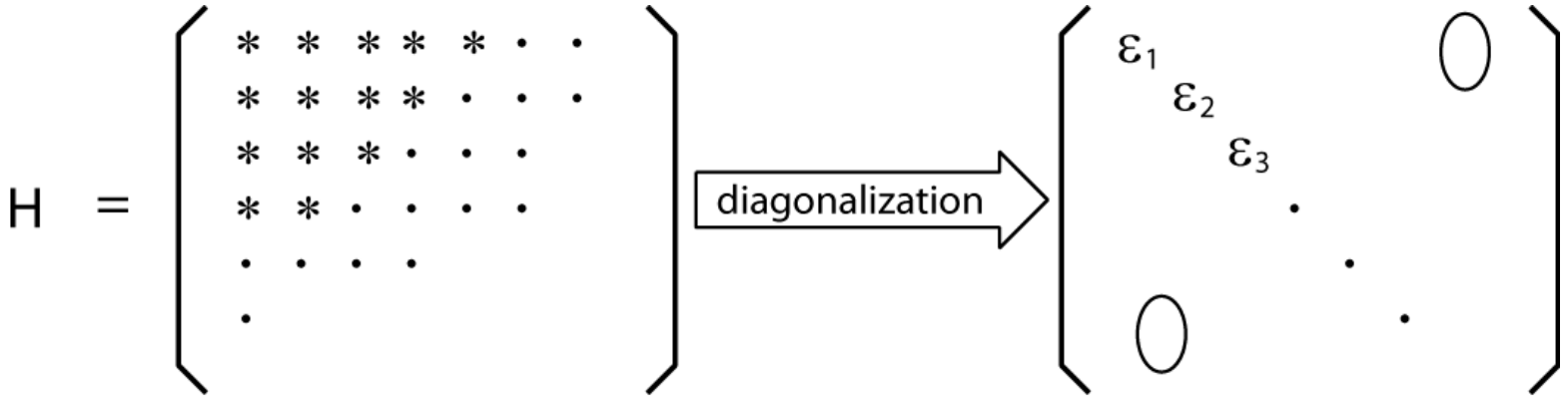

Conventional Shell Model

all Slater determinants

Direct diagonalization

For bigger problems

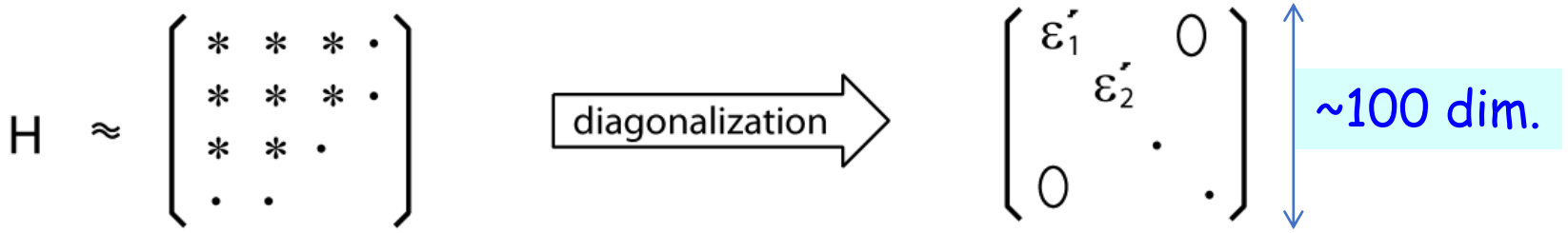

Monte Carlo Shell Model

bases important for a specific eigenstate

Selected important basis vectors

Outline

1. Basics of traditional shell model and Monte Carlo Shell Model
2. Shell evolution: from an introduction to the current landscape of magic numbers
3. Type-II Shell evolution: shape coexistence (parabola or linear or …)
4. Ellipsoidal nuclear shapes: Aage Bohr vs. Davydov
5. Shapes and driplines: who limits isotopes
6. α-clustering and nuclear matter: who likes α-cluster

Shell Evolution

The evolution of shell structure,
for instance,
as a function of Z or N

stable nuclei

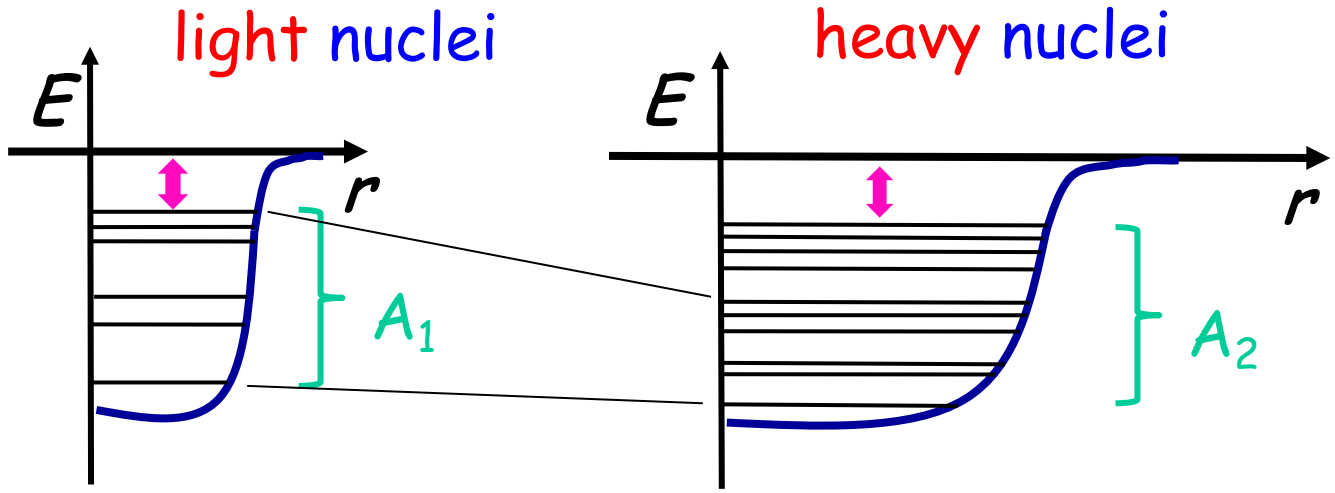

The shell structures are preserved "topologically"

exotic nuclei with Z << N

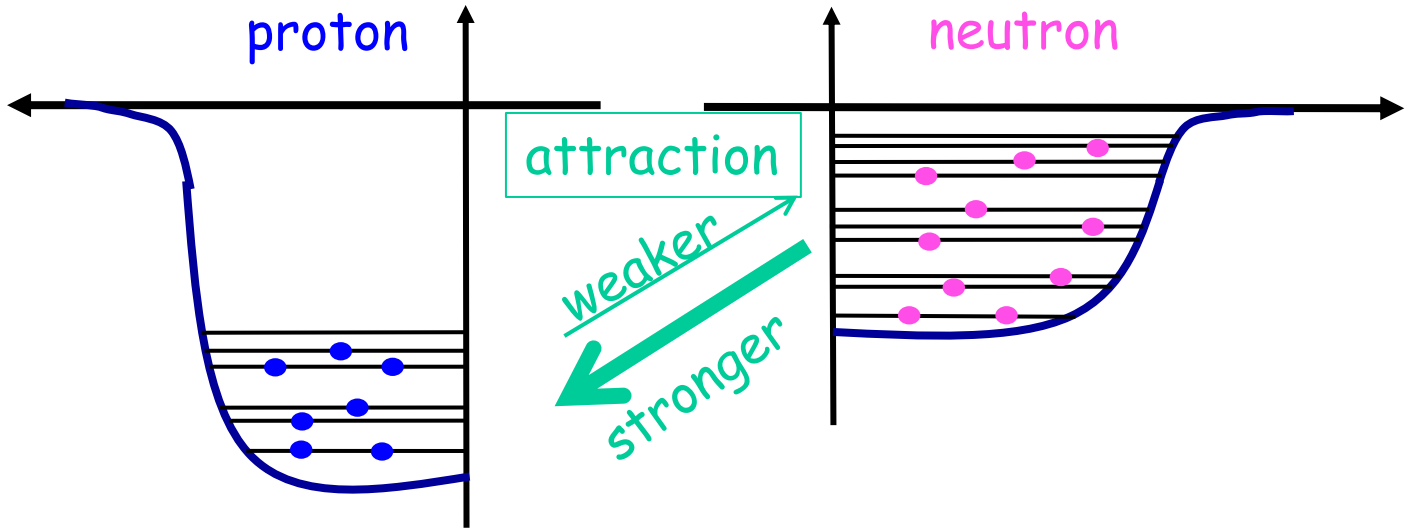

Observed excitation energies of the lowest excited 2^+ states of even-even nuclei

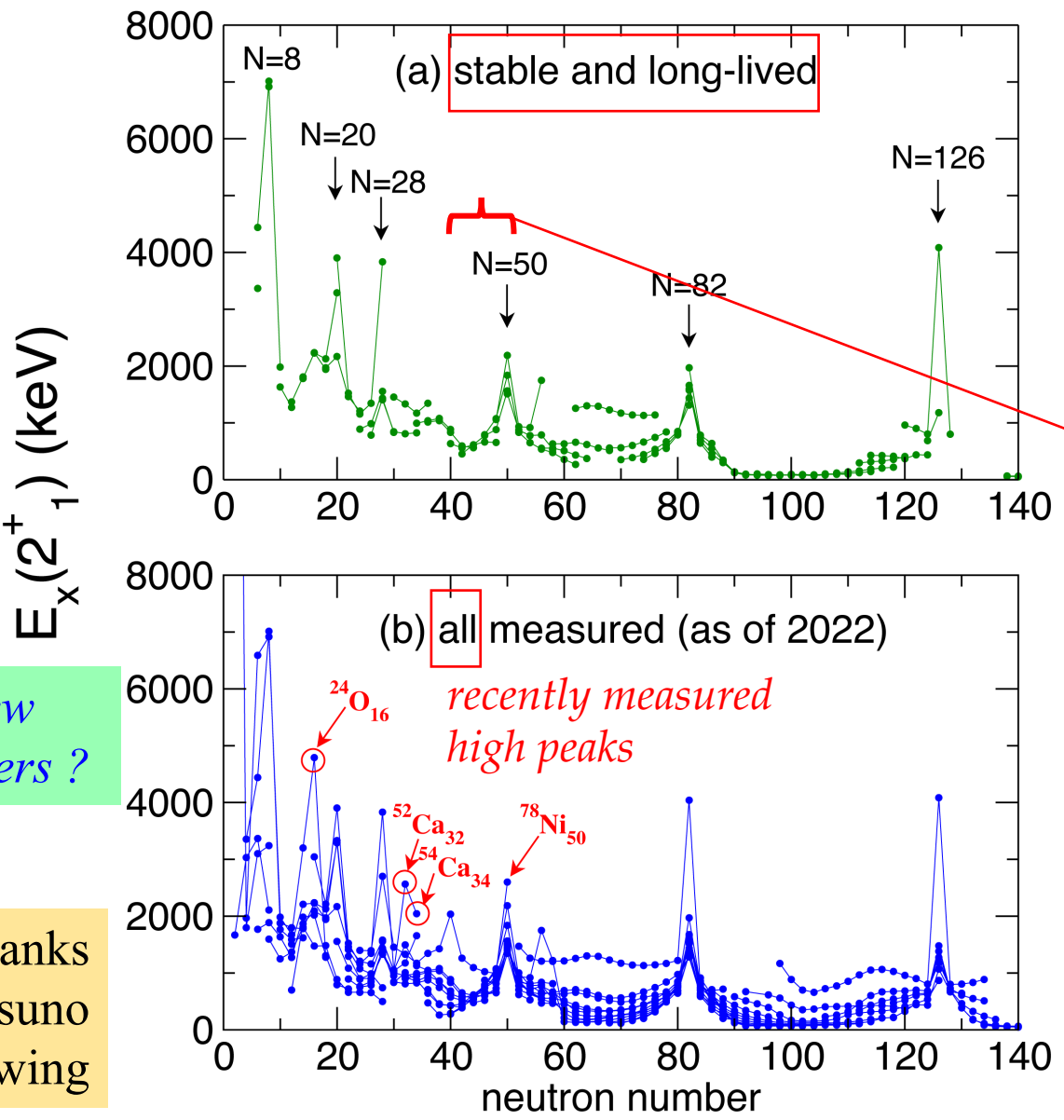

$E_x(2^+_1)$ is higher at magic numbers.

←Magic numbers

2, 8, 20, 28, 50, 82, 126

are visible

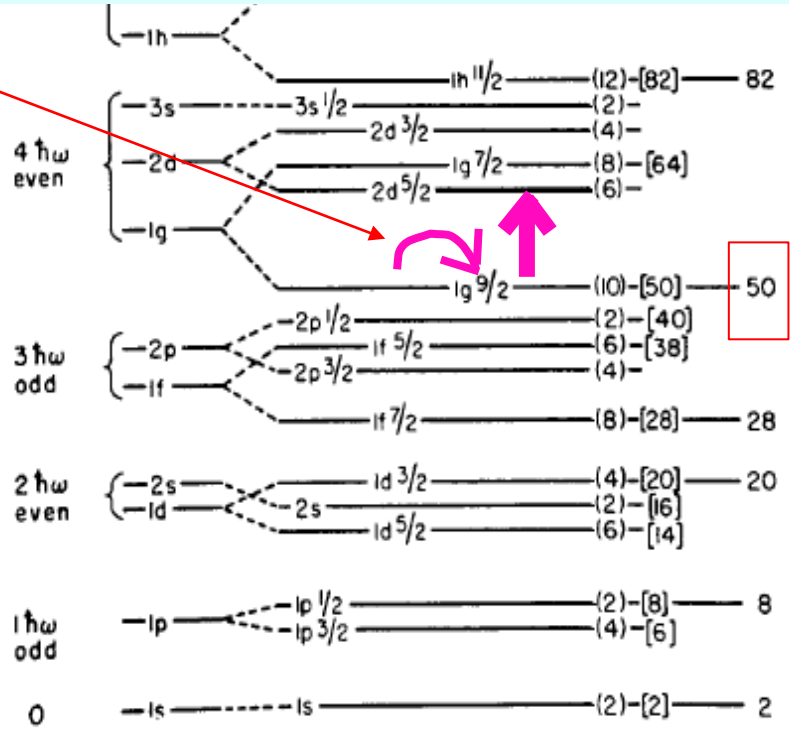

Fig. 7. Realistic level diagram for protons.

Emerging new magic numbers ?

Special thanks to Y. Utsuno for drawing

Many of new features, including new magic numbers, can be understood as consequences of the shell evolution.

Shell evolution means changes of the single-particle energies (SPE), up to inversion of their ordering, for instance, as functions of Z or N, due to specific components of nuclear forces.
The shell evolution results in substantial deviations from the Mayer-Jensen scheme (or paradigm).

The next slide shows a recent systematic survey of "measured" SPEs reported by Schiffer *et al*. (PRC 105, L041302 (2022)) .

John Schiffer made great contributions to experimental study of the shell evolution and related subjects among others. He passed away last May.

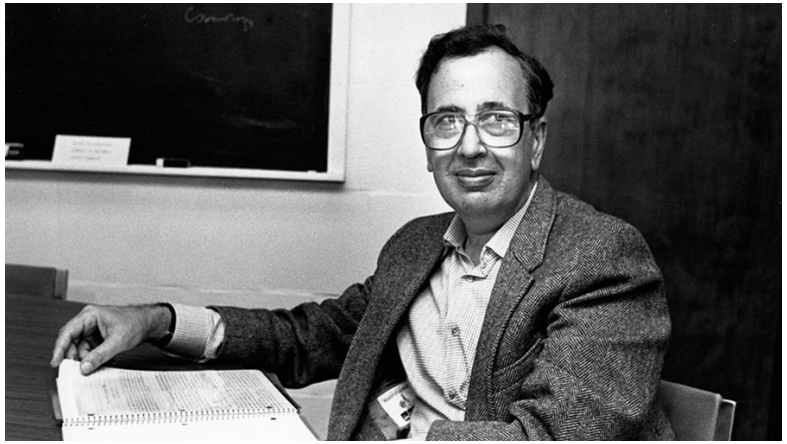

Credit: Photo by Keith Swinden/Courtesy University of Chicago Hanna Holborn Gray Special Collections Research Center

Experimentally obtained single-particle energies (SPE)

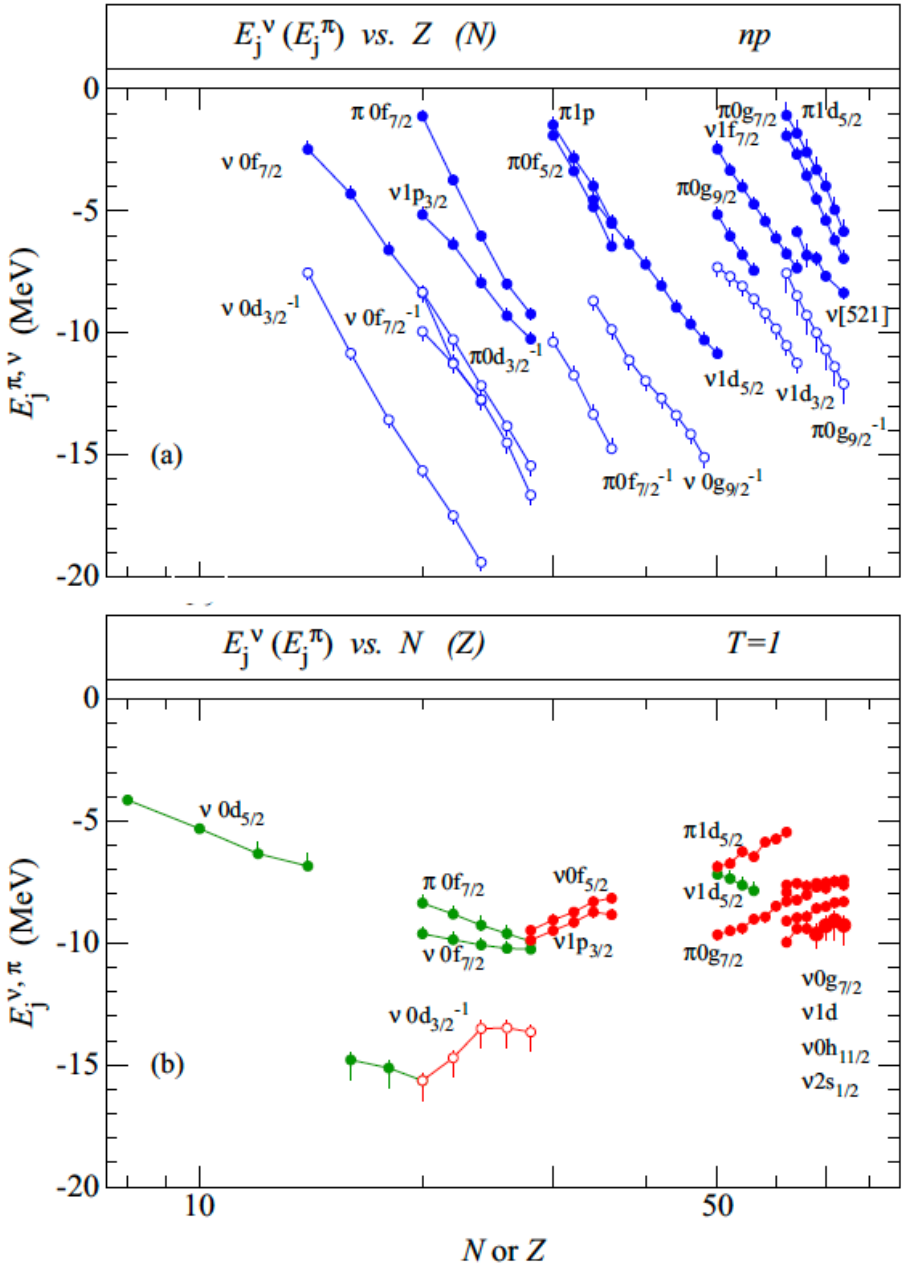

The changes are not uniform.

The SPEs get closer or apart.
Why ?
What consequences ?

Upper panel:
Neutron SPEs as Z changes,
and proton SPEs as N changes.

Lower panel:
Neutron SPEs as N changes,
and proton SPEs as Z changes.

from Schiffer et al. PRC 105, L041302 (2022)

The key to understand such SPE changes is the monopole interaction defined by monopole matrix elements:

cf: Bansal-French, Poves-Zuker

$$V^{\mathrm{mono}}(j,j') = \frac{\Sigma_{(m,m')} \langle j,m\,;\,j',m'|\hat{V}|j,m\,;\,j',m'\rangle}{\Sigma_{(m,m')}\,1}$$

$$= \frac{\langle \uparrow\uparrow | v | \uparrow\uparrow \rangle + \langle \uparrow\nearrow | v | \uparrow\nearrow \rangle + \langle \uparrow\rightarrow | v | \uparrow\rightarrow \rangle + \cdots}{\text{number of matrix elements in the summation}}$$

$$+ \langle \nearrow\uparrow | v | \nearrow\uparrow \rangle + \cdots \quad \cdots \quad \cdots \quad \cdots + \langle \downarrow\downarrow | v | \downarrow\downarrow \rangle$$

$\uparrow \nearrow \cdots \downarrow$: magnetic substates of the orbit j

$\uparrow \nearrow \cdots \downarrow$: magnetic substates of the orbit j'

from TO *et al.*, RMP (2020)

Monopole interaction V^{mono} is an angular-average of a given interaction V acting between orbitals j and j'

The monopole interaction between neutrons is written as

$$\hat{V}_{nn}^{\mathrm{mono}} = \Sigma_j \boxed{V_{nn}^{\mathrm{mono}}(j,j)} \frac{1}{2} \hat{n}_j^n \, (\hat{n}_j^n - 1) + \Sigma_{j<j'} \boxed{V_{nn}^{\mathrm{mono}}(j,j')} \hat{n}_j^n \, \hat{n}_{j'}^n$$

The monopole interaction between protons is given similarly.

The monopole interaction between a proton and a neutron is given, in a good approximation, by

$$\begin{aligned}
\hat{V}_{pn}^{\mathrm{mono}} &= \Sigma_{j \neq j'} \, \frac{1}{2} \left\{ \boxed{V_{T=0}^{\mathrm{mono}}(j,j')} + \boxed{V_{T=1}^{\mathrm{mono}}(j,j')} \right\} \hat{n}_j^p \, \hat{n}_{j'}^n \\
&\quad + \Sigma_j \, \frac{1}{2} \left\{ \boxed{V_{T=0}^{\mathrm{mono}}(j,j)} \frac{2j+2}{2j+1} + \boxed{V_{T=1}^{\mathrm{mono}}(j,j)} \frac{2j}{2j+1} \right\} \hat{n}_j^p \hat{n}_j^n \\
&= \Sigma_{j,j'} \boxed{\tilde{V}_{pn}^{\mathrm{mono}}(j,j')} \, \hat{n}_j^p \, \hat{n}_{j'}^n
\end{aligned}$$

Note: $\hat{V}$ can be any (component of) Nucleon-Nucleon (NN) interaction, e.g., total, central, tensor, etc.

The (total) monopole interaction becomes,

$$\hat{V}^{\text{mono}} = \hat{V}^{\text{mono}}_{pp} + \hat{V}^{\text{mono}}_{nn} + \hat{V}^{\text{mono}}_{pn}$$

The monopole Hamiltonian is given as,

$$\hat{H}^{\text{mono}} = \hat{H}_0 + \hat{V}^{\text{mono}} = \Sigma_j \, \epsilon^{p}_{0;j} \, \hat{n}^{p}_{j} + \Sigma_j \, \epsilon^{n}_{0;j} \, \hat{n}^{n}_{j} + \hat{V}^{\text{mono}}$$

The multipole term is defined

$$\hat{V}^{\text{multi}} = \hat{V} - \hat{V}^{\text{mono}}$$

The monopole and multipole terms contribute in very different ways to nuclear structure, and their interplay produces a variety of exciting physics.

Effects of the monopole interaction can be represented by Effective Single-Particle Energy (ESPE)

ESPE of a proton single-particle orbit, $\hat{\epsilon}^p_j$, is defined as the change of the monopole Hamiltonian due to the addition of one proton into the orbit *j*.

This can be obtained, theoretically, by replacing $\hat{n}^p_j$ by $\hat{n}^p_j + 1$, and evaluate the difference: $\hat{H}^{\rm mono}\ (\hat{n}^p_j \rightarrow \hat{n}^p_j + 1) - \hat{H}^{\rm mono}$.

$$\hat{H}^{\rm mono} = \hat{H}_0 + \hat{V}^{\rm mono} = \Sigma_j\, \epsilon^p_{0;j}\, \hat{n}^p_j + \Sigma_j\, \epsilon^n_{0;j}\, \hat{n}^n_j + \hat{V}^{\rm mono}$$

proton ESPE

pp monopole int.

pn monopole int.

$$\hat{\epsilon}^p_j = \epsilon^p_{0;j} + \Sigma_{j'}\, V^{\rm mono}_{pp}(j, j')\, \hat{n}^p_{j'} + \Sigma_{j'}\, \tilde{V}^{\rm mono}_{pn}(j, j')\, \hat{n}^n_{j'}$$

Effective single-particle energy is an operator

$$\hat{\epsilon}^p_j = \epsilon^p_{0;j} + \Sigma_{j'} V^{\rm mono}_{pp}(j, j')\, \hat{n}^p_{j'} + \Sigma_{j'} \tilde{V}^{\rm mono}_{pn}(j, j')\, \hat{n}^n_{j'}$$

$$\hat{\epsilon}^n_j = \epsilon^n_{0;j} + \Sigma_{j'} V^{\rm mono}_{nn}(j, j')\, \hat{n}^n_{j'} + \Sigma_{j'} \tilde{V}^{\rm mono}_{pn}(j', j)\, \hat{n}^p_{j'}$$

small large

By taking expectation values such as $\langle \hat{n}^p_{j'} \rangle$, we can look into essential features of dynamical variations of (effective) SPEs.

In particular, the difference between two states is very useful, for instance, between the ground states of two nuclei. An example is the plots of Schiffer *et al.* paper (2022), while they are experimental values.

Monopole interactions depict characteristic features

for Central force

Stronger attraction between single-particle orbits of similar radial wave functions

ex.: $f_{7/2} - f_{5/2}$, $g_{9/2} - h_{11/2}$ *cf: Federman-Pittel (1977)*

for Tensor force

(long-range part,
or 1π, 2π exchange)

$j_> = l + ½$

$j_< = l - ½$

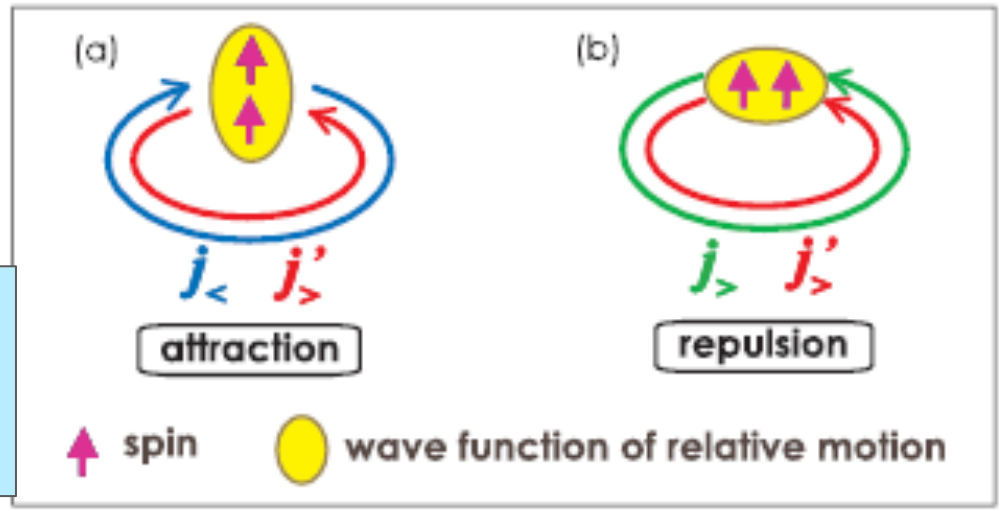

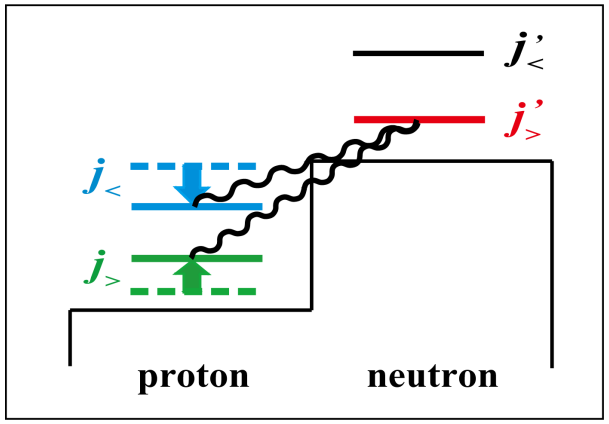

for Three-nucleon force (Δ-hole) : overall repulsive effect

An earlier experimental research by Schiffer et al.

Probably (one of) the first systematic experimental studies

VOLUME 92, NUMBER 16 PHYSICAL REVIEW LETTERS week ending 23 APRIL 2004

Is the Nuclear Spin-Orbit Interaction Changing with Neutron Excess?

J. P. Schiffer,[1] S. J. Freeman,[1,2] J. A. Caggiano,[3] C. Deibel,[3] A. Heinz,[3] C.-L. Jiang,[1] R. Lewis,[3] A. Parikh,[3] P. D. Parker,[3] K. E. Rehm,[1] S. Sinha,[1] and J. S. Thomas[4]

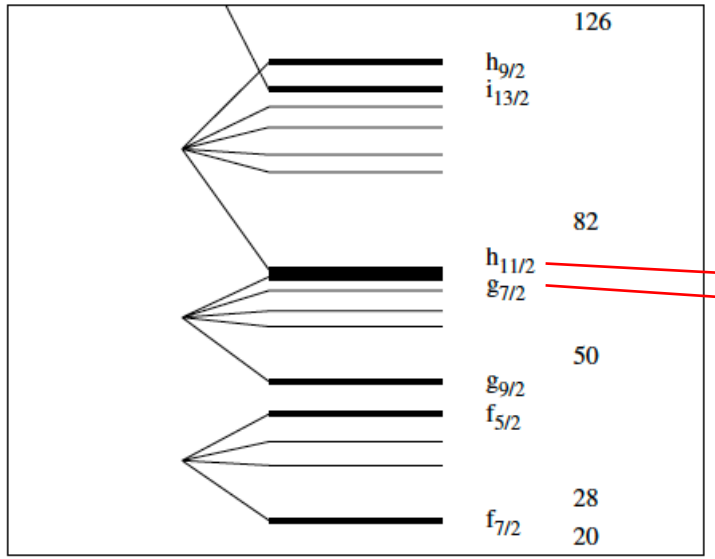

Mayer-Jensen scheme

A question why this widening occurs ?

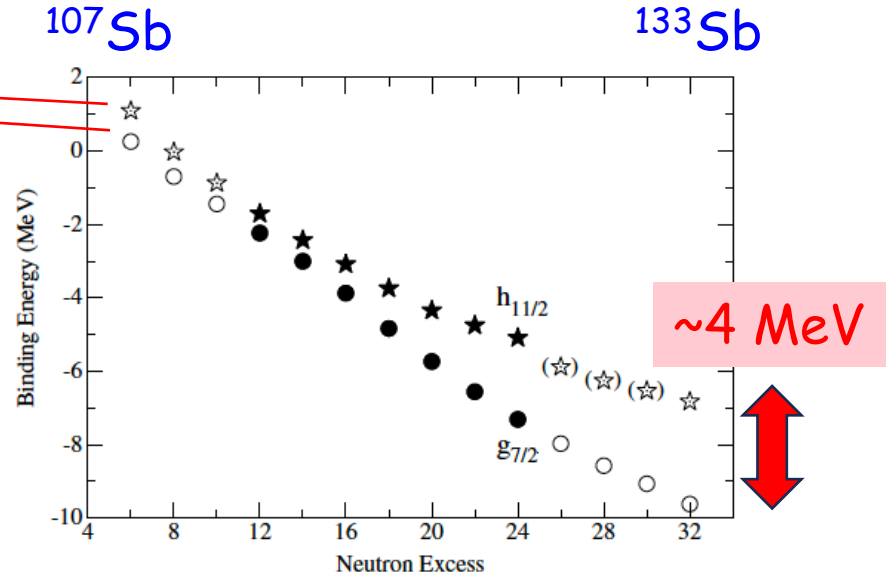

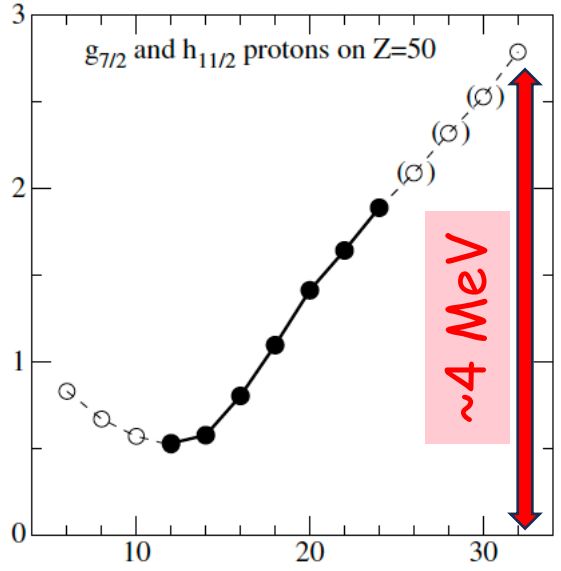

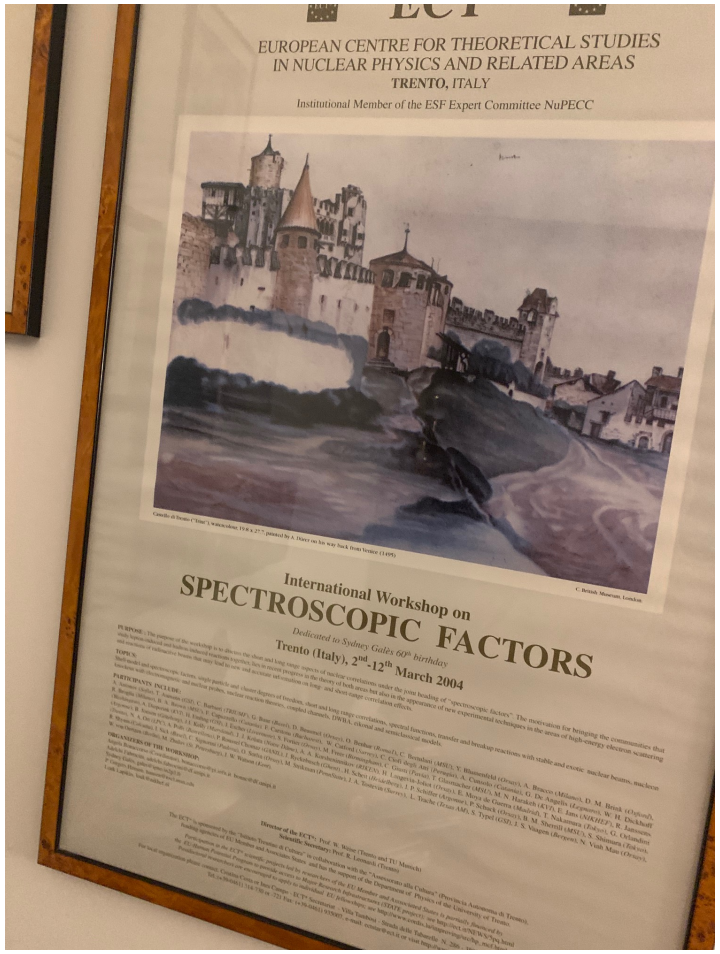

John and I met in the ect* (Trento, Italy) workshop held in March 2004 (Sydney Gales' 60th birthday).

I had the idea of the tensor force effect (*NN* conf. 2003), but was not so sure that it could be supported by experiments.

Schiffer showed his data in ect* (2004), requesting theoretical account. It was like a thunder strike from the heaven to me.

Schiffer experiment in PRL 2004

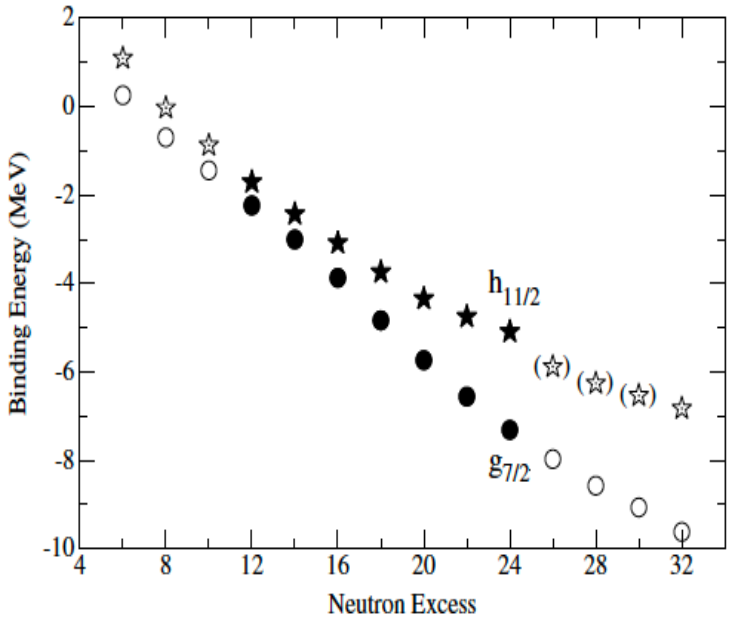

Our theory (PRL 95, 232502 (2005))

Symbols are from Schiffer et al.

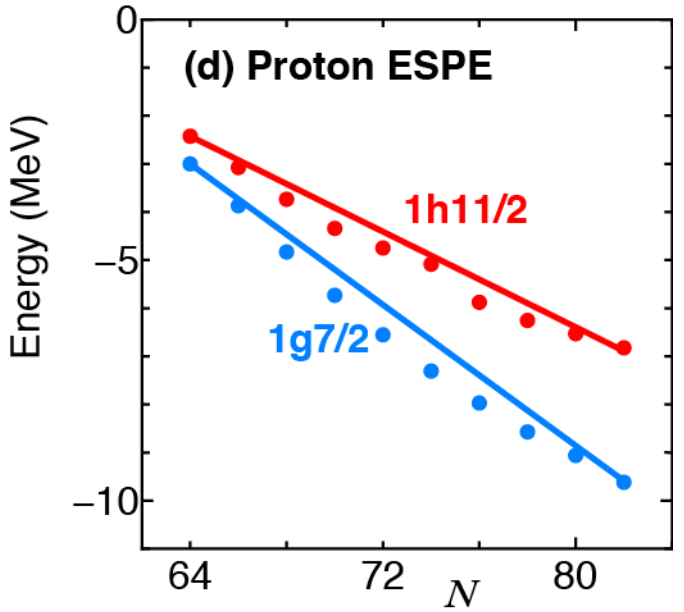

PRL 95, 232502 (2005) PHYSICAL REVIEW LETTERS week ending 2 DECEMBER 2005

Evolution of Nuclear Shells due to the Tensor Force

Takaharu Otsuka,[1,2,3,*] Toshio Suzuki,[4] Rintaro Fujimoto,[1] Hubert Grawe,[5] and Yoshinori Akaishi[6]

Fig. 4

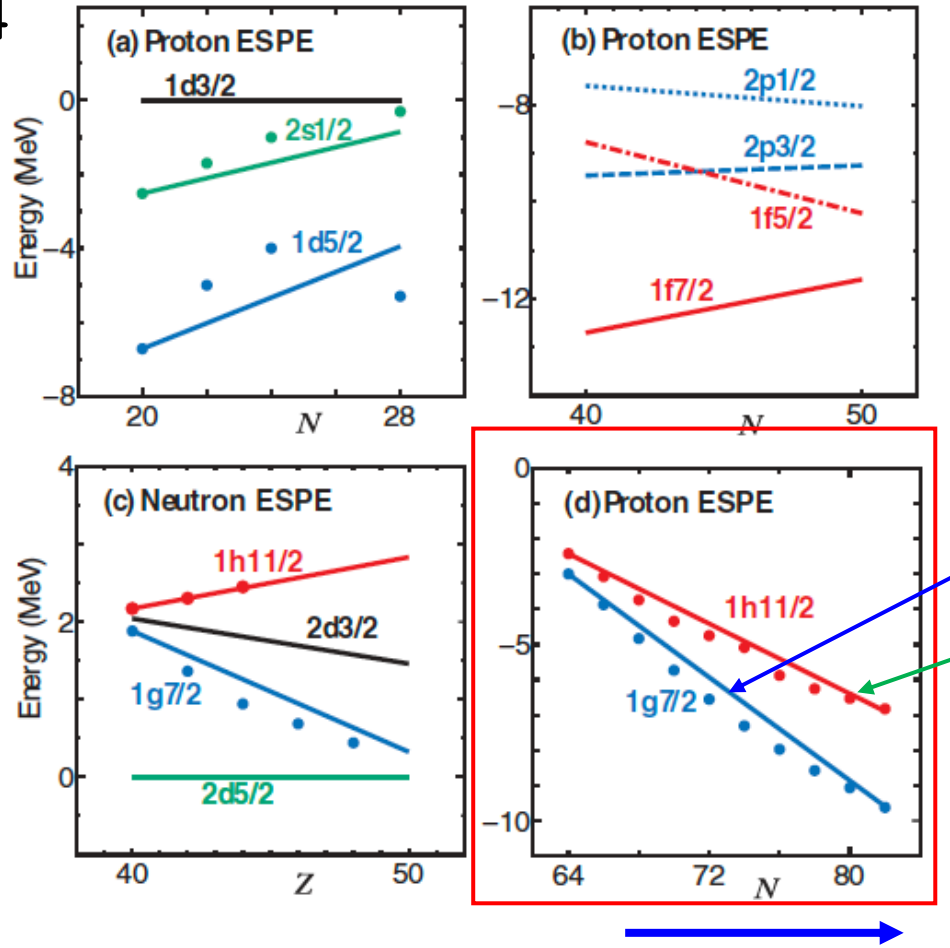

neutron $h_{11/2}$ occupied

general rule

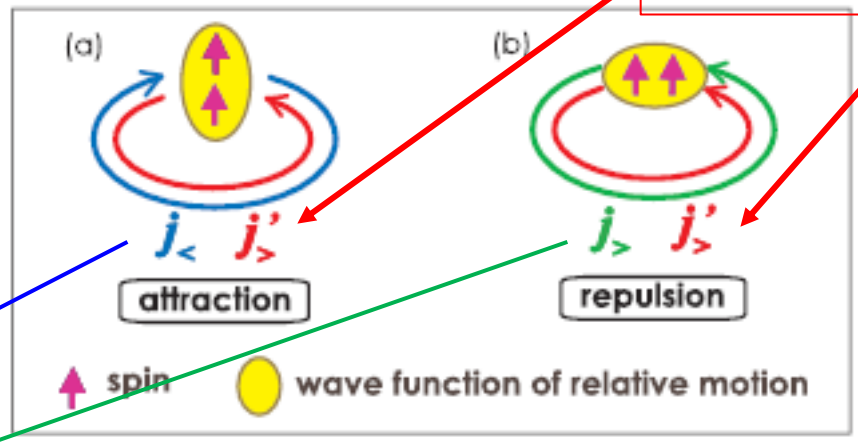

neutron $h_{11/2}$

Schiffer's data were crucial then, covering a wider span.

Now the paper has more than 1200 citations with many other experimental evidences.

ESPEs in exotic Ca isotopes

$$\hat{\epsilon}^n_j = \epsilon^n_{0;j} + \Sigma_{j'} V^{\mathrm{mono}}_{nn}(j, j')\, \hat{n}^n_{j'} + \Sigma_{j'} \tilde{V}^{\mathrm{mono}}_{pn}(j', j)\, \hat{n}^p_{j'}$$

Neutron shell structure in Ni isotopes ($f_{7/2}$ fully occupied)

a la Mayer-Jensen

N=34 magic number appears if proton $f_{7/2}$ becomes vacant (Ca)

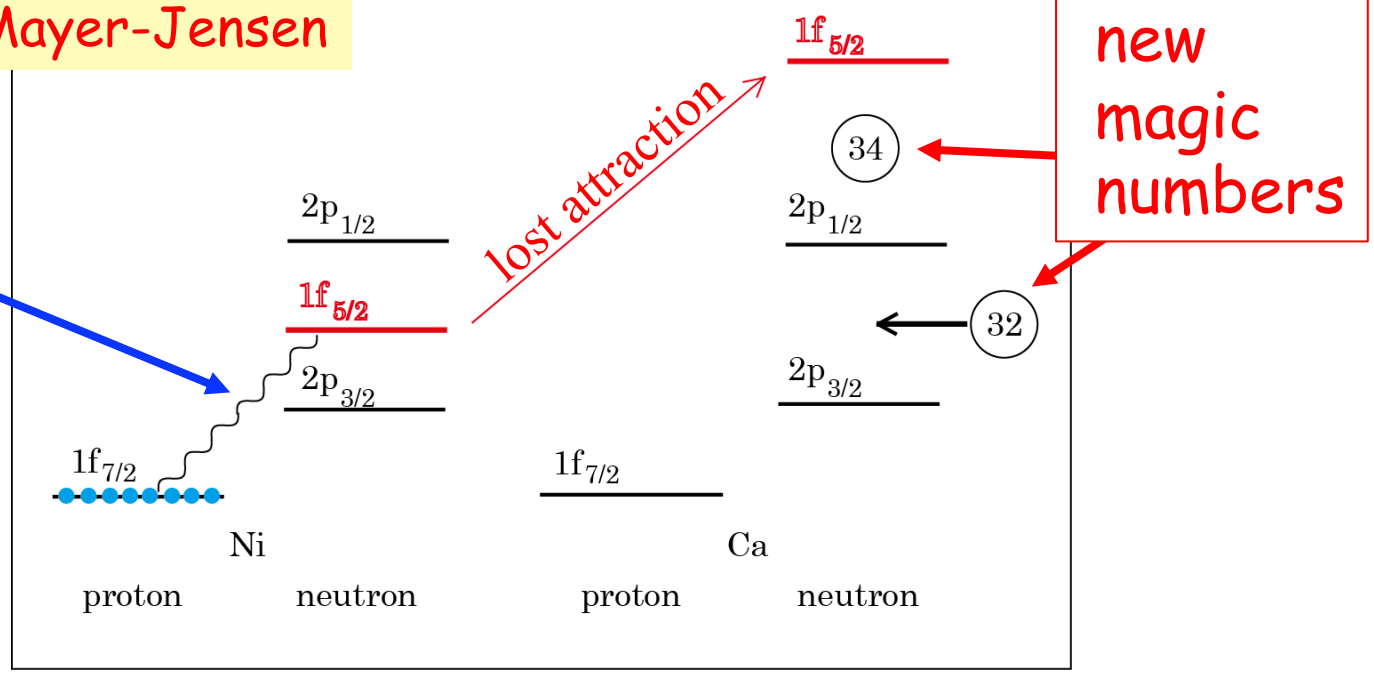

new magic numbers

strong attractive effect due to tensor force

$f_{7/2}$ /+ 1/2

$f_{5/2}$ /- 1/2

$\langle \hat{n}^p_{j'} \rangle = 8$

stable (e.g. ^{56}Ni)

$\langle \hat{n}^p_{j'} \rangle = 0$

exotic (neutron-rich, e.g. ^{54}Ca)

Experiment @ RIBF

12 years after prediction (2001)

excitation energy of the 2+ state

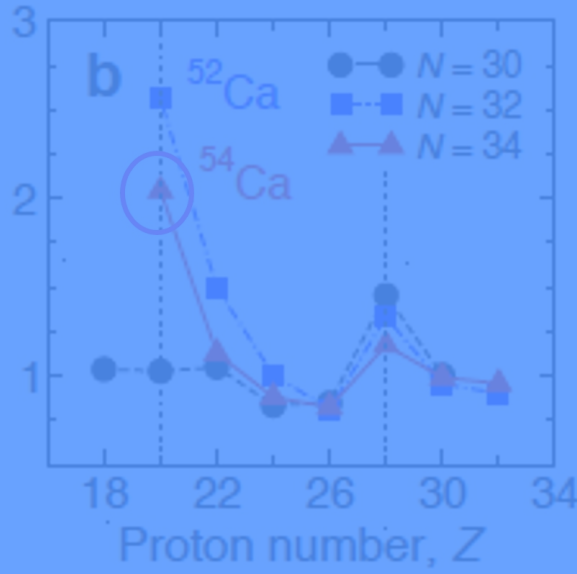

Steppenbeck *et al.* Nature 502 (2013)

TO and Tsunoda, J. Phys. G 43, 024009 (2016)

A bit of history

N=34 magic number was not trivial at all.

In comparison to N=32 magic number known experimentally (1985) for nearly 40 years (next page).

> Moving back to heavier nuclei, from the strong interaction in Fig. 1(c), we can predict other magic numbers, for instance, $N = 34$ associated with the $0f_{7/2}$-$0f_{5/2}$ interaction. In heavier nuclei, $0g_{7/2}$, $0h_{9/2}$, etc. are shifted upward in neutron-rich exotic nuclei, disturbing the magic numbers $N = 82$, 126, etc. It is of interest how the r process of nucleosynthesis is affected by it.

TO et al.
PRL 87 (2001)

relevant later

Pessimism in experiment

NATURE|Vol 435|16 June 2005

NUCLEAR PHYSICS

Elusive magic numbers

Robert V. F. Janssens

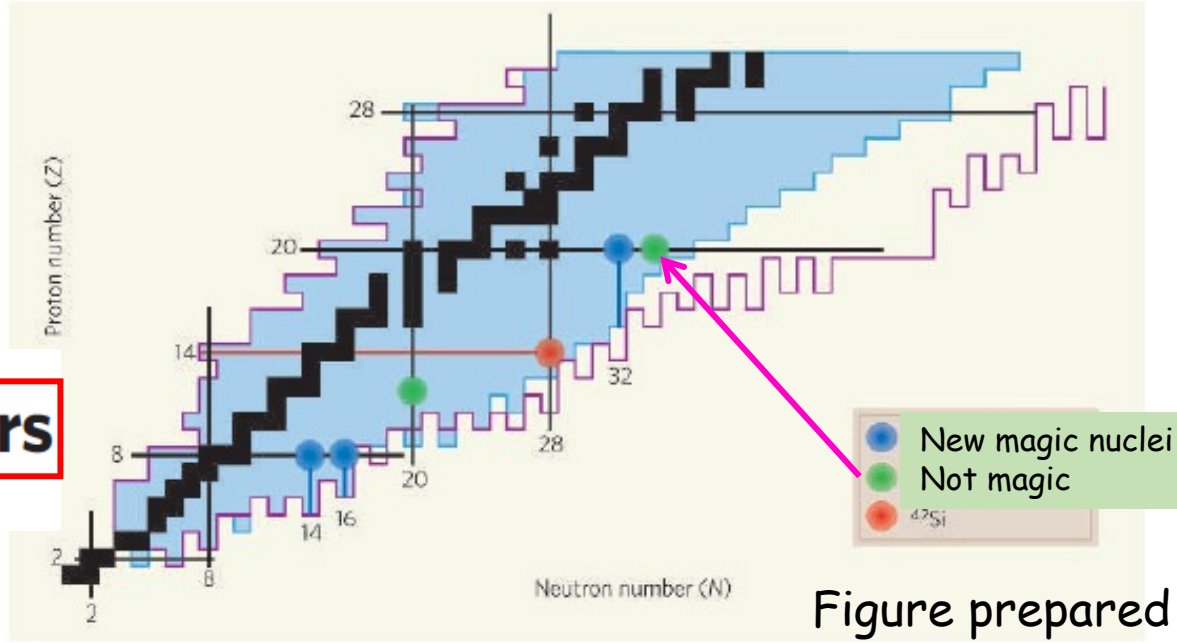

Figure prepared by MSU

ESPEs in exotic Ca isotopes

$$\hat{\epsilon}^n_j = \epsilon^n_{0;j} + \Sigma_{j'} V^{\mathrm{mono}}_{nn}(j,j')\,\hat{n}^n_{j'} + \Sigma_{j'} \tilde{V}^{\mathrm{mono}}_{pn}(j',j)\,\hat{n}^p_{j'}$$

Neutron shell structure in Ni isotopes ($f_{7/2}$ fully occupied)

a la Mayer-Jensen

N=34 magic number appears if proton $f_{7/2}$ becomes vacant (Ca)

Experiment @ RIBF
12 years after prediction (2001)

strong attractive effect due to tensor force
$f_{7/2}$ /+ 1/2
$f_{5/2}$ /- 1/2

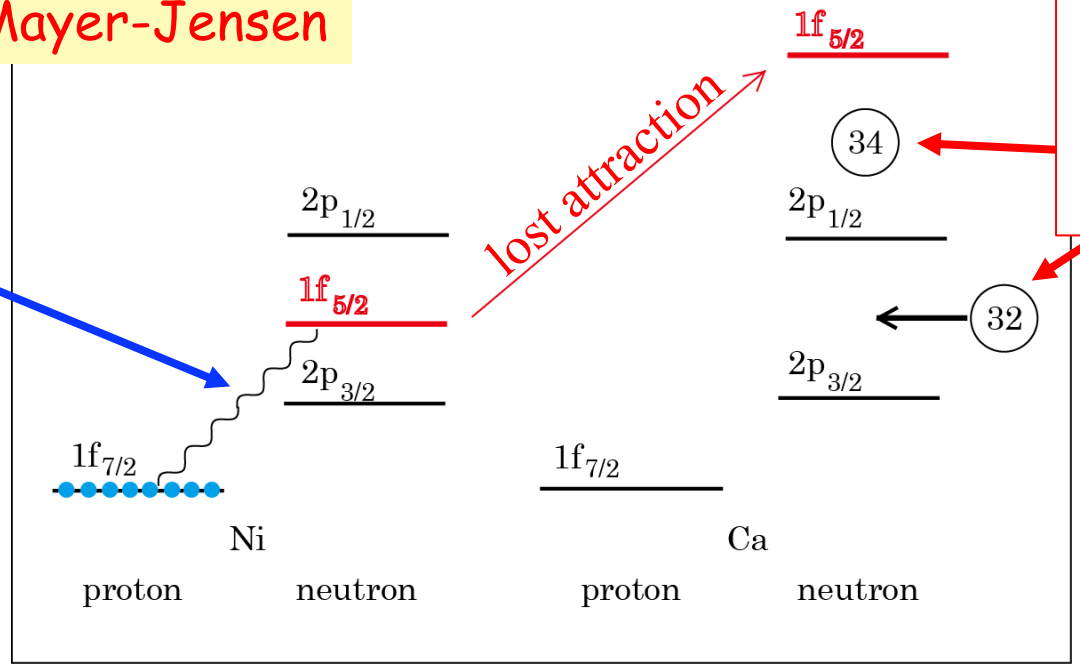

new magic numbers

$\langle \hat{n}^p_{j'} \rangle = 8$

stable (e.g. ^{56}Ni)

$\langle \hat{n}^p_{j'} \rangle = 0$

exotic (neutron-rich, e.g. ^{54}Ca)

excitation energy of the 2+ state

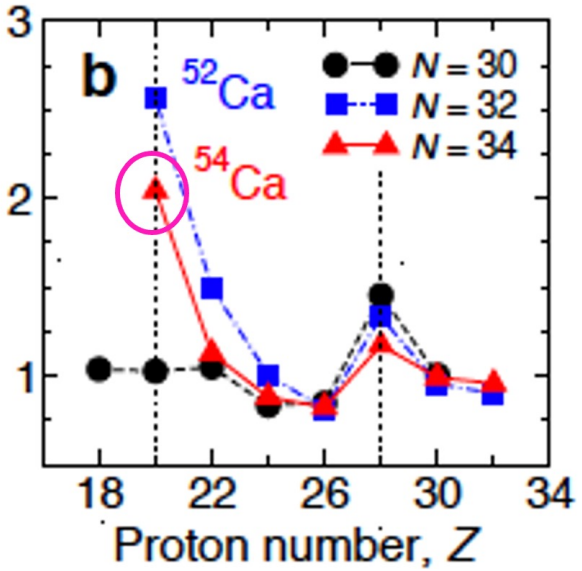

Steppenbeck *et al.*
Nature 502 (2013)

TO and Tsunoda,
J. Phys. G 43, 024009 (2016)

A bit of history

N=34 magic number was not trivial at all.

In comparison to N=32 magic number known experimentally (1985) for nearly 40 years (next page).

Moving back to heavier nuclei, from the strong interaction in Fig. 1(c), we can predict other magic numbers, for instance, $N = 34$ associated with the $0f_{7/2}$-0 interaction. In heavier nuclei, $0g_{7/2}$, $0h_{9/2}$, etc. upward in neutron-rich exotic nuclei, disturb… magic numbers $N = 82$, 126, etc. It is of inte… the r process of nucleosynthesis is affected…

TO et al.
PRL 87 (2001)

relevant later

Don't give up too quickly.

Pessimism in experim…

NATURE|Vol 435|16 June 2005

NUCLEAR PHYSICS

Elusive magic numbers

Robert V. F. Janssens

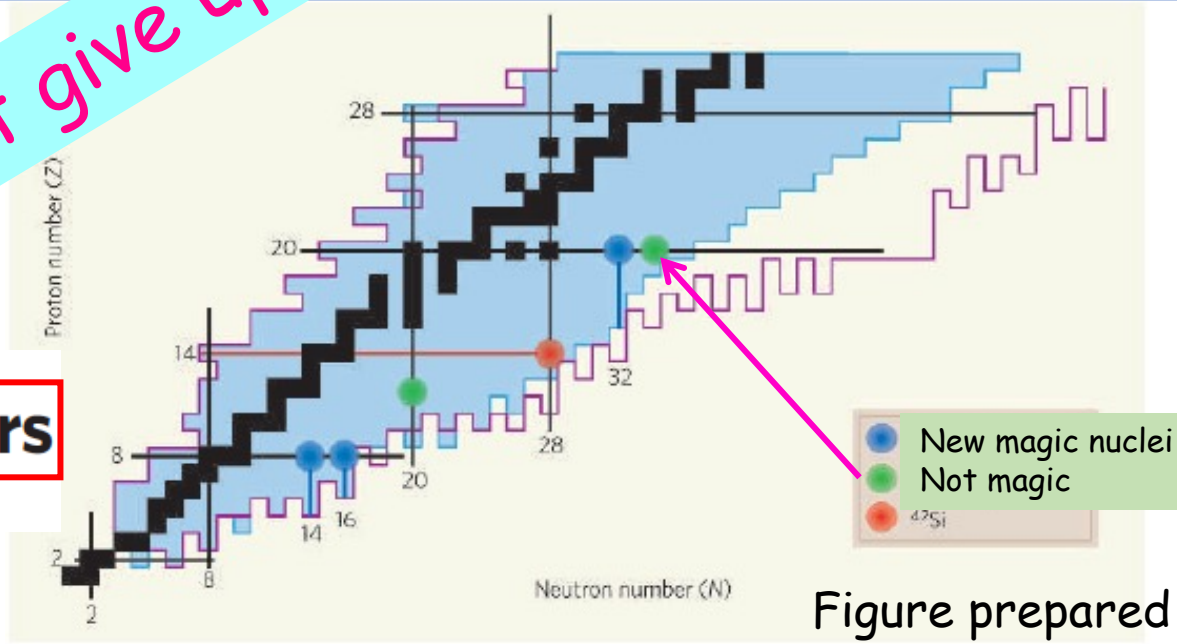

Figure prepared by MSU

The shell evolution now occurs almost everywhere on the nuclear chart.

➔one of the major subjects of RI-beam facilities for exotic nuclei

This word did not exist before 2004.

"Shell evolution"* : 0 hit in Google Scholar in 2003
1 2004

~140 hits/year ~2021

*Combine with "atomic nuclei", to avoid biology, … .

Earlier empirical analyses such as Grawe, Sorlin-Porquet, ….
with different nomenclatures for instance,"orbital migration", …

The shell evolution becomes visible mostly due to constructive contributions of tensor and central forces.

New magic gaps are generally smaller, but the closed-shell formation has been seen by direct reactions.

- Spectroscopic Factors -> closed shell at N=34

Chen, Lee, *et al*. PRL 123, 142501(2019)

^{54}Ca (p, pn) ^{53}Ca

↓

SF (C^2S)

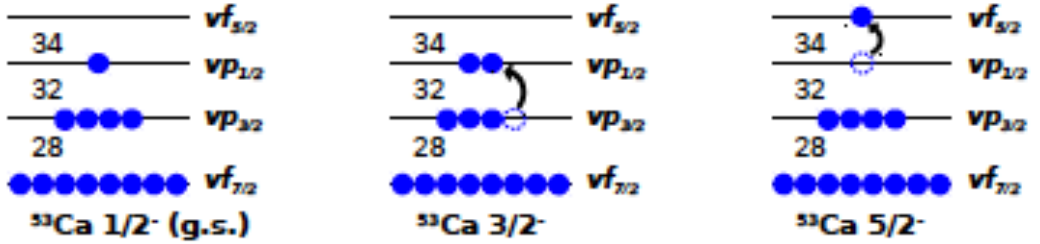

FIG. 1. Illustration of the most representative neutron single-particle configurations for ground and bound excited states of ^{53}Ca.

	J^π	-1n	σ_{-1n}	DWIA σ_{sp}	GXPF1Bs E_x(keV)	GXPF1Bs C^2S	GXPF1Bs σ^{th}_{-1n}
g.s.	$1/2^-$	$p_{1/2}$	15.9(17)	7.27	0	1.82	13.2
2220(13)	$3/2^-$	$p_{3/2}$	19.1(12)	6.24	2061	3.55	22.2
1738(17)	$5/2^-$	$f_{5/2}$	1.0(3)	4.19	1934	0.19	0.8
Inclusive			36.0(12)				36.2

C^2S exp	max
2.2(2)(3)	2
3.1(2)(5)	4

full occupancy

Being closed shell => the most direct indicator of magicity.

N=34 magic number disappears if a proton occupies $f_{7/2}$ (Sc (Z=21))

new mass experiment on Sc, Ti and V by MR-TOF at RIBF
mass difference Δ_{2n} ~ gap

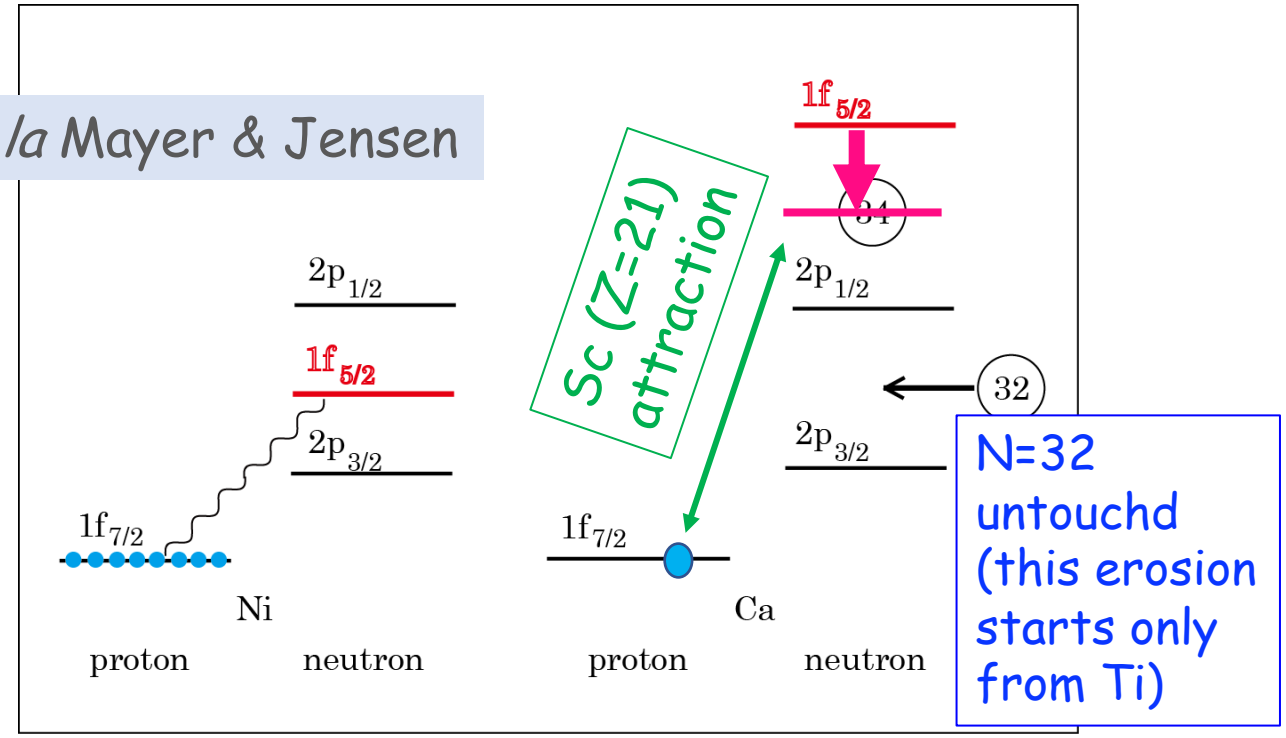

stable (e.g. ^{58}Ni)
a la Mayer-Jensen

exotic
(neutron-rich, e.g. ^{55}Sc)

Iimura *et al*. PRL 130, 012501 (2023)

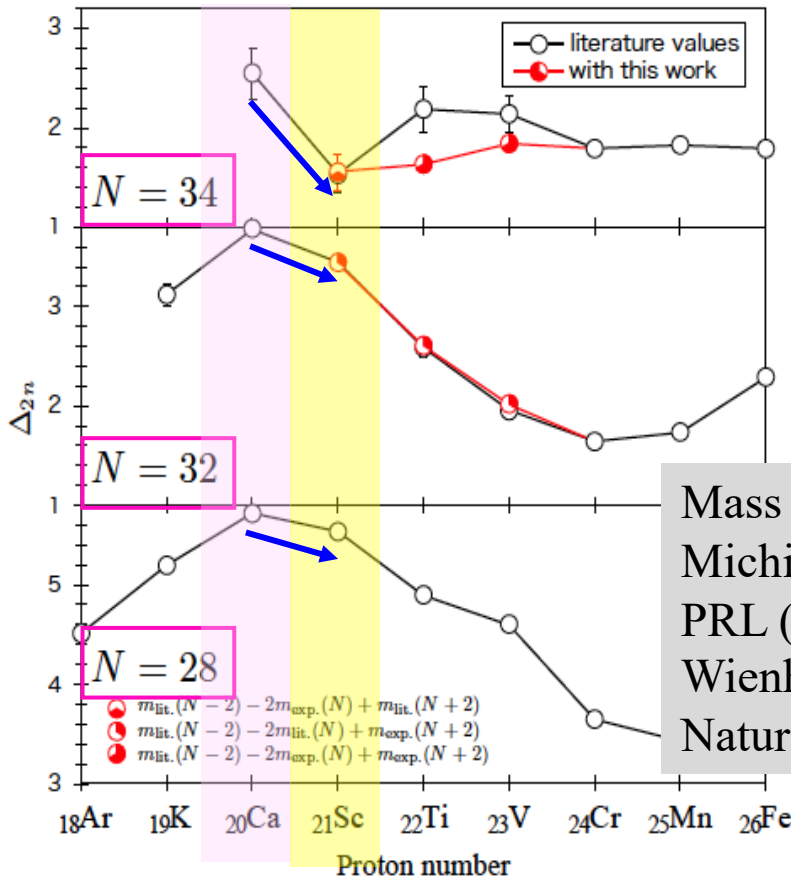

Mass measurement:
Michimasa *et al*. PRL (2018),
Wienholtz *et al*. Nature (2013)

Magic numbers are not universal. They emerge and fade away on the chart.

More recent experimental results of magic numbers

$E_x(2^+)$ of Ar (Z=19)

Liu et al. PRL (2019)

N=34 magic gap may remain, but
N=32 magic gap is fading away.

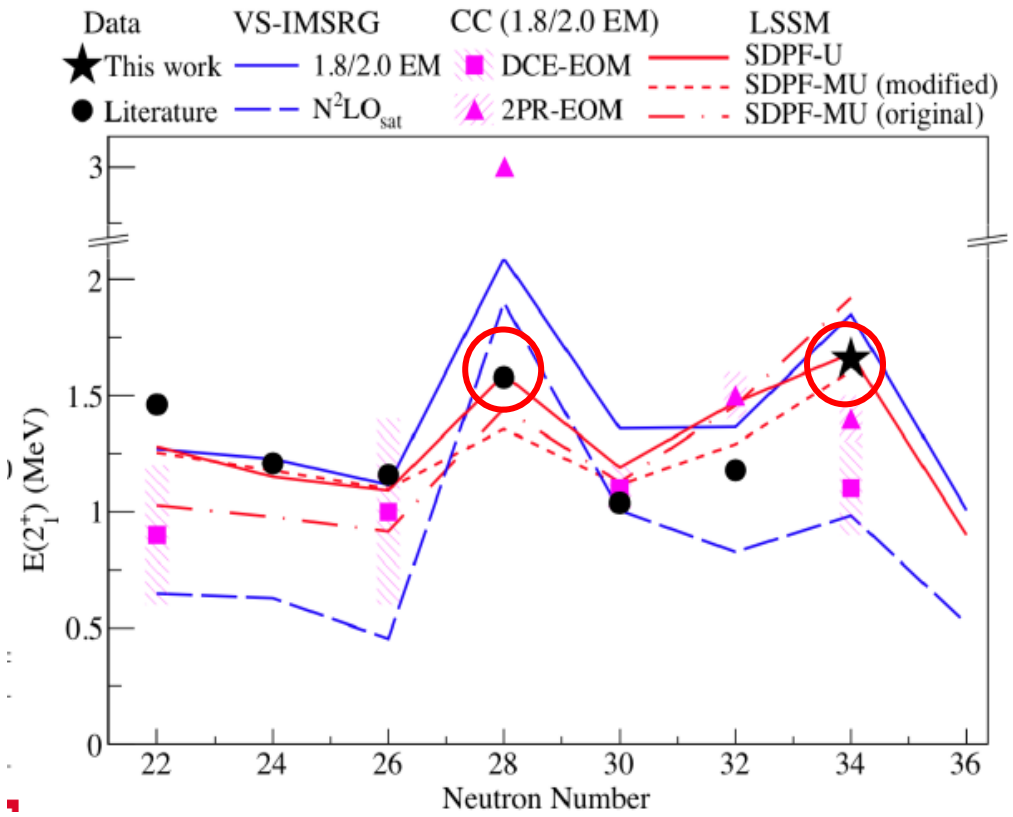

$E_x(2^+)$ of ^{56,58}Ca

S.D. Chen *et al.* to be published in PLB

These data suggest neutron $g_{9/2}$ is not far above $f_{5/2}$ ➔ pushing Ca dripline far away

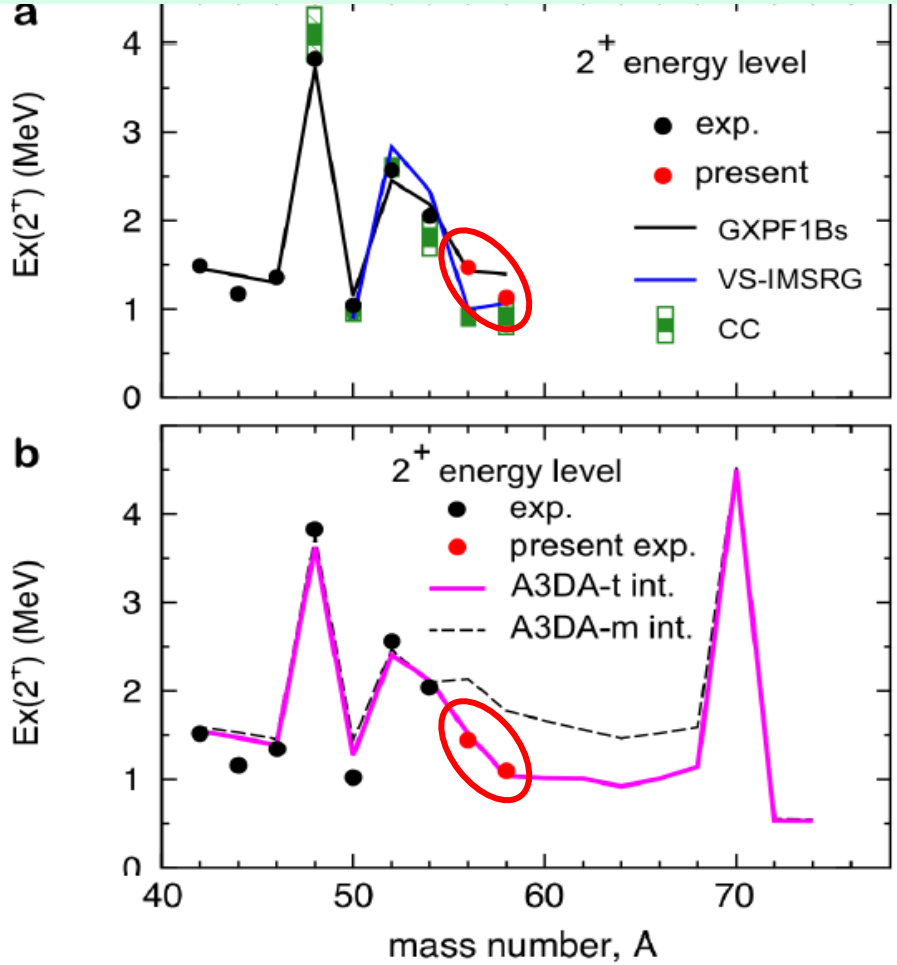

A review paper

REVIEWS OF MODERN PHYSICS, VOLUME 92, JANUARY–MARCH 2020

Evolution of shell structure in exotic nuclei

by T. Otsuka, A. Gade, O. Sorlin, T. Suzuki and Y. Utsuno

CONTENTS

Shell evolution in the Density Functional Theories

D.M. Brink
1930-2021

Skyrme formally included tensor force. NPA (1958)

Stancu, Brink and Flocard, PRC (1977)
proposed a formulation being used in literatures.

Brink and Stancu, PLB (2007) showed shell evolution.

After 2006, many papers have been published taking the SBF formulation

Lesinski, Bender, Bennaceur, Duguet, Meyer, PRC (2007)
Skyrme model is not flexible enough for including the tensor force

Gogny force has been extended so as to include the tensor force.

TO, Matsuo and Abe, PRL 97, 162501 (2006). → *GT2 interction*

Relativistic Hartree-Fock was improved closer to the shell model.

Wang, Naito and Liang, PRC (2021) may show the right direction.

Despite confirmed feasibilities, actual formulation is to come

Remarks up to here

From here, 2nd lecture

The decomposition to monopole and multipole interactions facilitates our understanding of nuclear structure, although actual outcome of the shell model calculation is obtained by including both of them.

The monopole interaction effectively changes the energies of single-particle orbits, resulting in the shell evolution.

The effective single-particle energy (ESPE) is then introduced as an operator, and is, of course, state-dependent. In many cases, the essential physics can be learned by taking appropriate expectation values of the operator.

$$\hat{\epsilon}^n_j = \epsilon^n_{0;j} + \Sigma_{j'} V^{\rm mono}_{nn}(j, j')\, \hat{n}^n_{j'} + \Sigma_{j'} \tilde{V}^{\rm mono}_{pn}(j', j)\, \hat{n}^p_{j'}$$

A good example is the emergence of new magic numbers N=32 and 34. Neither can be understood within the Major-Jensen scheme.

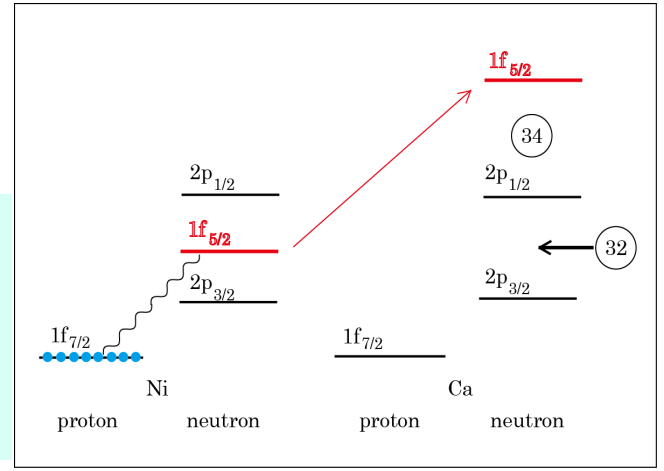

Note for practitioner: monopole matrix elements can be calculated by the formula

$$V_T^{\text{mono}}(j,\ j') = \frac{\sum_J (2J+1)\langle j, j'; J, T|\hat{V}|j, j'; J, T\rangle}{\sum_J (2J+1)} \quad \text{for } T = 0 \text{ and } 1.$$

which is equivalent to what are discussed.

USD interaction

i	j	k	l	J	T	v
1	1	1	1	0	1	-2.1845
1	1	1	1	1	0	-1.4151
1	1	1	1	2	1	-0.0665
1	1	1	1	3	0	-2.8842
2	1	1	1	1	0	0.5647
2	1	1	1	2	1	-0.6149
2	1	1	1	3	0	2.0337
2	1	2	1	1	0	-6.5058
2	1	2	1	1	1	1.0334
2	1	2	1	2	0	-3.8253
2	1	2	1	2	1	-0.3248
2	1	2	1	3	0	-0.5377
2	1	2	1	3	1	0.5894
2	1	2	1	4	0	-4.5062
2	1	2	1	4	1	-1.4497
2	1	3	1	1	0	-1.7080
2	1	3	1	1	1	0.1874
2	1	3	1	2	0	0.2832
2	1	3	1	2	1	-0.5247
2	1	3	3	1	0	2.1042
2	2	1	1	0	1	-3.1856
2	2	1	1	1	0	0.7221
2	2	1	1	2	1	-1.6221
2	2	1	1	3	0	1.8949
2	2	2	1	1	0	2.5435

1 = d3/2

2= d5/2

3= s1/2

T=0 monopole int. between $d_{3/2}$ and $d_{5/2}$

-6.506 x 3 = -19.518

-3.825 x 5 = -19.125

-0.538 x 7 = -3.766

-4.506 x 9 = -40.554

Sum -82.963

Sum of (2J+1) = 24

$= V^{\text{mono}} = -3.457$ (T=0)

Outline

1. Basics of traditional shell model and Monte Carlo Shell Model

2. Shell evolution: from an introduction to the current landscape of magic numbers

3. Type-II Shell evolution: shape coexistence (parabola or linear or …)

4. Ellipsoidal nuclear shapes: Aage Bohr vs. Davydov

5. Shapes and driplines: who limits isotopes

6. α-clustering and nuclear matter: who likes α-cluster

The (total) monopole interaction becomes,

$$\hat{V}^{\mathrm{mono}} = \hat{V}^{\mathrm{mono}}_{pp} + \hat{V}^{\mathrm{mono}}_{nn} + \hat{V}^{\mathrm{mono}}_{pn}$$

The monopole Hamiltonian is given as,

$$\hat{H}^{\mathrm{mono}} = \hat{H}_0 + \hat{V}^{\mathrm{mono}} = \Sigma_j \, \epsilon^{p}_{0;j} \, \hat{n}^{p}_{j} + \Sigma_j \, \epsilon^{n}_{0;j} \, \hat{n}^{n}_{j} + \hat{V}^{\mathrm{mono}}$$

The multipole term is defined

$$\hat{V}^{\mathrm{multi}} = \hat{V} - \hat{V}^{\mathrm{mono}}$$

The monopole and multipole terms contribute in very different ways to nuclear structure, and **their interplay** produces a variety of exciting physics.

The linear dependence of ESPE is unique: the effect grows all the way

- schematic pictures -

effective single-particle energy

due to monopole interaction

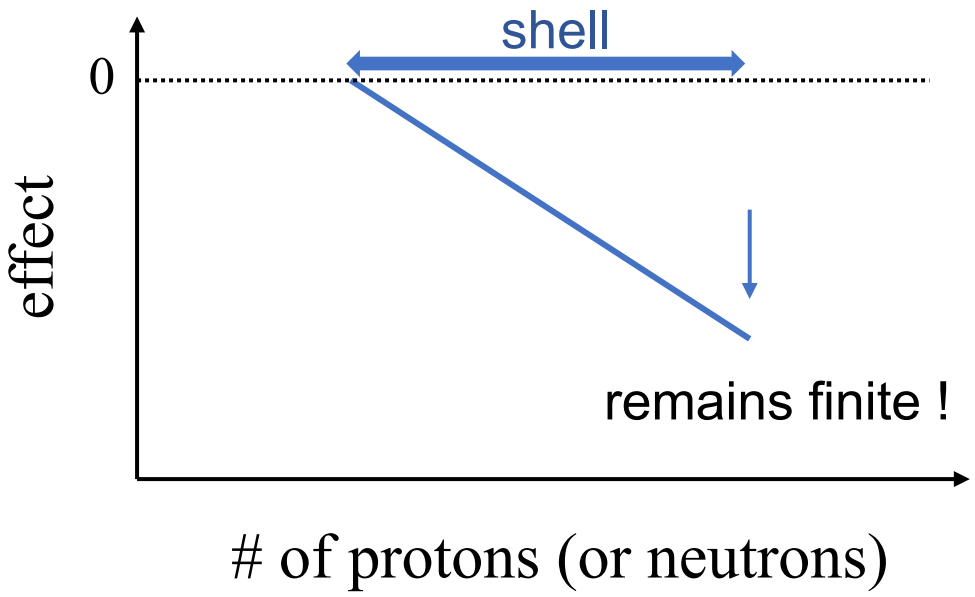

effect of a multipole interaction

example: deformation energy

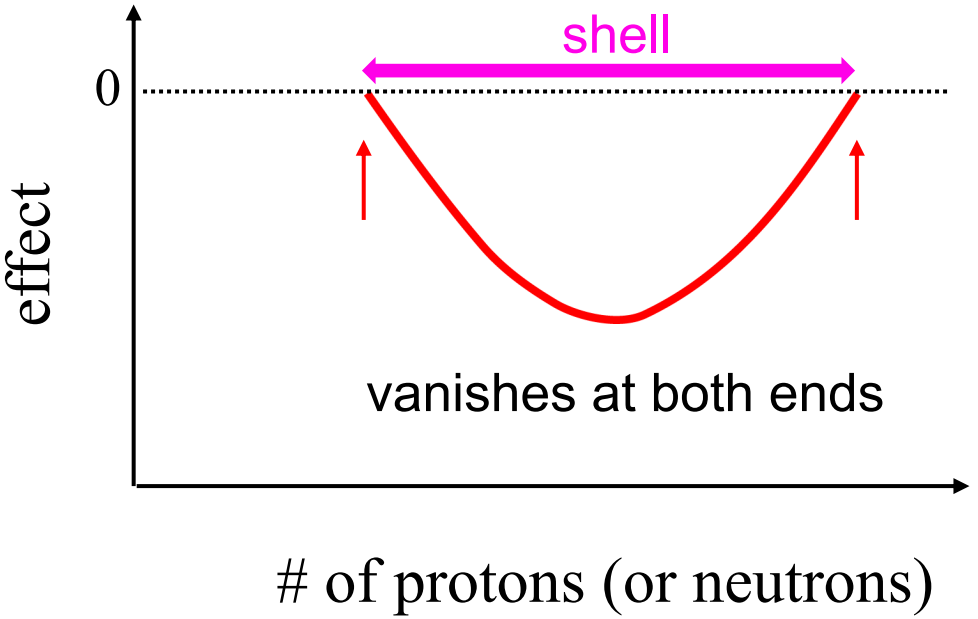

$$\hat{\epsilon}^n_j = \epsilon^n_{0;j} + \Sigma_{j'} V^{\mathrm{mono}}_{nn}(j, j')\, \hat{n}^n_{j'} + \Sigma_{j'} \tilde{V}^{\mathrm{mono}}_{pn}(j', j)\, \hat{n}^p_{j'}$$

$< \text{proton-neutron} \quad \hat{V}^{\mathrm{multi}} >$

Shape coexistence

Traditional view of "quadratic dependence" of excitation energies of deformed bands

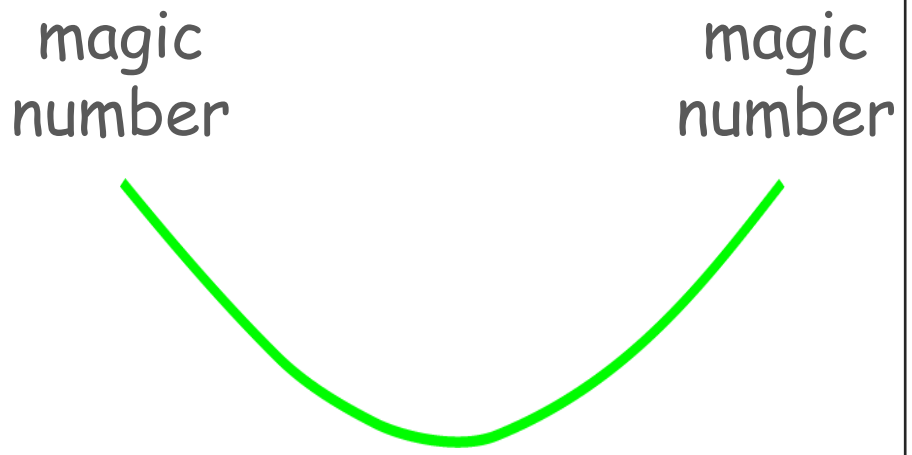

neutron number, N

Fig. 10 of Heyde & Wood, RMP 83, 1467 (2011)

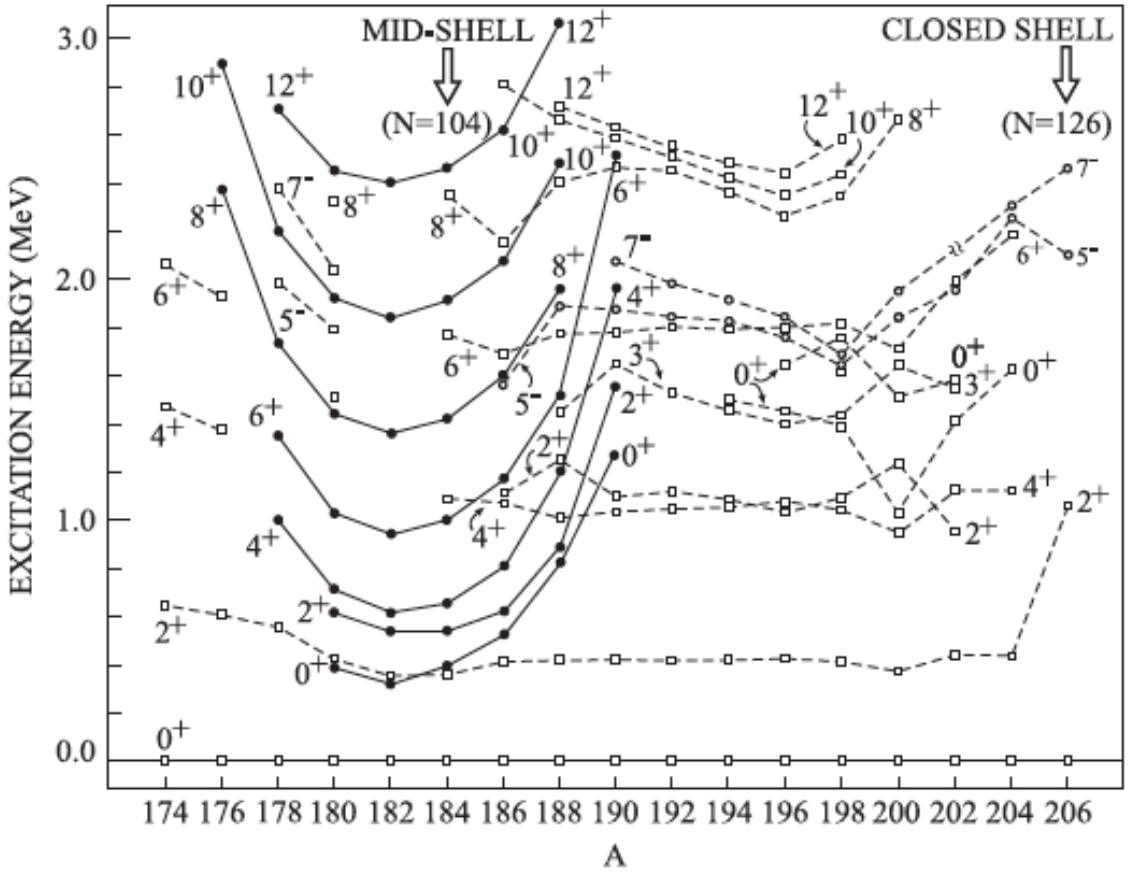

FIG. 10. Systematics of excited states in the even-Hg isotopes. Note the "parabolic intrusion" of the closely spaced bands of states (marked with solid lines) with $J = 0, 2, 4, \ldots$ centered on ^{182}Hg ($N = 102$). The data are taken from Nuclear Data Sheets. Some recent lifetime data can be found in Grahn *et al.* (2009).

Energy levels and B(E2) values of Ni isotopes

Description by the A3DA-m Hamiltonian

× exp.
— calc.

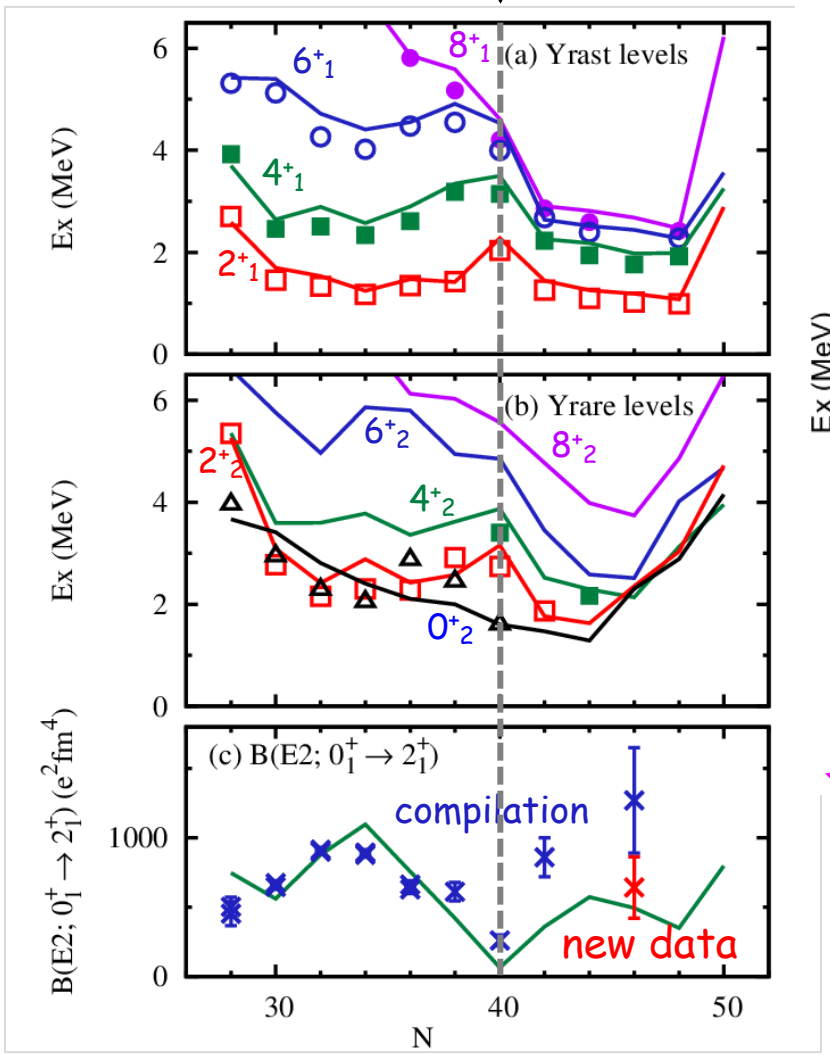

Shape coexistence in ^{68}Ni

^{68}Ni

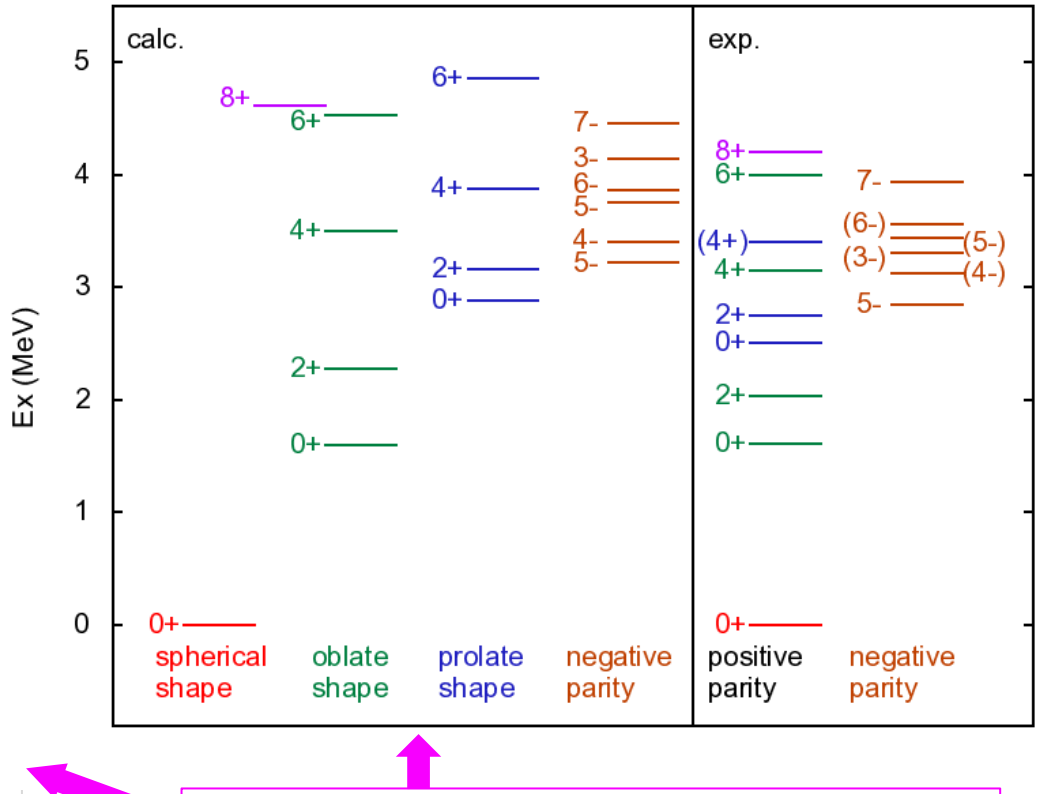

Calc. : Monte Carlo Shell Model

Figures:
Y. Tsunoda, TO, Shimizu, Honma and Utsuno,
PRC 89, 031301 (R) (2014)

Occupation numbers

0^+_3 state
(prolate)

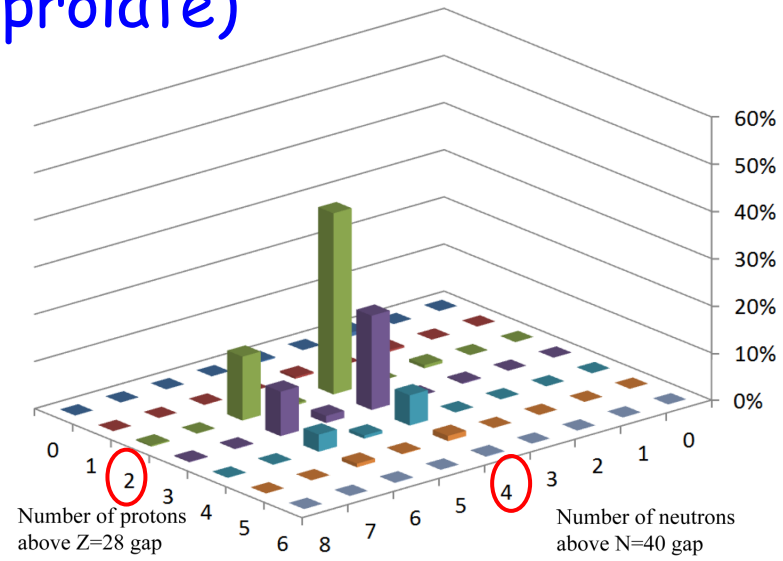

6p6h+ excitations

0^+_2 state
(oblate)

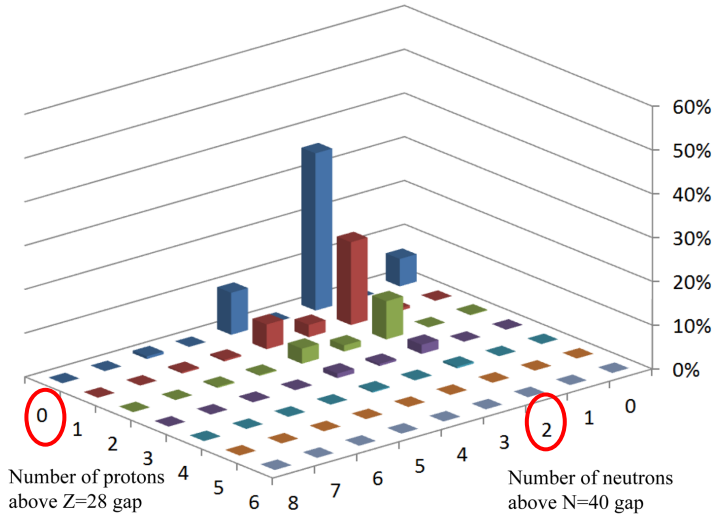

2p2h+ excitations

sudden jump

ground state
(spherical
-> closed shell)

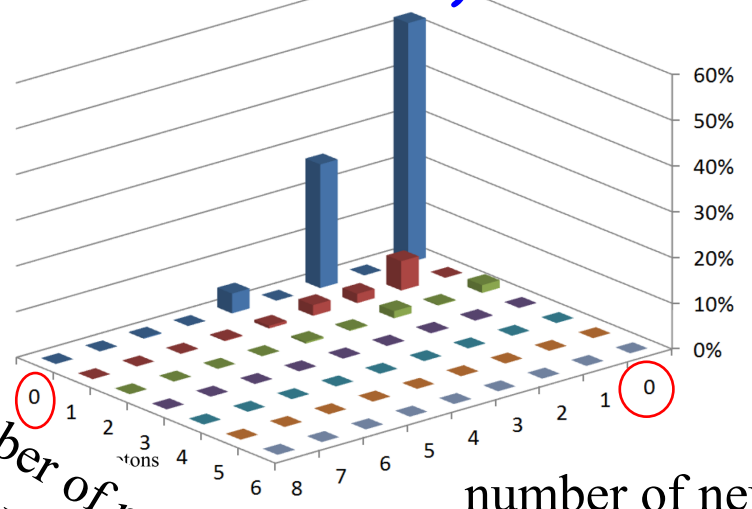

0p0h with 25% mixture of 2p2h excitation over N=40 gap

Potential energy surface (PES)

Constrained Hartree-Fock calculation for the shell-model Hamiltonian with constraints by β_2 and γ.

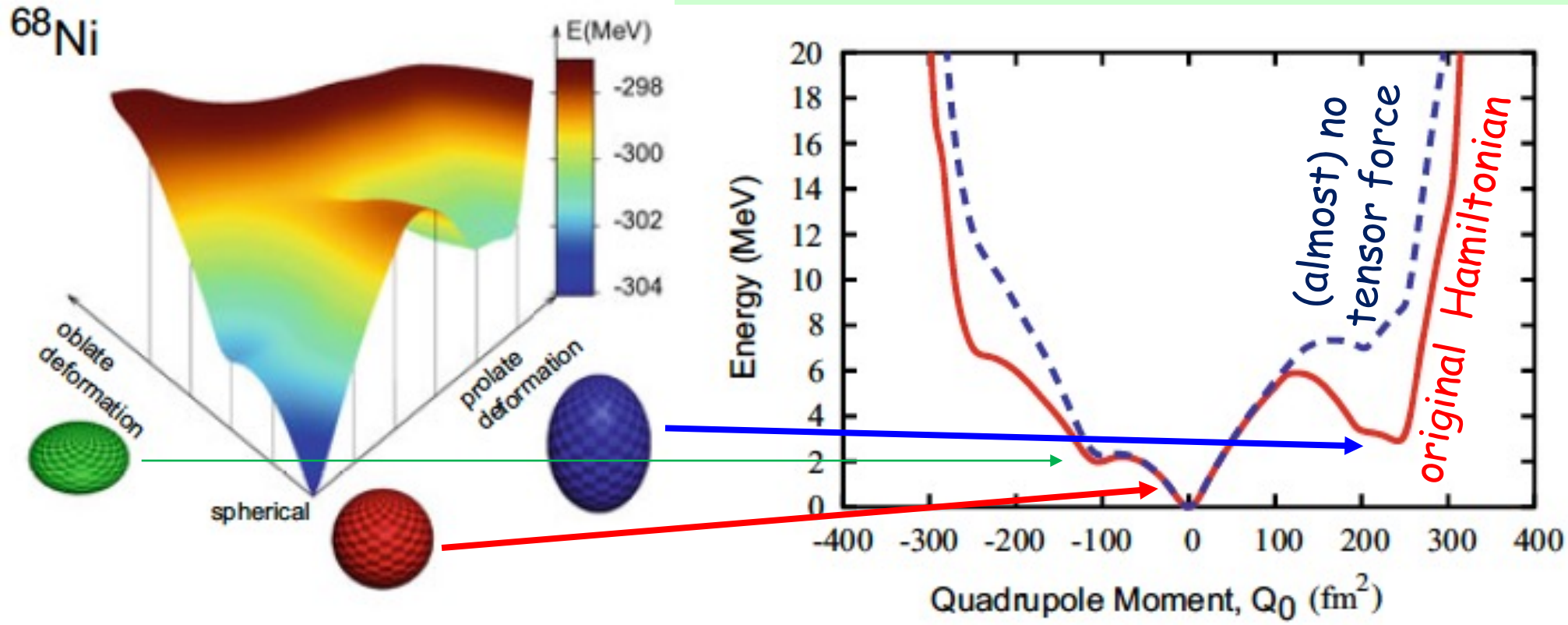

Fig. 17 (left) Potential energy surface (PES) of ^{68}Ni. (Taken from Fig. 5 of Otsuka and Tsunoda 2016). (right) PES of ^{68}Ni for axially symmetric shapes. The solid line shows the PES of the full Hamiltonian, whereas the dashed line is the PES with practically no tensor force contribution. (Taken from Fig. 6 of Otsuka and Tsunoda 2016)

Key concept is the deformation from spherical shape to ellipsoidal shape

Ellipsoid of classical uniform object

triaxial prolate

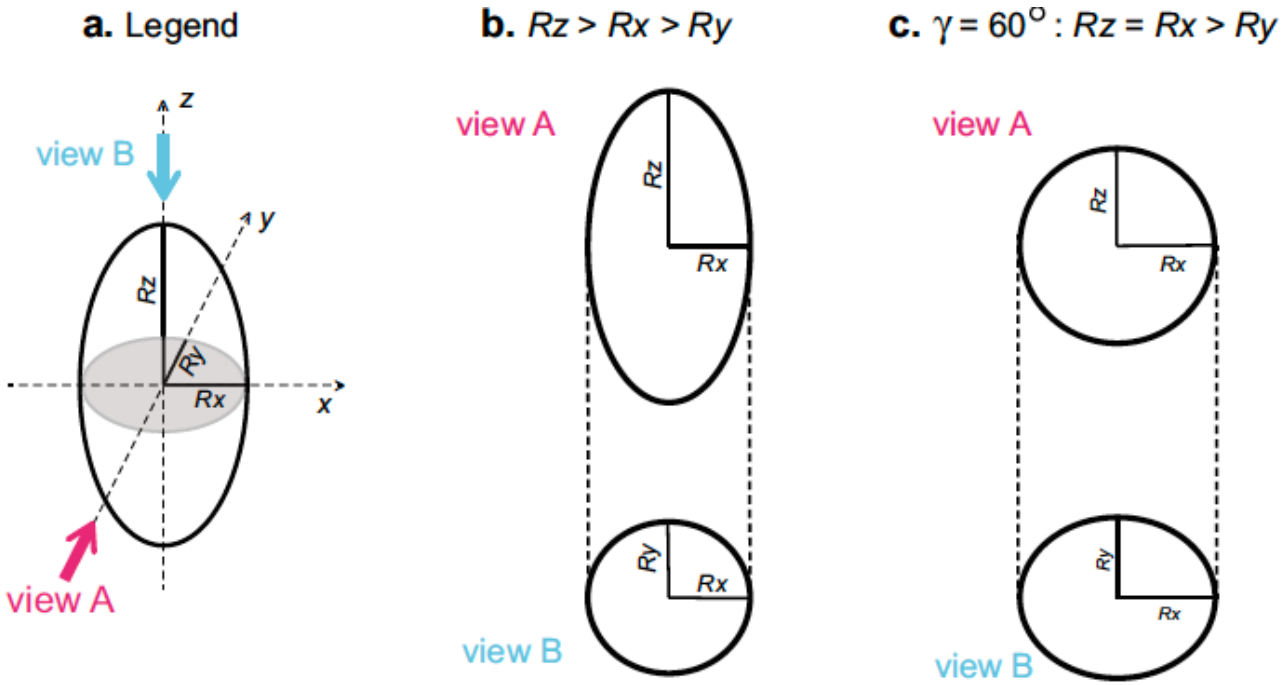

$$R_z = \{1 + 0.63\,\beta_2 \cos\gamma\}\, R_0,$$

$$R_x = \{1 + 0.63\,\beta_2 \sin(\gamma - 30^\circ)\}\, R_0,$$

$$R_y = \{1 - 0.63\,\beta_2 \cos(60^\circ - \gamma)\}\, R_0,$$

Nuclear quantum states:

$$Q_0 = \langle\eta| \sum_i (2z^2 - x^2 - y^2)_i \,|\eta\rangle$$

$$Q_2 = \sqrt{3/2}\,\langle\eta| \sum_i (x^2 - y^2)_i \,|\eta\rangle$$

quantum Q_0 and Q_2

⇕

classical Q_0 and Q_2

⇕

R_x , R_y , R_z

deformation parameters β_2 and γ

$0 <= \gamma <= 60$ deg

Bohr-model calc. by HFB with **Gogny** force, Girod, Dessagne, Bernes, Langevin, Pougheon and Roussel, PRC 37,2600 (1988)

Present with full monopole effects

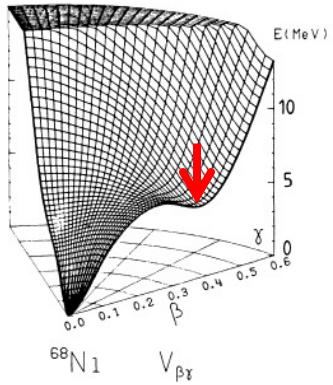

^{68}Ni $V_{\beta\gamma}$

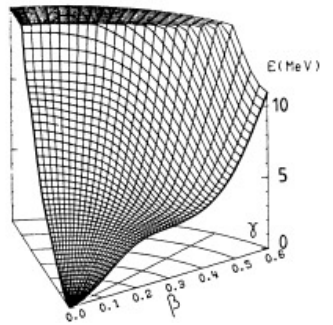

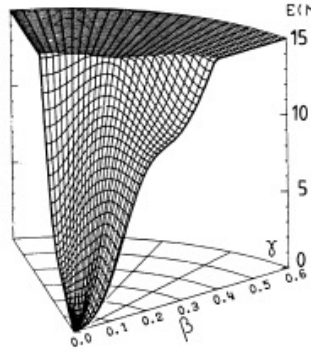

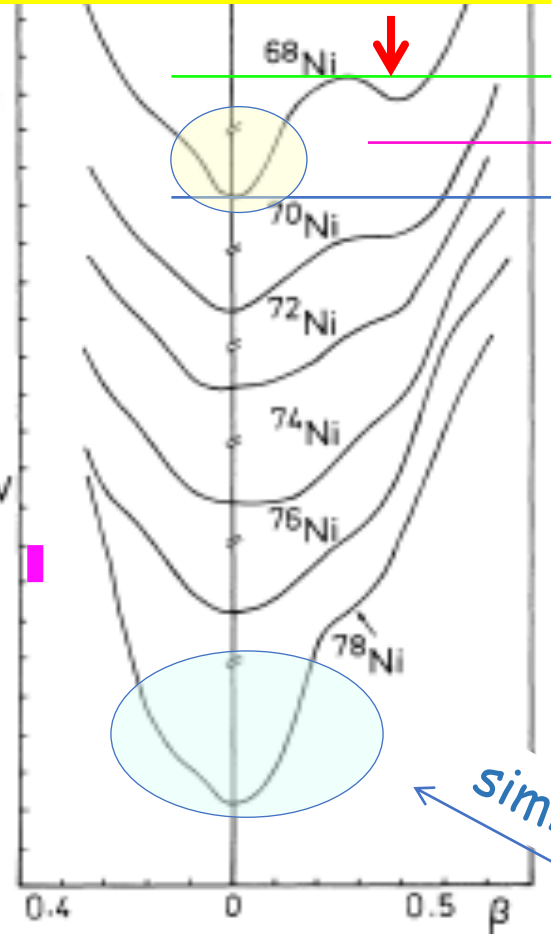

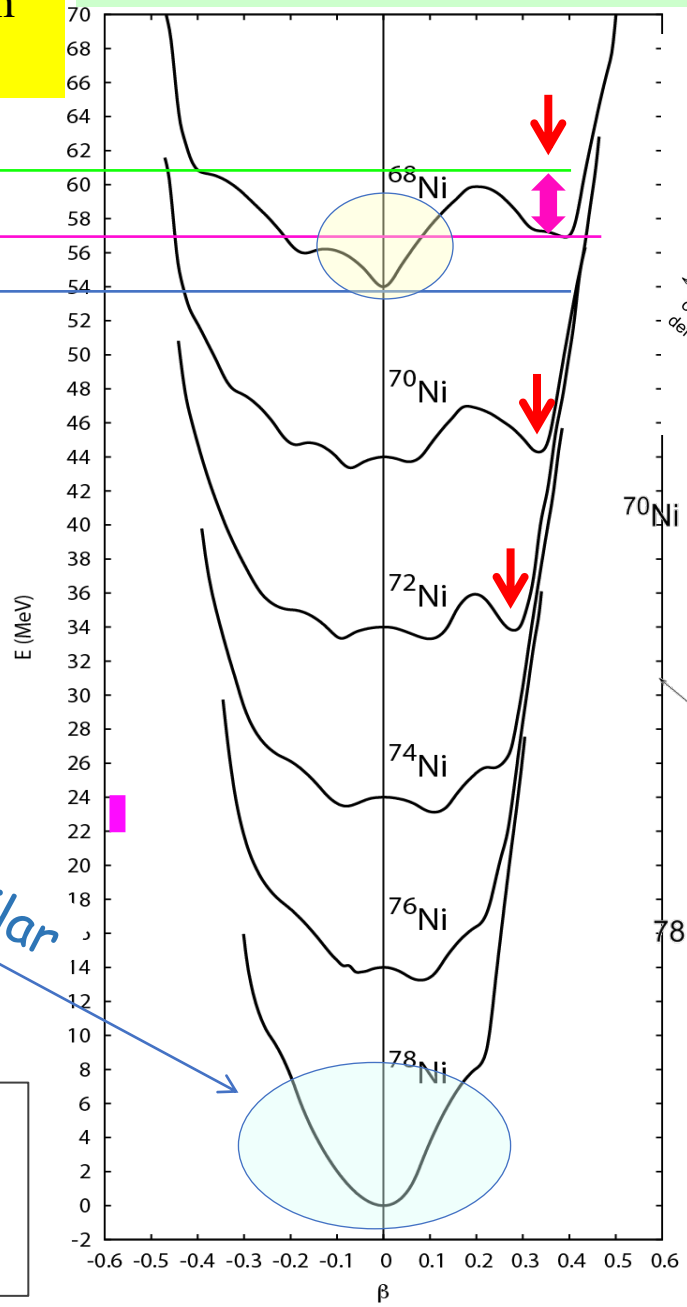

similar

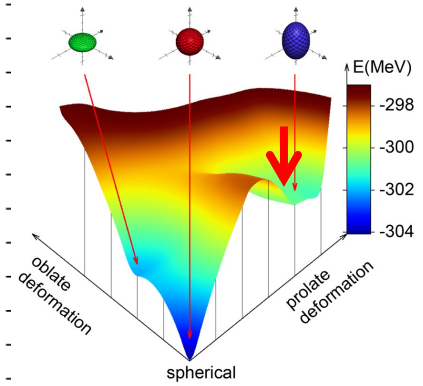

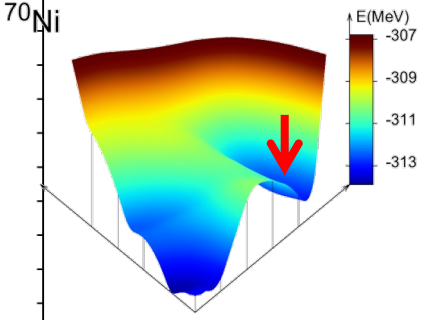

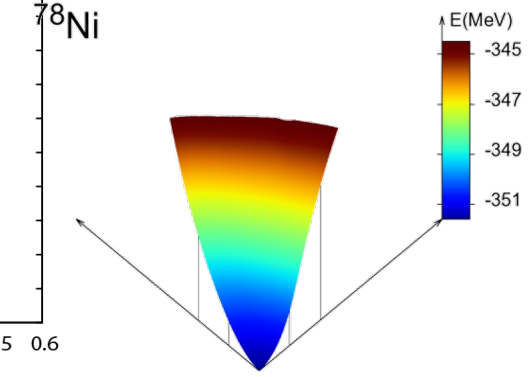

The same scale of energy between two figures.

Extended Shell Evolution due to the tensor force

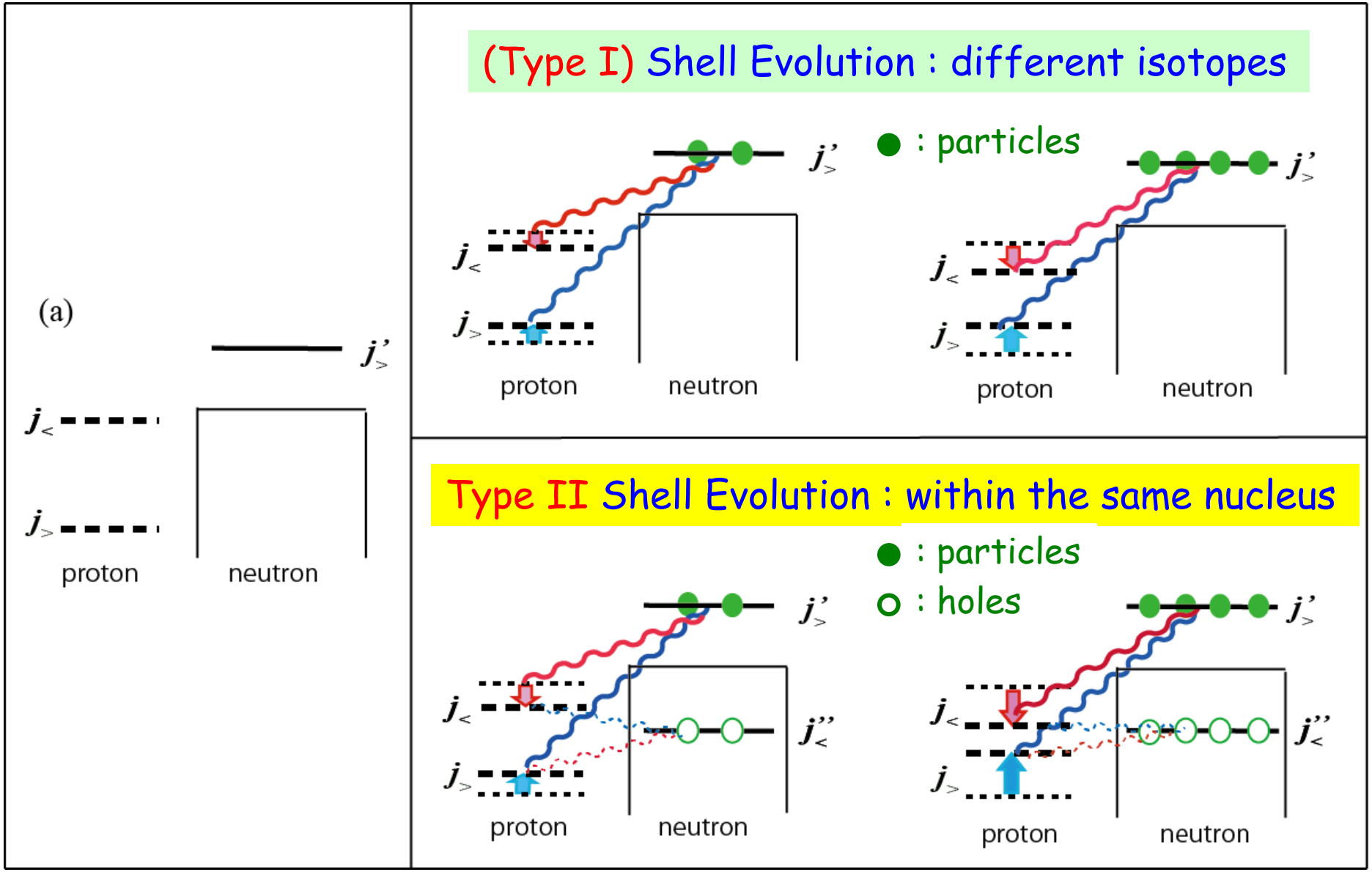

TO and Y. Tsunoda, J. Phys. G: Nucl. Part. Phys. 43 (2016) 024009

Another advantage: Identification of nuclear shape by T-plot of MCSM

- Location of circle: shape
  quadrupole deformation of unprojected MCSM basis vector
- Area of circle: importance
  overlap probability between each projected basis vector and eigen wave function
- Potential energy surface (PES) is calculated by Constrained HF for the same interaction

T-plot of 0^+ states of ^{78}Ni (Z=28, N=50)

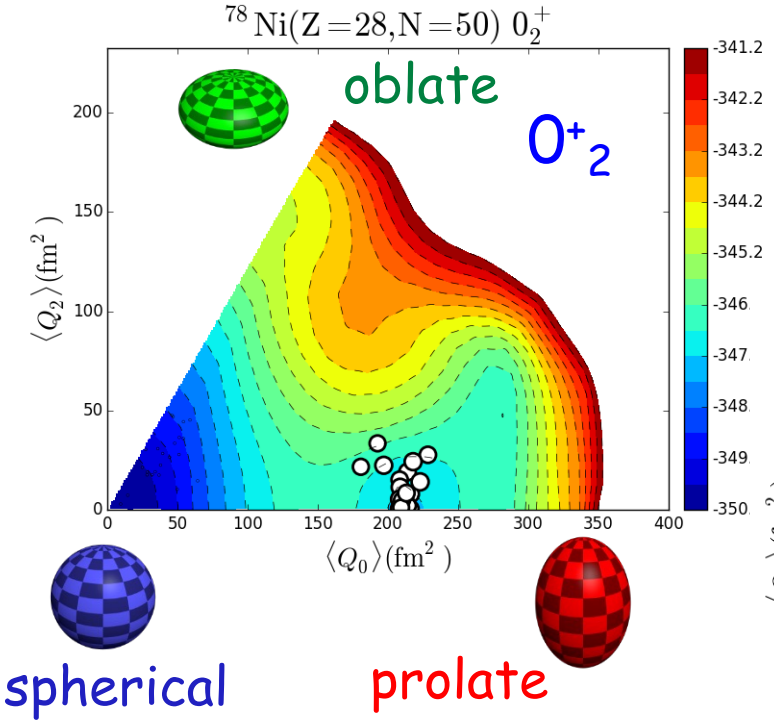

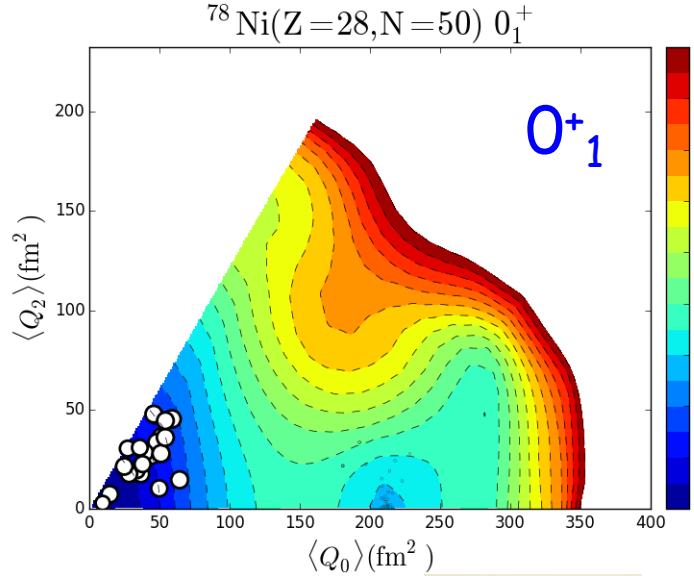

Angular-momentum, parity projection

Slater determinant

$$|\Psi\rangle = \sum_n f_n P^{J\pi} |\psi_n\rangle$$

MCSM eigen wave function

MCSM basis vector

Y. Tsunoda, *et al.*
PRC 89, 031301 (R) (2014)

Evolution of shapes in Ni isotopes

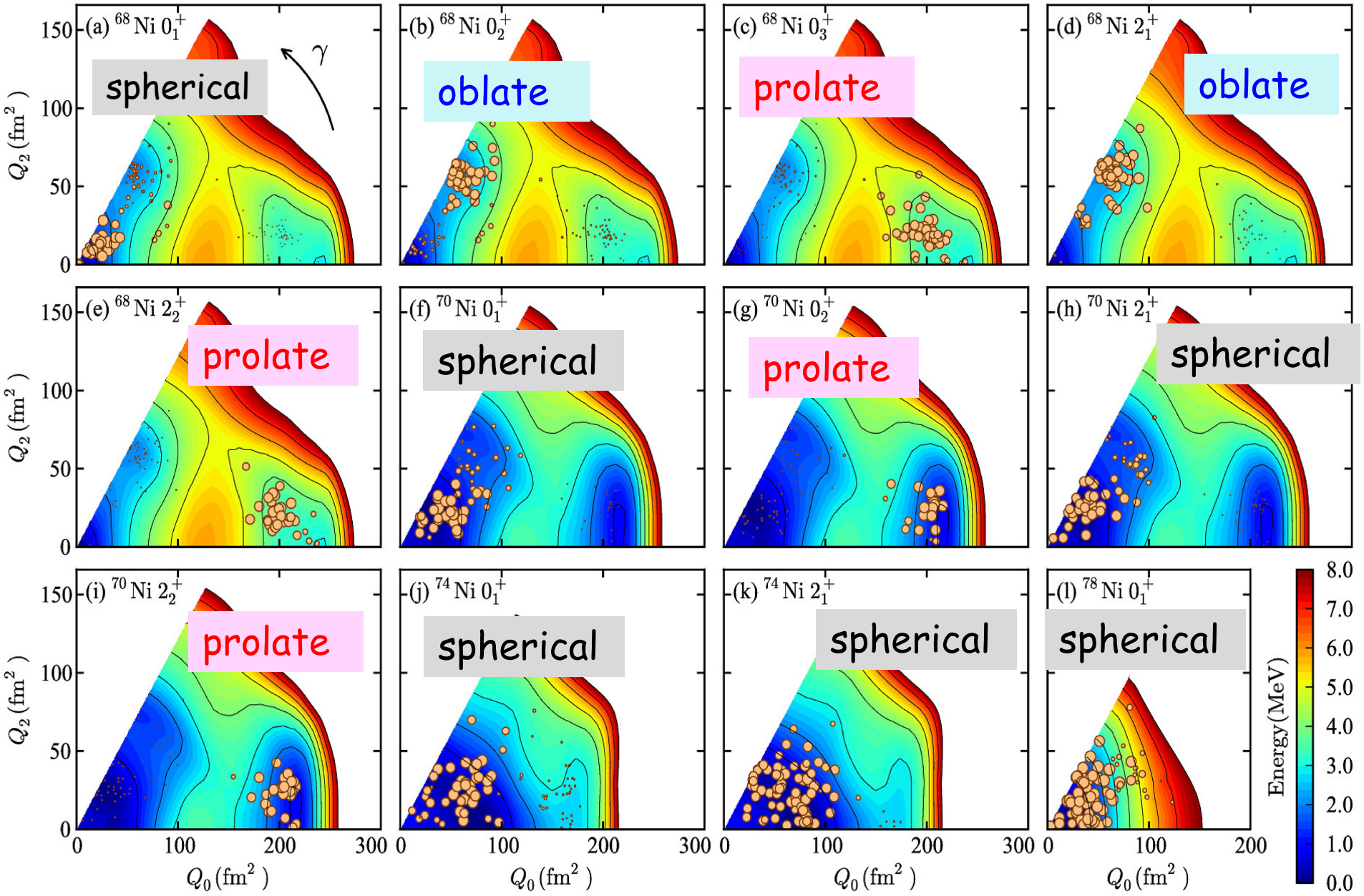

Shape coexistence with a lowest excitation energy

Physics Letters B 765 (2017) 328–333

Type II shell evolution in $A = 70$ isobars from the $N \geq 40$ island of inversion

A.I. Morales [a,b,*], G. Benzoni [a], H. Watanabe [c,d], Y. Tsunoda [e], T. Otsuka [f,g,h], S. Nishimura [d], F. Browne [i,d], R. Daido [j], P. Doornenbal [d], Y. Fang [j], G. Lorusso [d], Z. Patel [k,d], S. Rice [k,d], L. Sinclair [l,d], P.-A. Söderström [d], T. Sumikama [m], J. Wu [d], Z.Y. Xu [f,d], A. Yagi [j], R. Yokoyama [f], H. Baba [d], R. Avigo [a,b], F.L. Bello Garrote [n], N. Blasi [a], A. Bracco [a,b], F. Camera [a,b], S. Ceruti [a,b], F.C.L. Crespi [a,b], G. de Angelis [o], M.-C. Delattre [p], Zs. Dombradi [q], A. Gottardo [o], T. Isobe [d], I. Kojouharov [r], N. Kurz [r], I. Kuti [q], K. Matsui [f], B. Melon [s], D. Mengoni [t,u], T. Miyazaki [f], V. Modamio-Hoybjor [o], S. Momiyama [f], D.R. Napoli [o], M. Niikura [f], R. Orlandi [h,v], H. Sakurai [d,f], E. Sahin [n], D. Sohler [q], H. Schaffner [r], R. Taniuchi [f], J. Taprogge [w,x], Zs. Vajta [q], J.J. Valiente-Dobón [o], O. Wieland [a], M. Yalcinkaya [y]

[a] Istituto Nazionale di Fisica Nucleare, Sezione di Milano, Via Celoria 16, 20133 Milano, Italy
[b] Dipartimento di Fisica, Università degli Studi di Milano, Via Celoria 16, 20133 Milano, Italy

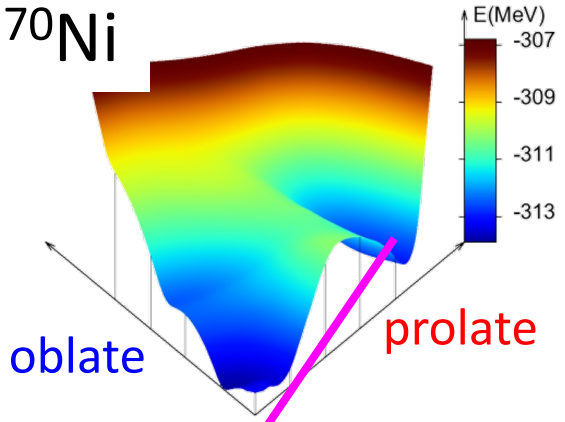

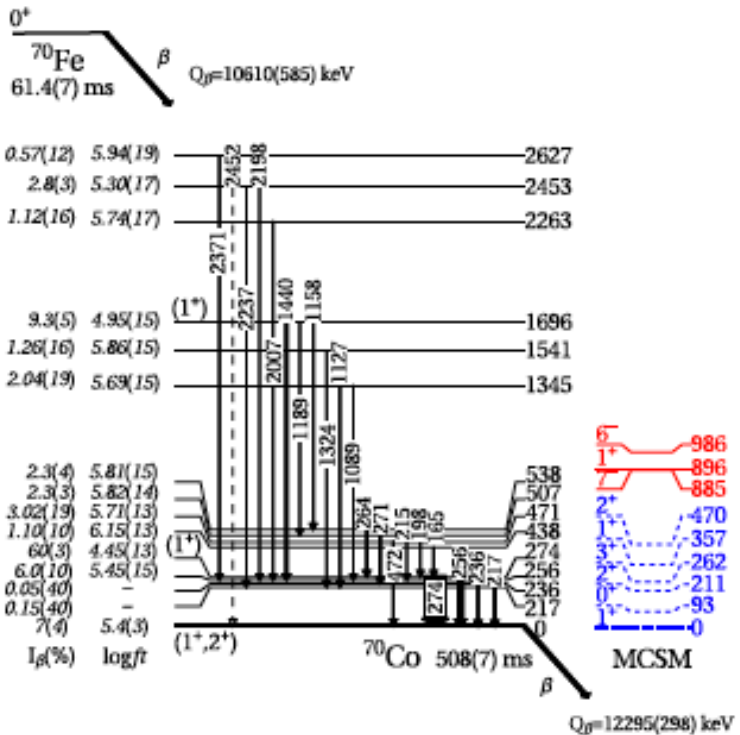

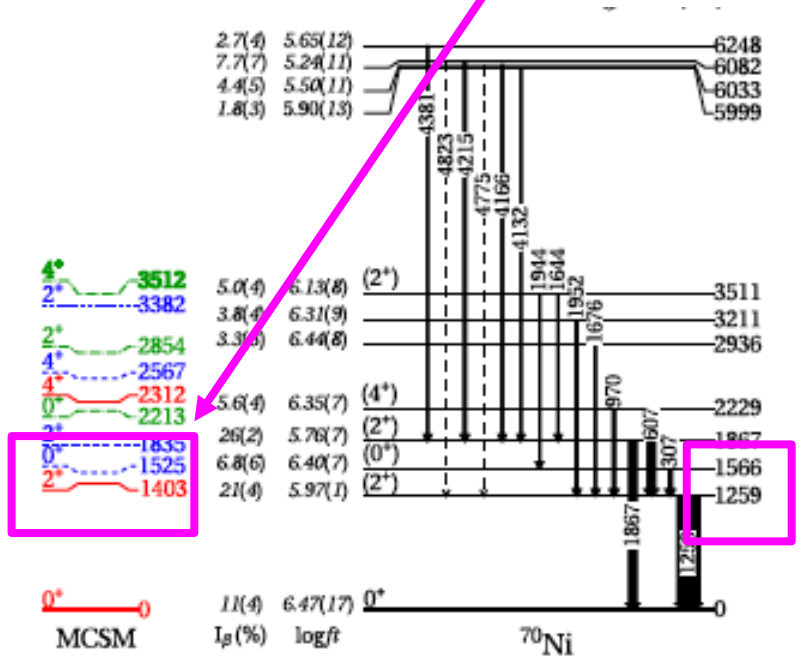

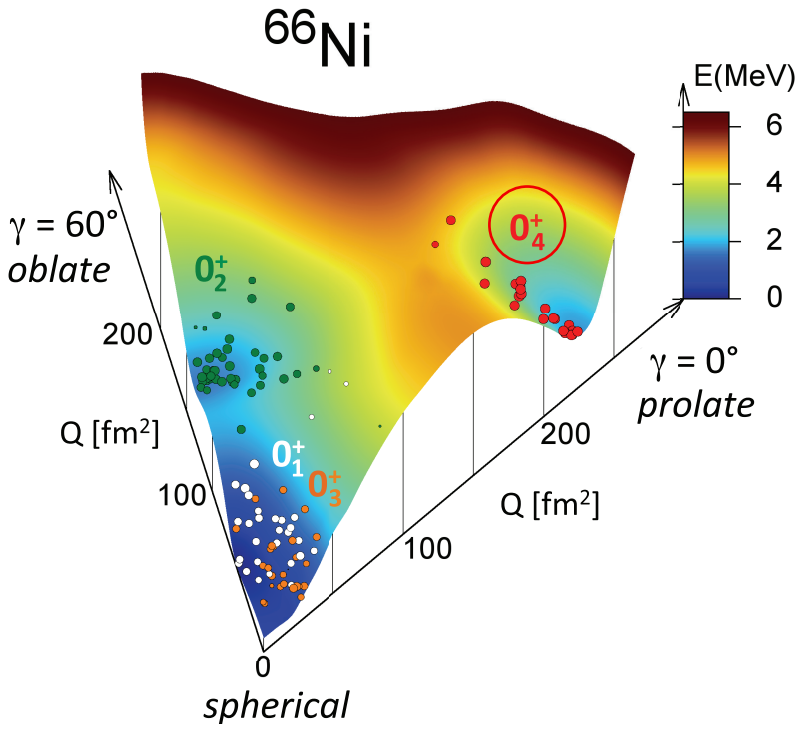

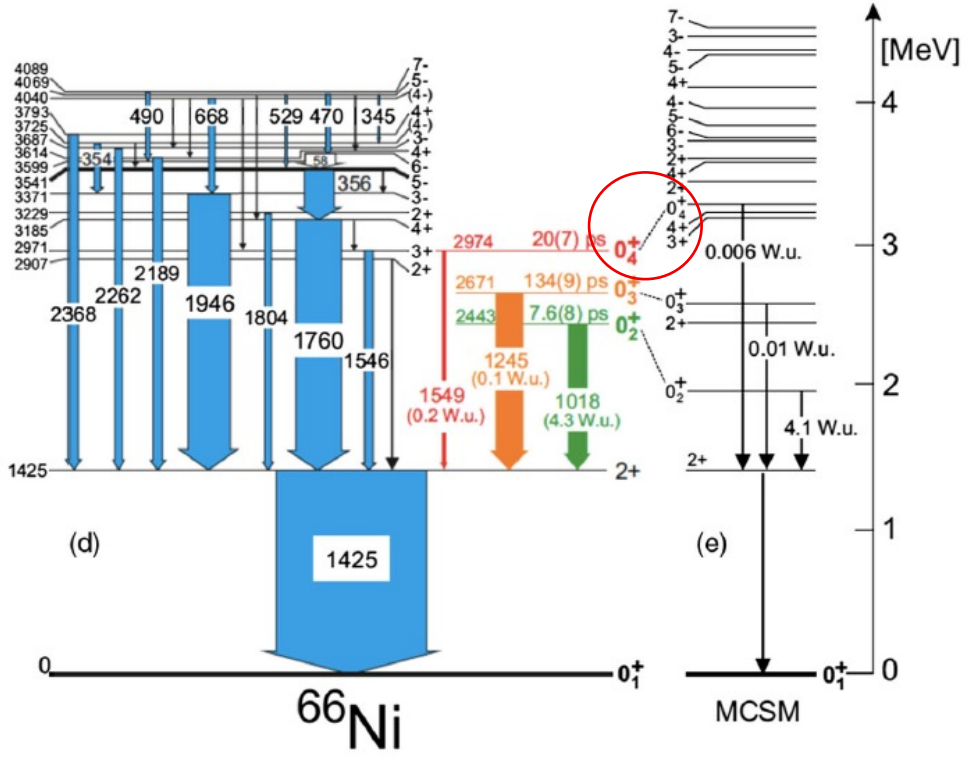

PRL 118, 162502 (2017) PHYSICAL REVIEW LETTERS week ending 21 APRIL 2017

Multifaceted Quadruplet of Low-Lying Spin-Zero States in ^{66}Ni: Emergence of Shape Isomerism in Light Nuclei

S. Leoni,[1,2,*] B. Fornal,[3] N. Mărginean,[4] M. Sferrazza,[5] Y. Tsunoda,[6] T. Otsuka,[6,7,8,9] G. Bocchi,[1,2] F. C. L. Crespi,[1,2] A. Bracco,[1,2] S. Aydin,[10] M. Boromiza,[4,11] D. Bucurescu,[4] N. Cieplicka-Oryńczak,[2,3] C. Costache,[4] S. Călinescu,[4] N. Florea,[4] D. G. Ghiţă,[4] T. Glodariu,[4] A. Ionescu,[4,11] Ł.W. Iskra,[3] M. Krzysiek,[3] R. Mărginean,[4] C. Mihai,[4] R. E. Mihai,[4] A. Mitu,[4] A. Negreţ,[4] C. R. Niţă,[4] A. Olăcel,[4] A. Oprea,[4] S. Pascu,[4] P. Petkov,[4] C. Petrone,[4] G. Porzio,[1,2] A. Şerban,[4,11] C. Sotty,[4] L. Stan,[4] I. Ştiru,[4] L. Stroe,[4] R. Şuvăilă,[4] S. Toma,[4] A. Turturică,[4] S. Ujeniuc,[4] and C. A. Ur[12]

^{64}Ni

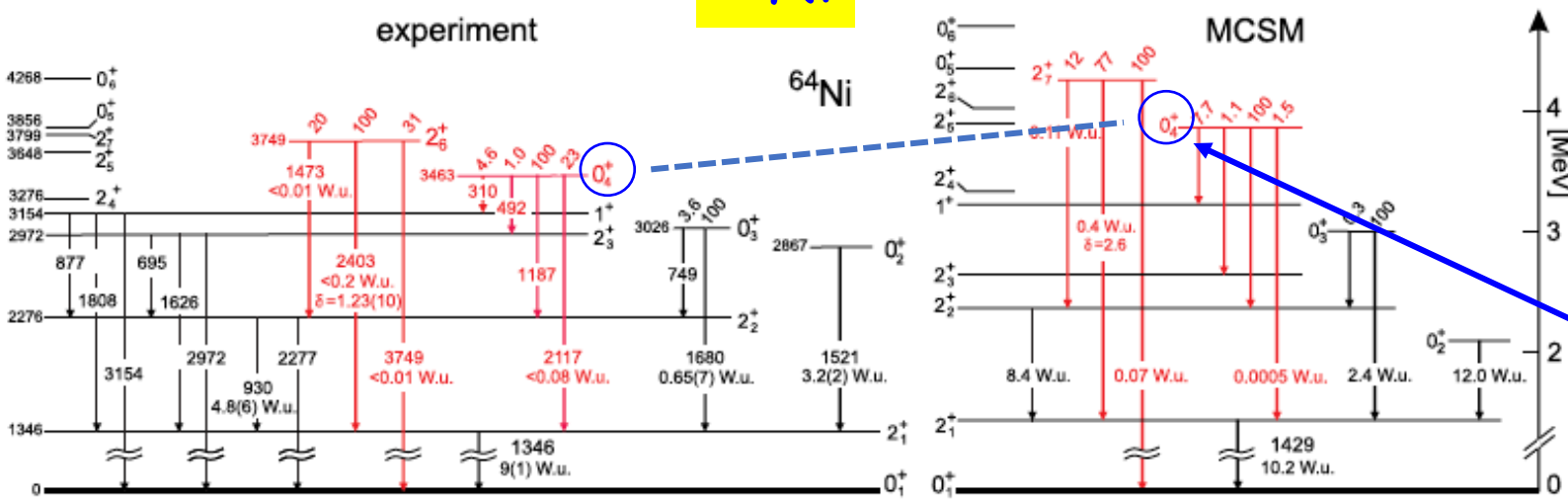

Lowering by the tensor force reduced only to 0.5+ MeV

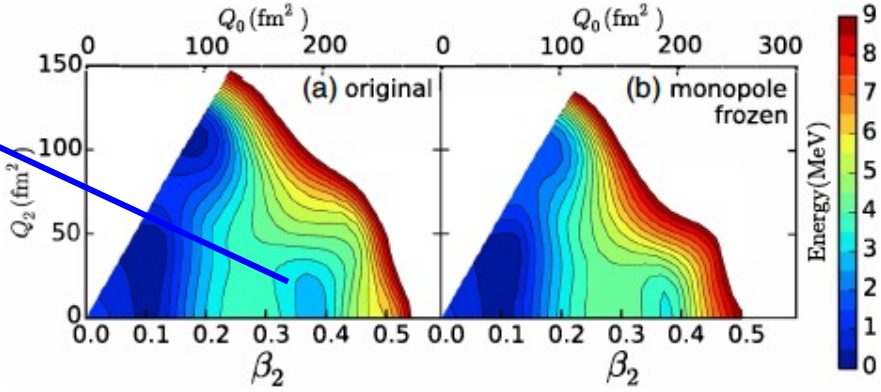

PHYSICAL REVIEW LETTERS 125, 102502 (2020)

Shape Coexistence at Zero Spin in ^{64}Ni Driven by the Monopole Tensor Interaction

N. Mărginean,[1,*] D. Little,[2,3] Y. Tsunoda,[4] S. Leoni,[5,6,†] R. V. F. Janssens,[2,3,‡] B. Fornal,[7,§] T. Otsuka,[8,9,10,‖] C. Michelagnoli,[11] L. Stan,[1] F. C. L. Crespi,[5,6] C. Costache,[1] R. Lica,[1] M. Sferrazza,[12] A. Turturica,[1] A. D. Ayangeakaa,[13] K. Auranen,[14,¶] M. Barani,[5,6,11] P. C. Bender,[15] S. Bottoni,[5,6] M. Boromiza,[1] A. Bracco,[5,6] S. Călinescu,[1] C. M. Campbell,[16] M. P. Carpenter,[14] P. Chowdhury,[15] M. Ciemała,[7] N. Cieplicka-Oryńczak,[7] D. Cline,[17] C. Clisu,[1] H. L. Crawford,[16] I. E. Dinescu,[1] J. Dudouet,[18] D. Filipescu,[1] N. Florea,[1] A. M. Forney,[19] S. Fracassetti,[5,6,**] A. Gade,[20,21] I. Gheorghe,[1] A. B. Hayes,[22] I. Harca,[1] J. Henderson,[23] A. Ionescu,[1] Ł. W. Iskra,[6] M. Jentschel,[11] F. Kandzia,[11] Y. H. Kim,[11] F. G. Kondev,[14] G. Korschinek,[24] U. Köster,[11] Krishichayan,[3] M. Krzysiek,[7] T. Lauritsen,[14] J. Li,[14,††] R. Mărginean,[1] E. A. Maugeri,[25] C. Mihai,[1] R. E. Mihai,[1] A. Mitu,[1] P. Mutti,[11] A. Negret,[1] C. R. Niţă,[1] A. Olăcel,[1] A. Oprea,[1] S. Pascu,[1] C. Petrone,[1] C. Porzio,[5,6] D. Rhodes,[20,21] D. Seweryniak,[14] D. Schumann,[25] C. Sotty,[1] S. M. Stolze,[14] R. Şuvăilă,[1] S. Toma,[1] S. Ujeniuc,[1] W. B. Walters,[19] C. Y. Wu,[23] J. Wu,[14] S. Zhu,[22] and S. Ziliani[5,6]

[1]*Horia Hulubei National Institute of Physics and Nuclear Engineering—IFIN HH, Bucharest 077125, Romania*

If not,
parabolic behavior arises

Traditional view of
"quadratic dependence"
of excitation energies
of deformed bands

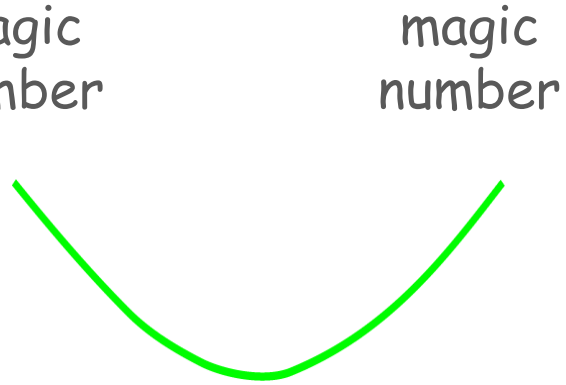

neutron number, N

Ni isotopes

type II shell evolution
occurs more strongly

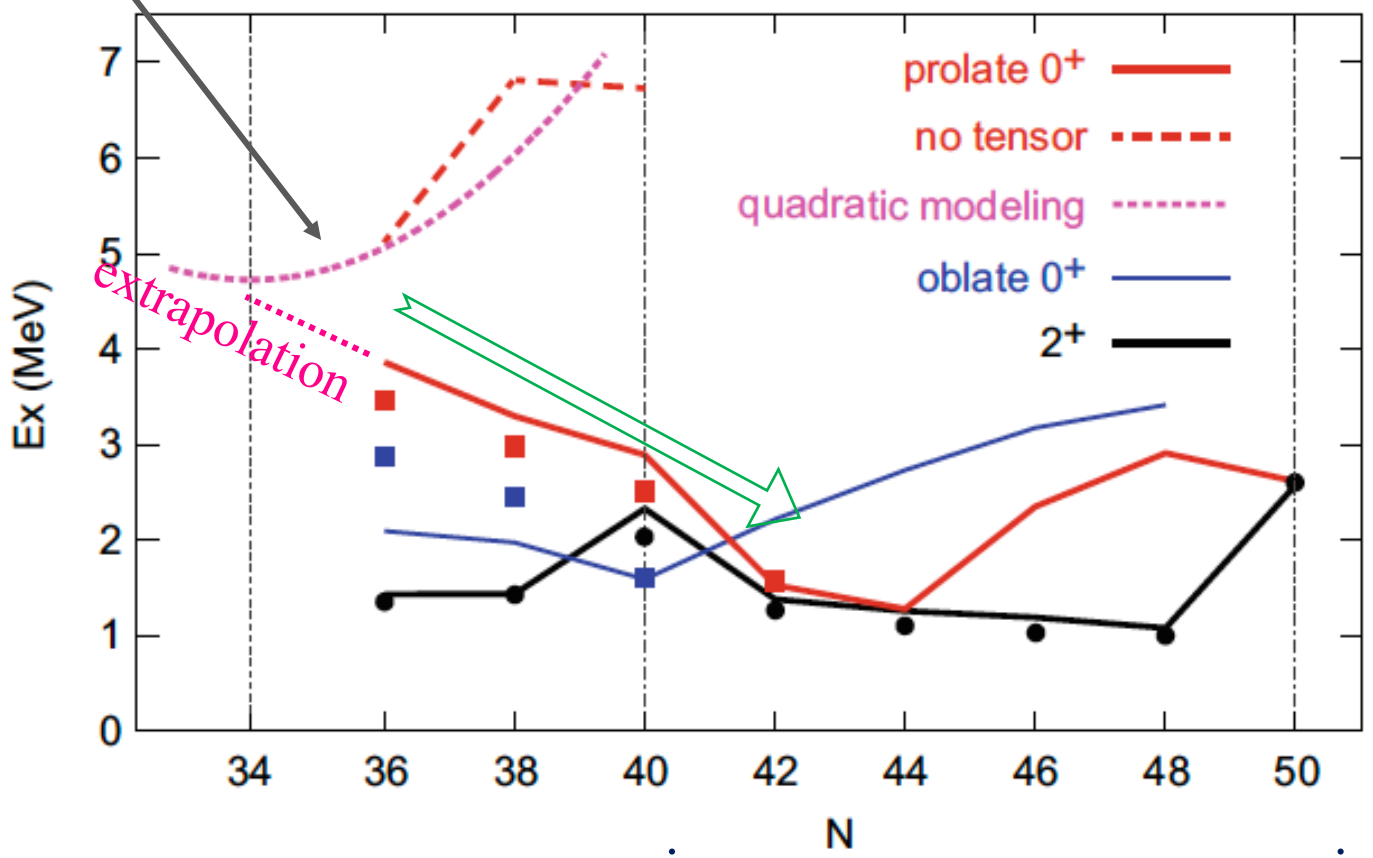

magic
number

magic
number

Outline

1. Basics of traditional shell model and Monte Carlo Shell Model
2. Shell evolution: from an introduction to the current landscape of magic numbers
3. Type-II Shell evolution: shape coexistence (parabola or linear or …)
4. Ellipsoidal nuclear shapes: Aage Bohr vs. Davydov
5. Shapes and driplines: who limits isotopes
6. α-clustering and nuclear matter: who likes α-cluster

Observed excitation energies of the first excited 2^+ states of even-even nuclei

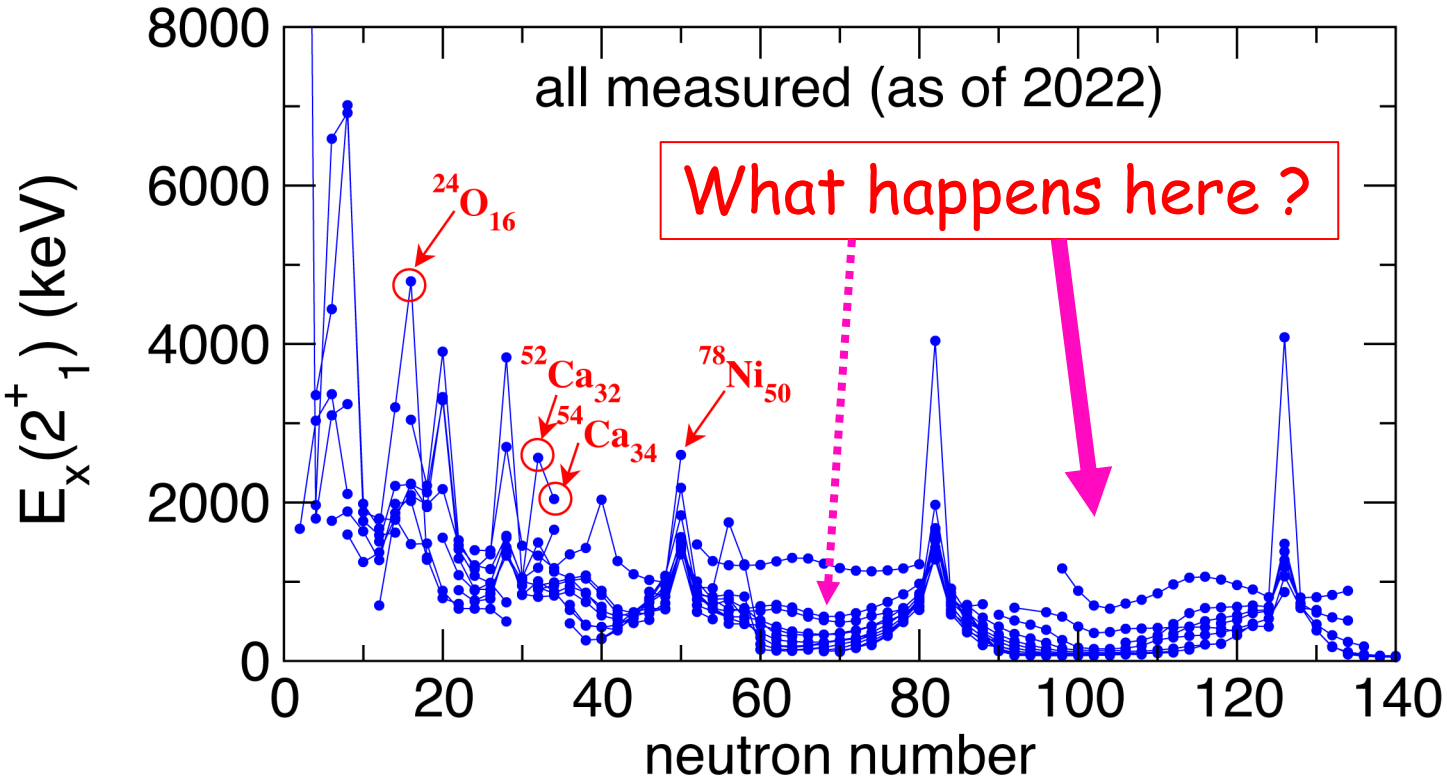

What happens in heavy deformed nuclei, where the structure is not of single-particle nature, but is dominated by strong ellipsoidal deformation.

Why is the deformation a "must" in (most of) nuclei ?

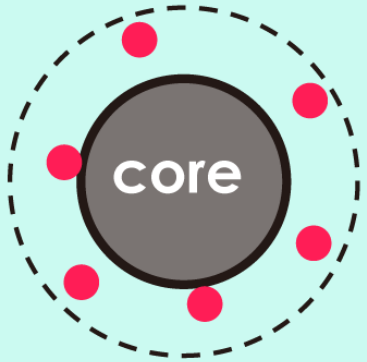

valence nucleons are sparsely
configured because of the shell structure

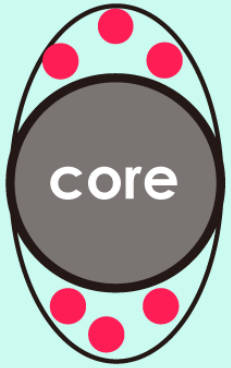

short-range
attractive
nuclear force
between
nucleons
produces more
binding energy

range of nuclear forces

<<

size of single-particle orbital
(the bigger the heavier)

Molecular and nuclear rotations

a. O_2 molecule

b. H_2O molecule

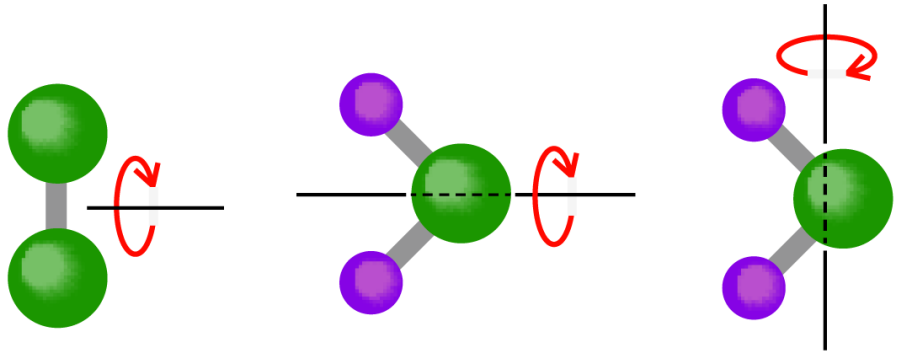

c. nucleus (prolate)

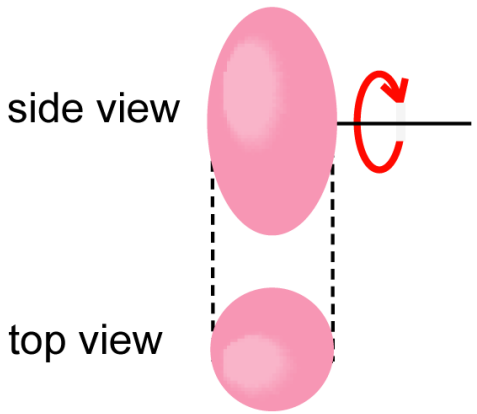

d. nucleus (triaxial)

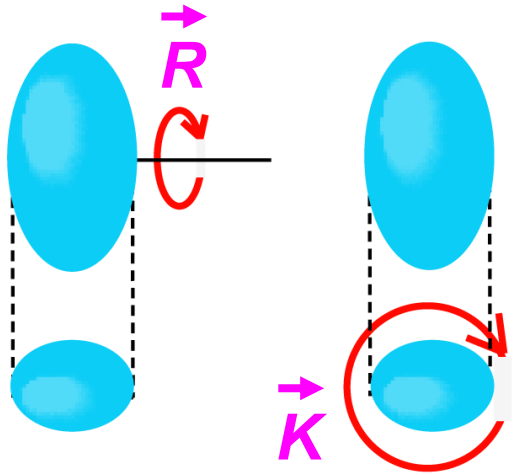

e. Legend

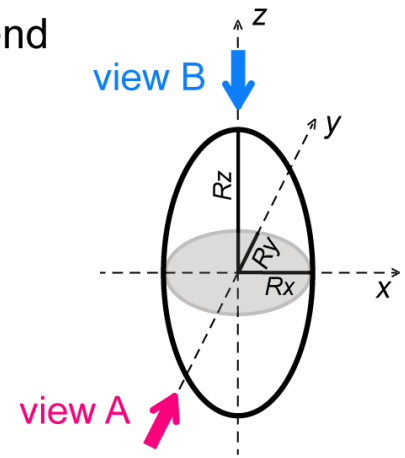

f. $Rz > Rx = Ry$
prolate

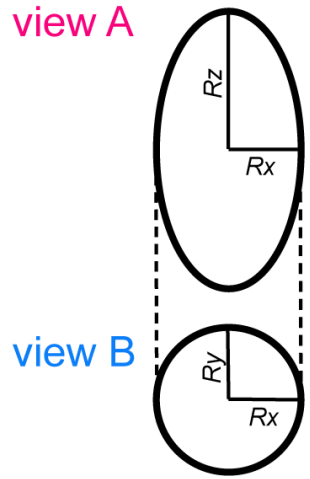

g. $Rz > Rx > Ry$
triaxial

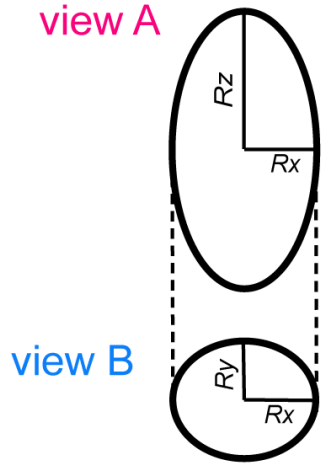

$\vec{J} = \vec{R} + \vec{K}$

caution: $\vec{R}$ and $\vec{K}$ are not independent

Multi-axis rotation is always fun !

Ayumu Hirano,
Gold medalist, 2022 Olympics

from NHK

Aage Bohr Novel Prize Lecture (1975)

Aage N. Bohr, 1922-2009
Nobel Foundation archive

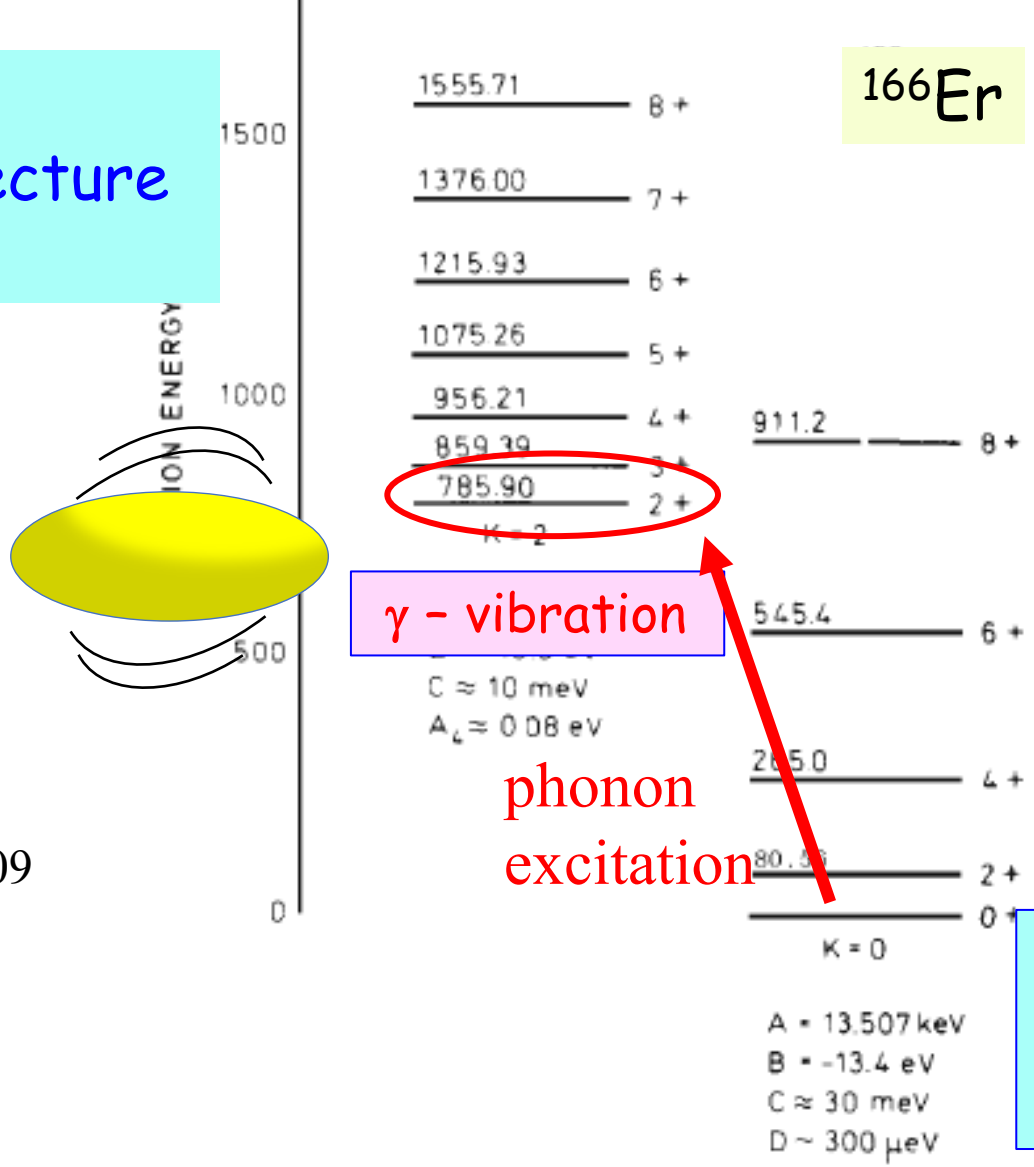

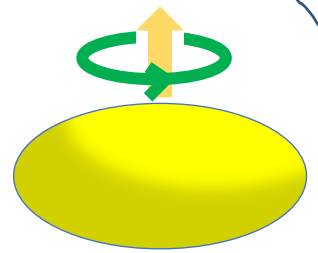

Axially symmetric prolate ellipsoid (equilibrium)

A case of the textbook example:

原子核 by M. Nogami

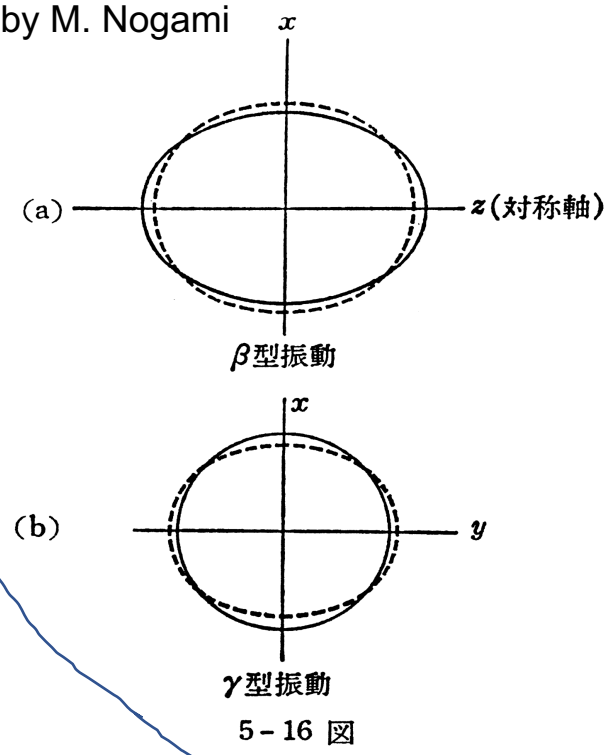

Fig. 9. Rotational bands in ^{166}Er. The figure is from (35) and is based on the experimental data by Reich and Cline (75). The bands are labelled by the component K of the total angular momentum with respect to the symmetry axis. The K = 2 band appears to represent the excitation of a mode of quadrupole vibrations involving deviations from axial symmetry in the nuclear shape.

Bohr & Mottelson, Nuclear Structure II, 1975

Two possibilities 1. Vibrational mode (most likely preferred)

2. Equilibrium shape deviating from axial symmetry

Interpretation of the $K\pi = 2+$ excitation ^{166}Er

The low-energy and large $E2$-matrix element for exciting the $K=2$ band suggests that we are dealing with a collective mode involving deviations of the nuclear shape from axial symmetry. (The $B(E2)$ value for exciting the $K=2, I=2$ state is about $28 B_W(E2)$, which is 14 times the appropriate single-particle unit (see p. 549).) Such a collective mode could have the character of a vibration around an axially symmetric equilibrium or might be associated with an equilibrium shape deviating from axial symmetry.

shape coexistence

Nobel lecture by A. Bohr (1975)

Only the possibility 1. was mentioned for ^{166}Er.

The dominance of axially-symmetric shapes was supported microscopically by the so-called Pairing + Quadrupole Model.

Kumar, K. and Baranger, M.
Nuclear deformations in the pairing-plus-quadrupole model (III).
Static nuclear shapes in the rare-earth region. Nucl. Phys. A 1968, 110, 529–554.

This paper presents statements such as

> While most of the deformed nuclei are found to be prolate,

and

> The preponderance of axially symmetric shapes (prolate or oblate)

Bes, D.R. and Sorensen, R.A.
The Pairing-Plus-Quadrupole Model.
In Advances in Nuclear Physics; Ed. by Baranger, M. and Vogt, E, (Plenum Press, New York, NY, USA, 1969)

This conclusion is correct, as far as the Pairing + Quadrupole Model is adopted.
However...

Questions were raised from experimental viewpoints ….

Eur. Phys. J. A (2019) 55: 15
DOI 10.1140/epja/i2019-12665-x

THE EUROPEAN PHYSICAL JOURNAL A

Review

"Stiff" deformed nuclei, configuration dependent pairing and the β and γ degrees of freedom

J.F. Sharpey-Schafer[1,a], R.A. Bark[2], S.P. Bvumbi[3], T.R.S. Dinoko[4], and S.N.T. Majola[5,b]

INSTITUTE OF PHYSICS PUBLISHING — JOURNAL OF PHYSICS G: NUCLEAR AND PARTICLE PHYSICS

J. Phys. G: Nucl. Part. Phys. 27 (2001) R1–R22 — www.iop.org/Journals/jg — PII: S0954-3899(01)18337-4

TOPICAL REVIEW

Characterization of the β vibration and 0_2^+ states in deformed nuclei

P E Garrett

And from empirical approaches….

P. Boutachkov, A. Aprahamian, Y. Sun, J.A. Sheikh & S. Frauendorf

The European Physical Journal A - Hadrons and Nuclei **15**, 455–458 (2002)

Furthermore, there have been microscopic approaches also, where the description of excited bands are still a challenge.

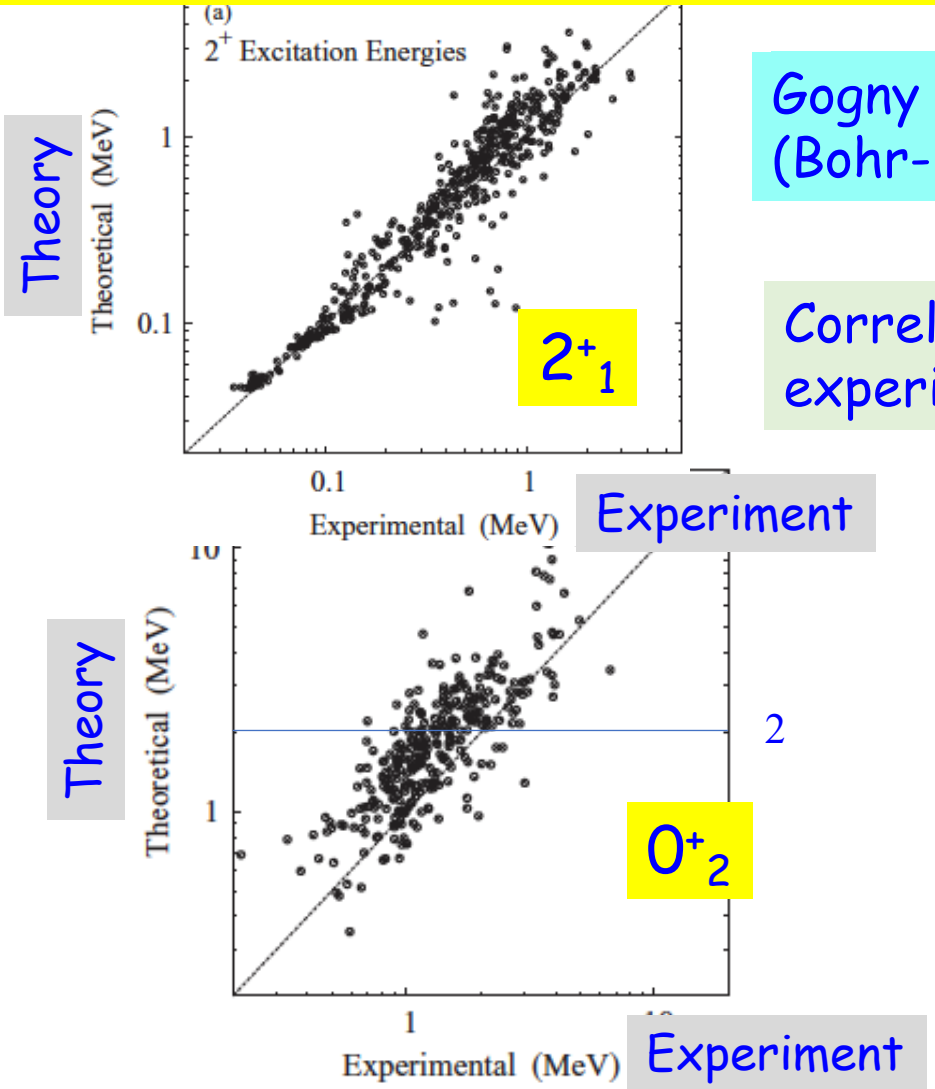

FIG. 20. Excitation energy of the 0_2^+ state compared with experiment [24].

Gogny -> 5DCH (Bohr-Hamiltonian)

Delaroche et al., PR C 81, 014303 (2010)

Correlations between theoretical & experimental values (scale: logarithmic)

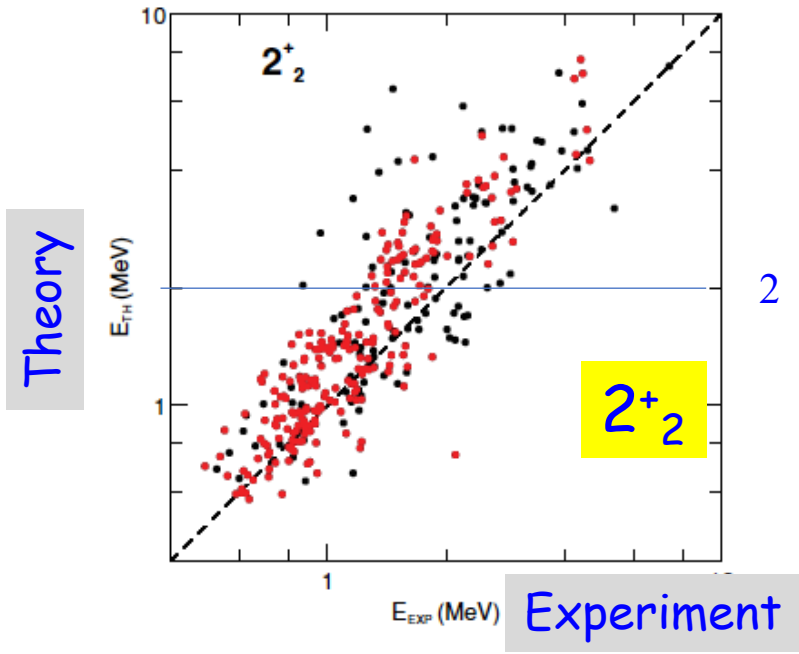

FIG. 19. (Color online) Excitation energy of the second $J = 2$ excitation, comparing 352 nuclei. Experimental data are from Ref. [24]. The 2_γ^+ levels are marked with red color.

Revisit with Monte Carlo Shell Model

Effective interaction:
G-matrix* + V_{MU}

* Brown, PRL 85, 5300 (2000)

Nucleons are excited fully within this model space (no truncation)

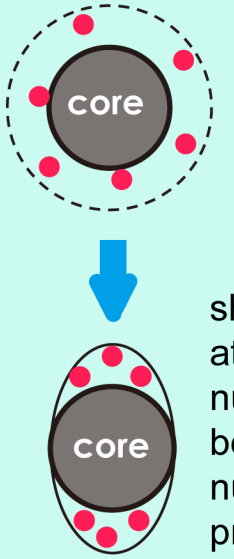

short-range attractive nuclear force between nucleons produces more binding energy

We performed Monte Carlo Shell Model (MCSM) calculations, where the largest case corresponds to the diagonalization of 4.8 x 10^{33} dimension matrix.
Its recent extension, Quasiparticle Vacua Shell Model (QVSM)* is used,
for most of the calculations to be shown. *
Shimizu *et al*, PRC 103, 014312 (2021)

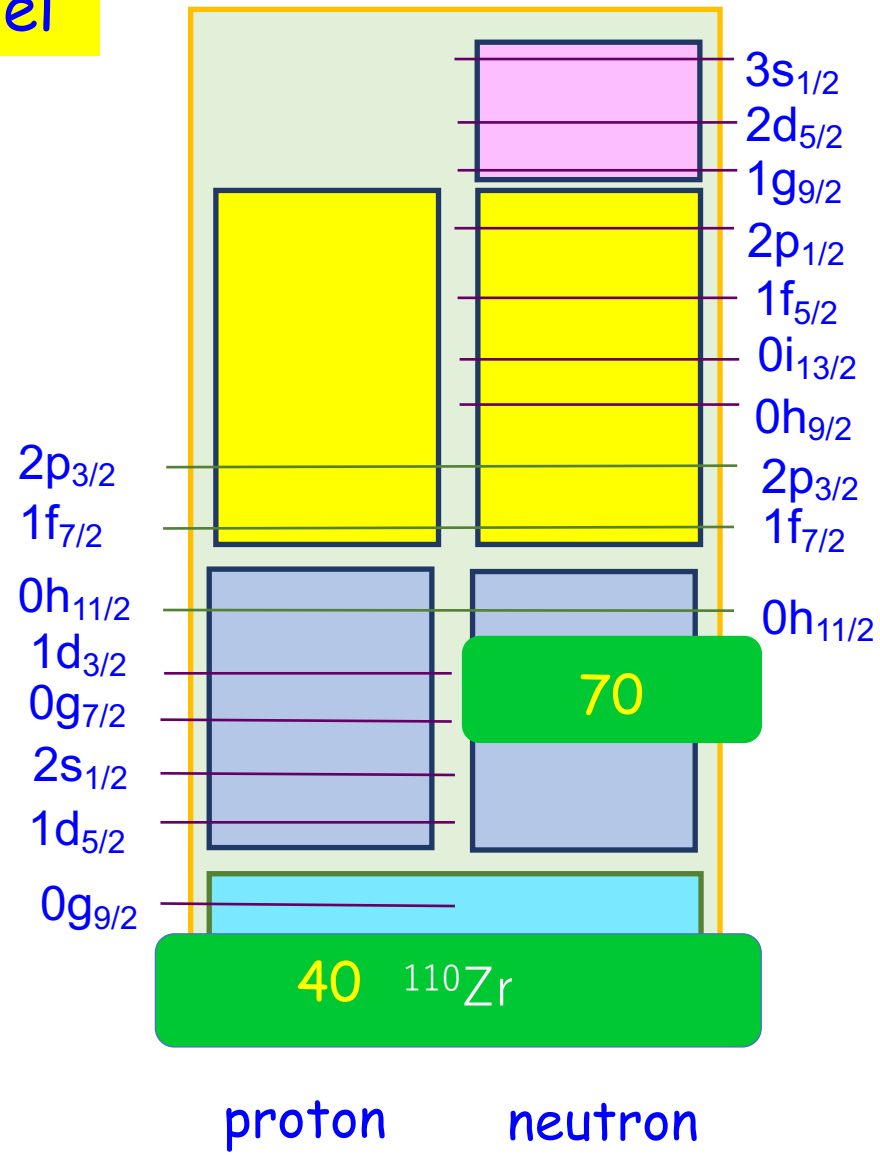

V_{MU} : same interaction for the description of shell evolution in exotic nuclei

Most advanced methodology in the MCSM is used

- (Ordinary) MCSM: superposed Slater determinants with angular momentum and parity projections

- QVSM(Quasiparticle Vacua Shell Model): superposed quasiparticle vacua with number, angular momentum, and parity projections

- Pairing correlations over many single-particle orbitals are already incorporated in each basis vector because of its BCS-type character

quasiparticle vacuum

$$|\phi\rangle = \prod_p (u_p + v_p a_p^\dagger a_{\bar{p}}^\dagger)|-\rangle$$

core (vacuum)

PHYSICAL REVIEW C **103**, 014312 (2021)

Variational approach with the superposition of the symmetry-restored quasiparticle vacua for nuclear shell-model calculations

Noritaka Shimizu,[1,*] Yusuke Tsunoda,[1] Yutaka Utsuno,[2,1] and Takaharu Otsuka[3,4,2]

The QVSM code was fully used, but huge computer resources were needed.

Shimizu

Aage Bohr's picture

a. conventinal picture (prolate)

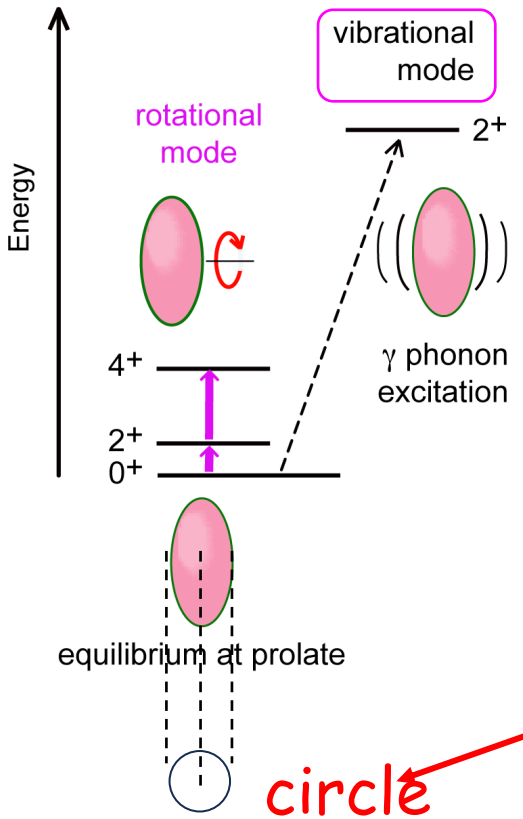

Our picture

b. present picture (triaxial)

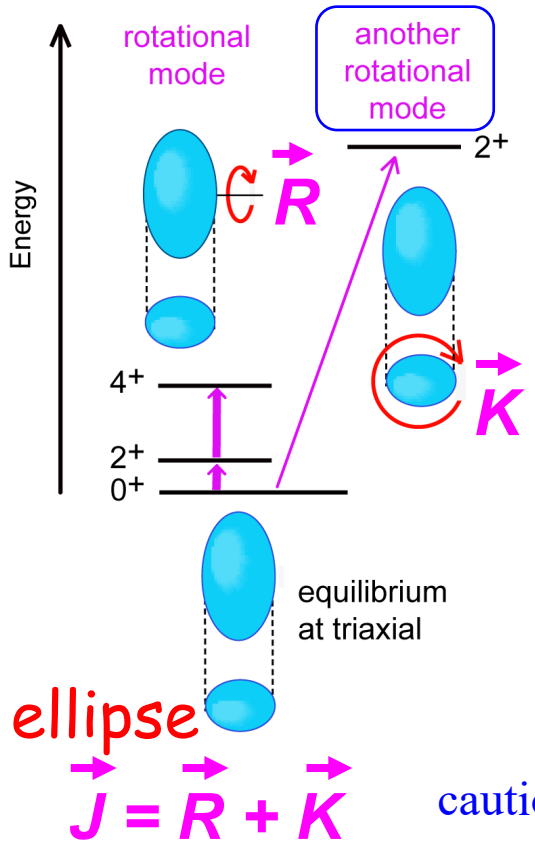

ellipse

circle

$\vec{J} = \vec{R} + \vec{K}$

caution: $\vec{R}$ and $\vec{K}$ are not independent

Result of MCSM calculation

c. level energies and E2 properties of ^{166}Er

E2 quantities in W.u.

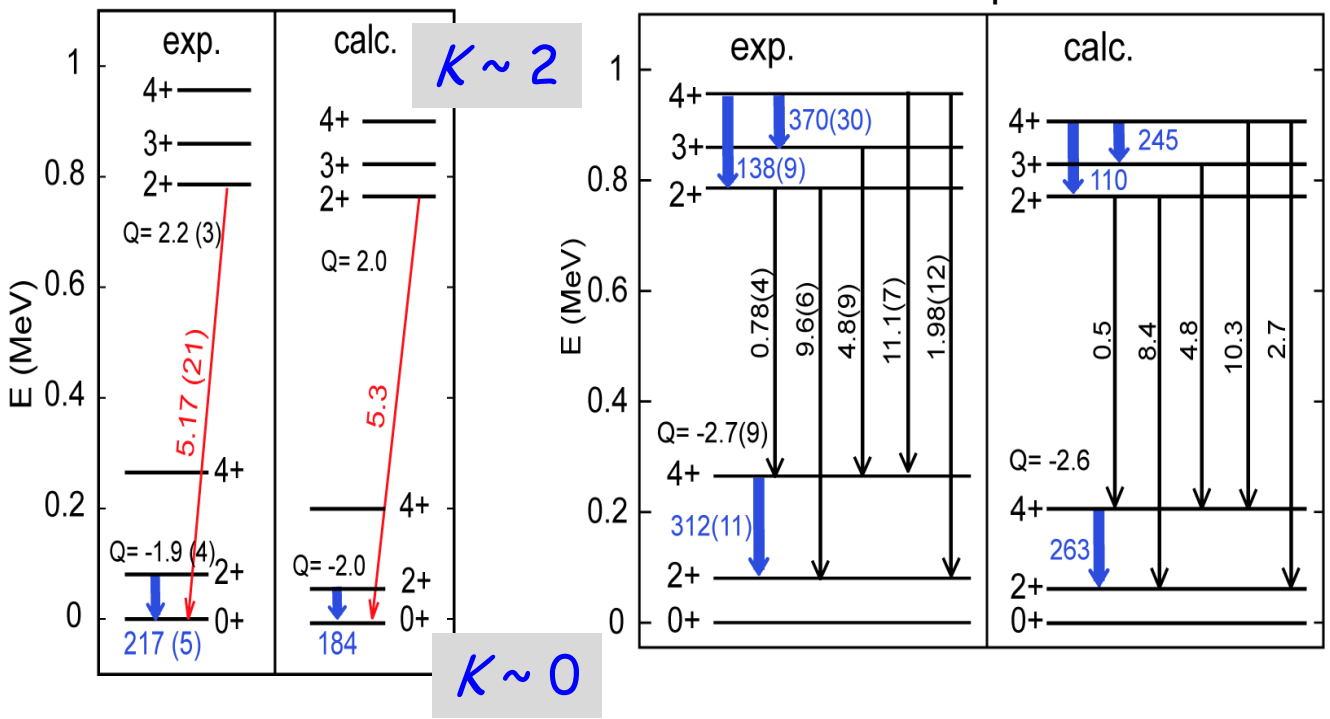

The R and K rotational modes are not completely independent, and are coupled by the Hamiltonian.

PES and T-plot of the ground and lowest states of ^{166}Er

a. legend

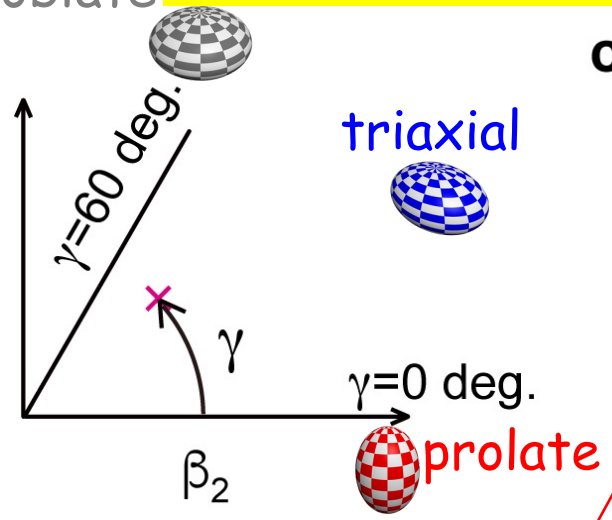

b. PES (^{166}Er, HFB, unprojected)

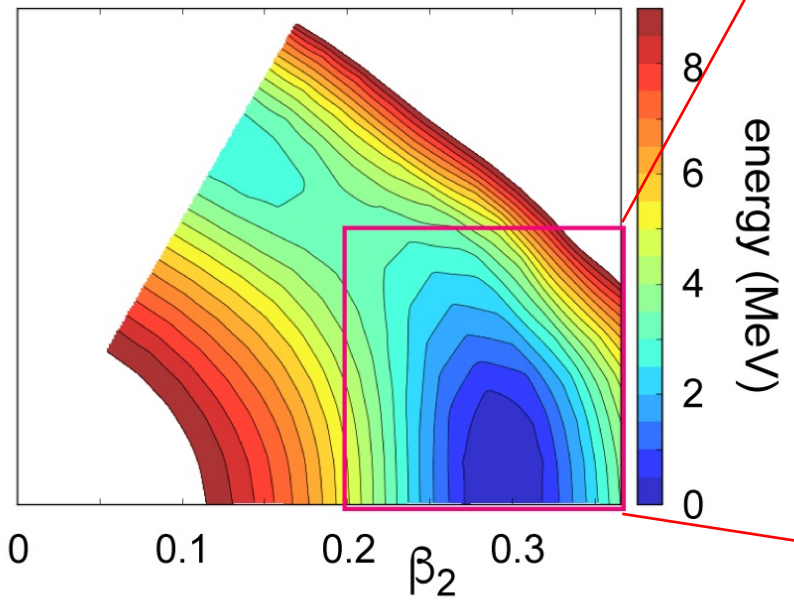

c. T plots

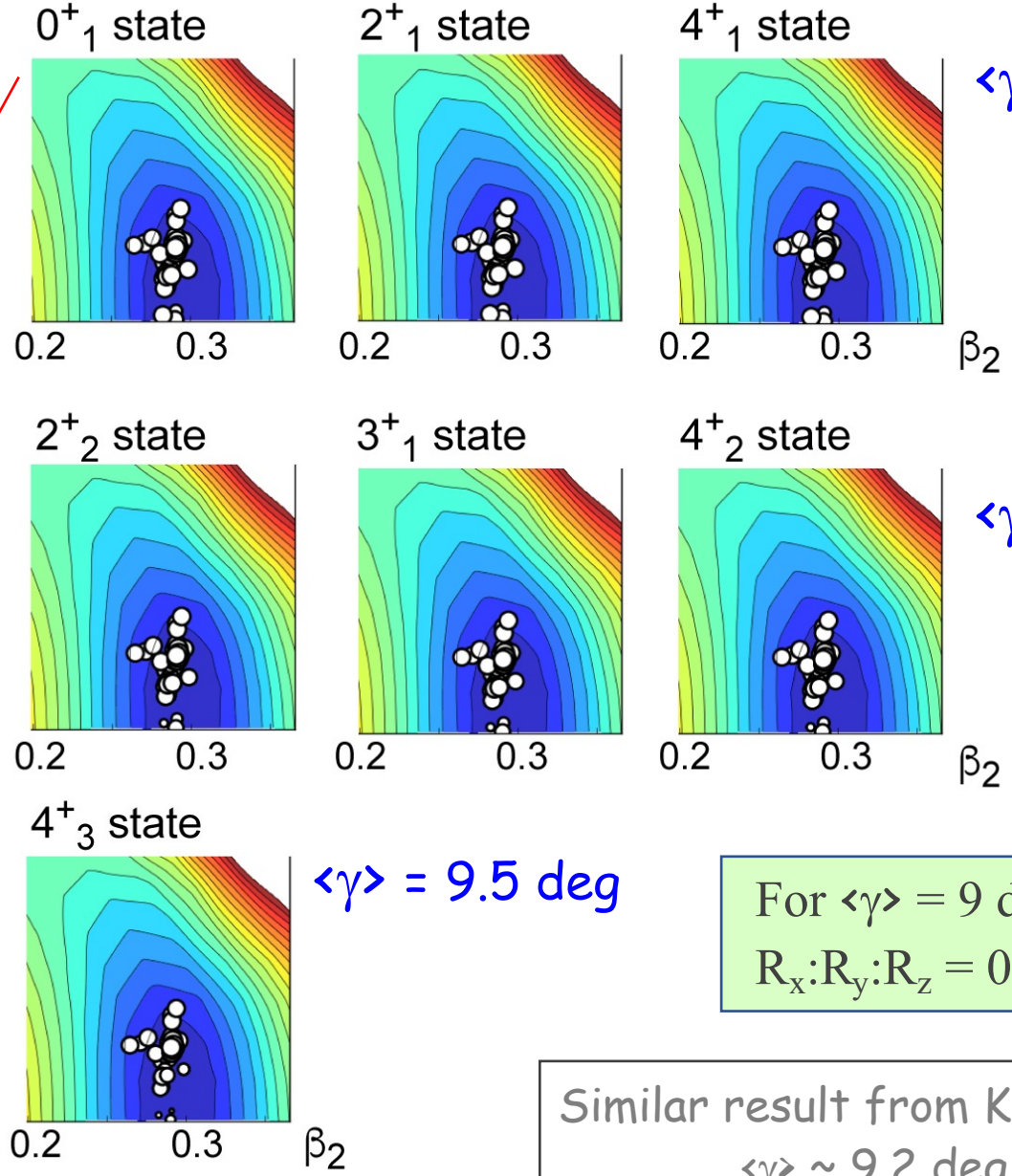

For $\langle\gamma\rangle = 9$ deg,
$R_x:R_y:R_z = 0.93 : 0.88 : 1.19$

Similar result from Kumar invariant
$\langle\gamma\rangle \sim 9.2$ deg, $\langle\beta_2\rangle \sim 0.30$

What makes such triaxial shapes
in ground and low-lying state.

Monopole interaction

PES near the minimum: refined contour plots

T plot of 0^+_1 state

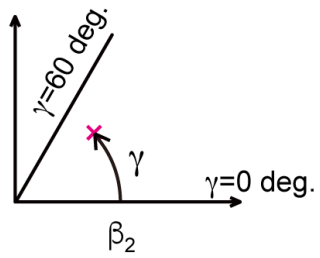

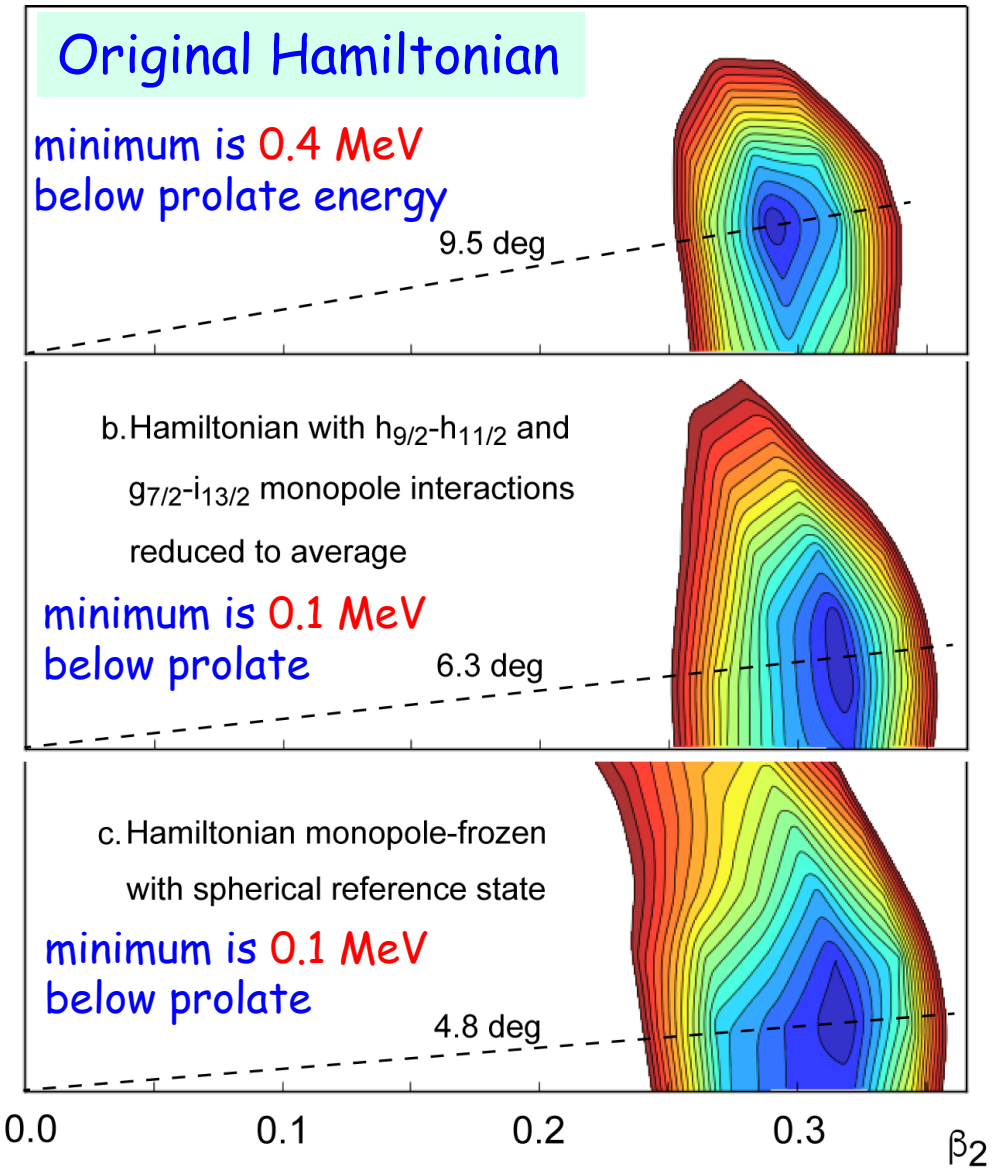

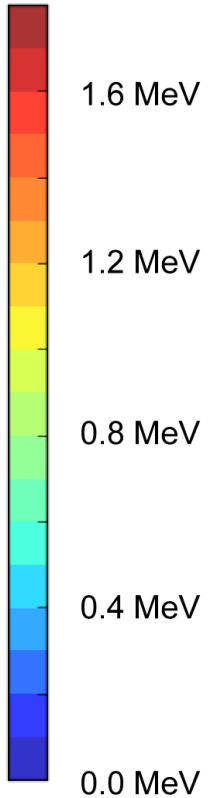

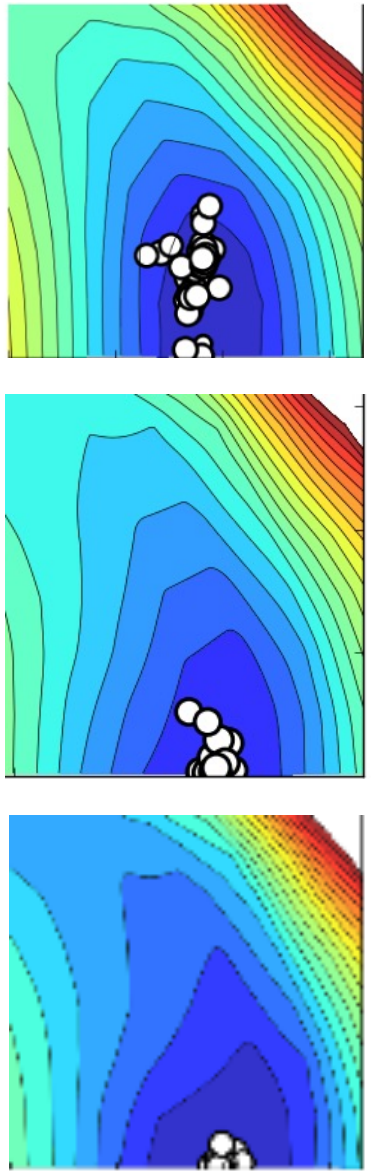

two most attractive monopole interactions $h_{11/2}$-$h_{9/2}$ and $g_{7/2}$-$i_{13/2}$ are weakened to average value

monopole interactions are replaced by constant SPEs assessed for spherical reference state (Monopole-Frozen)

Closely lying single-particle orbits of the same parity → axial symmetry

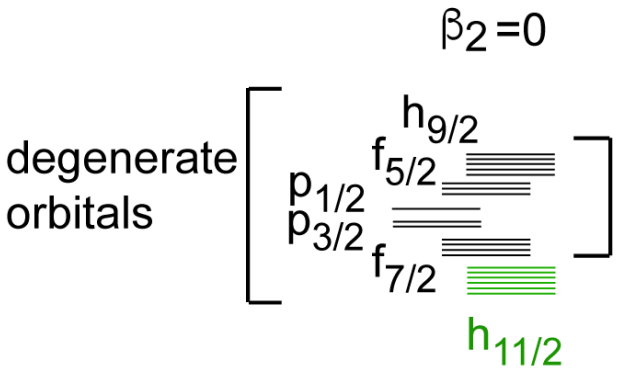

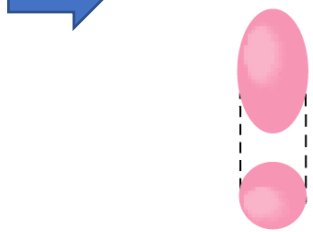

Q_0=large

Q_2=0

prolate
(axially-symmetric)
shape

- Closely lying single-particle orbits of the same parity → axial symmetry

A substantial effect needed to change this trend

A single-particle orbit with large j (e.g. $h_{11/2}$) can produce sizable triaxiality (i.e., Q_2), if the number of particles in the orbit is appropriate.

Proton single-particle orbit with large j_p and neutron orbit with large j_n are coupled by the monopole interactions of the central and tensor forces, as it occurs in the shell evolution.

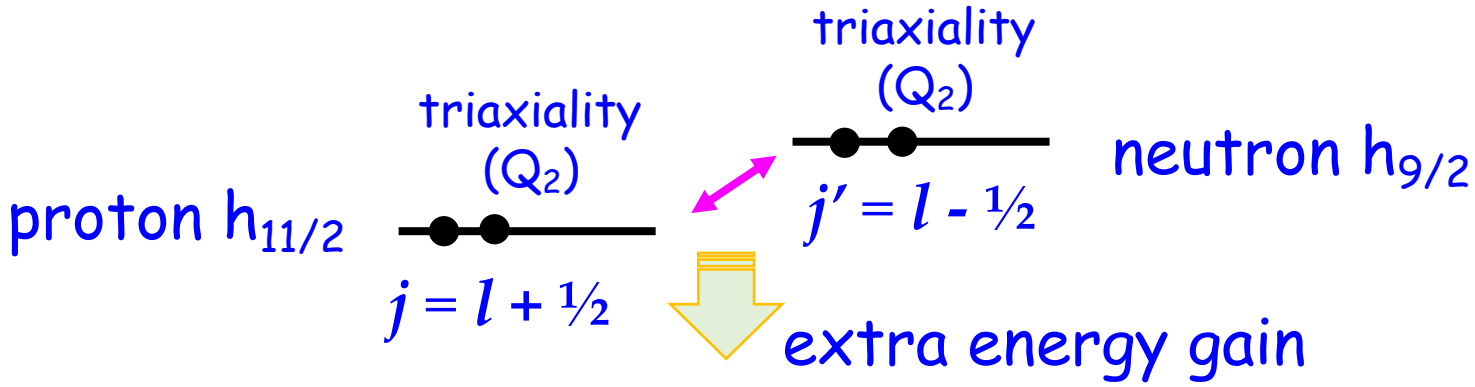

- Monopole interactions can be related to triaxiality

Monopole interactions are the key

for Central force

Stronger attraction between single-particle orbits of similar radial wave functions

ex.: $f_{7/2} - f_{5/2}$, $g_{9/2} - h_{11/2}$ *cf: Federman-Pittel (1977)*

for Tensor force

(long-range part,
or 1π, 2π exchange)

$j_> = l + ½$

$j_< = l - ½$

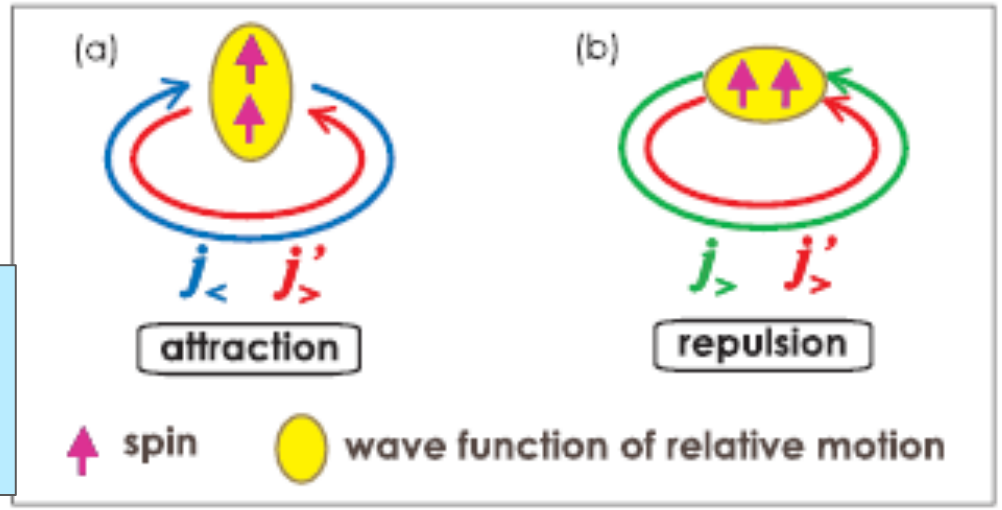

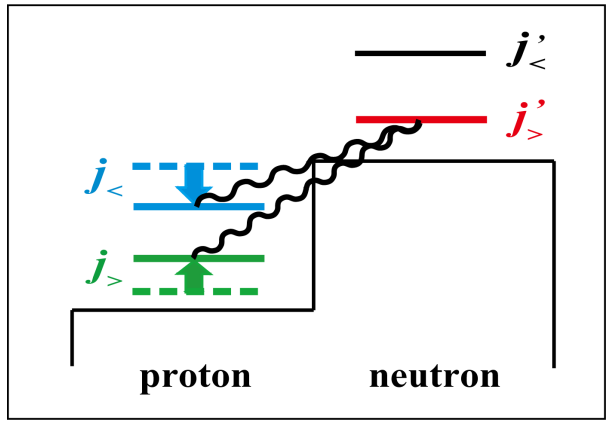

for Three-nucleon force (Δ-hole) : overall repulsive effect

Prolate shape produced by many single-particle orbitals

Triaxial shape produced by large-j single-particle orbital lowered by the monopole int.

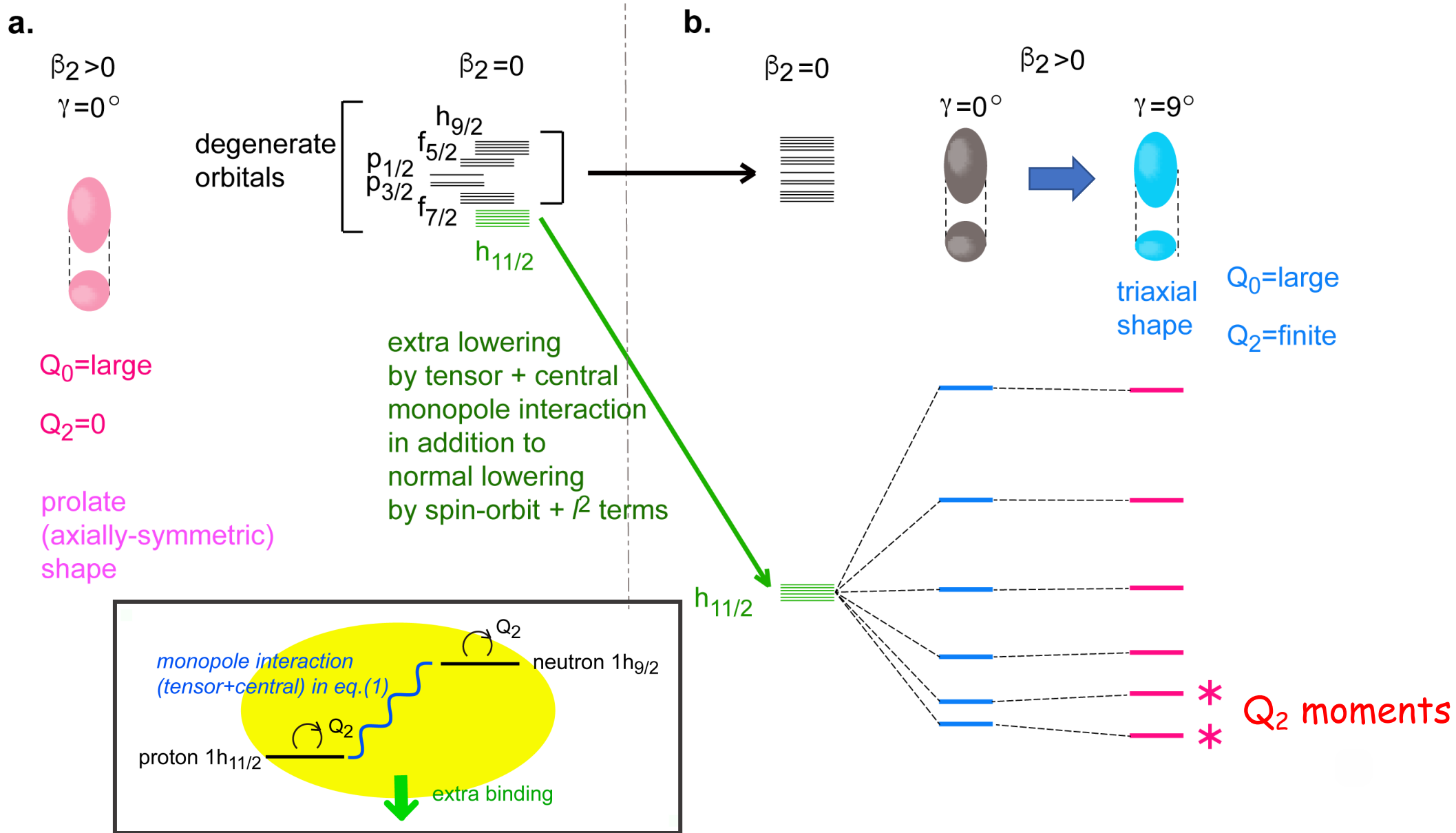

Aage Bohr's picture

a. conventinal picture (prolate)

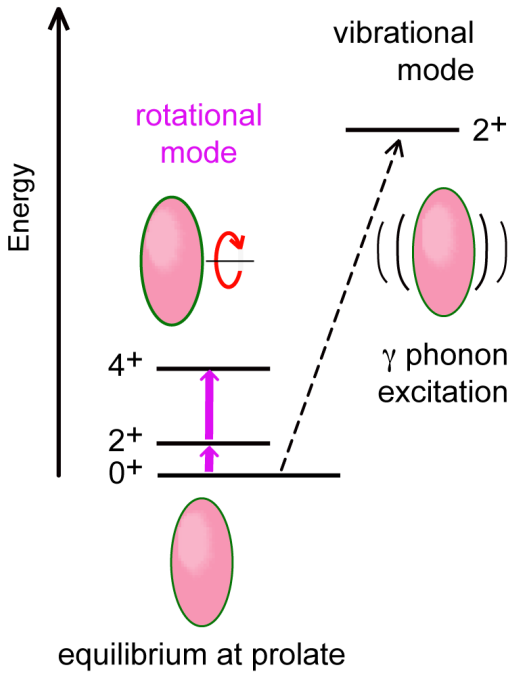

Our picture

b. present picture (triaxial)

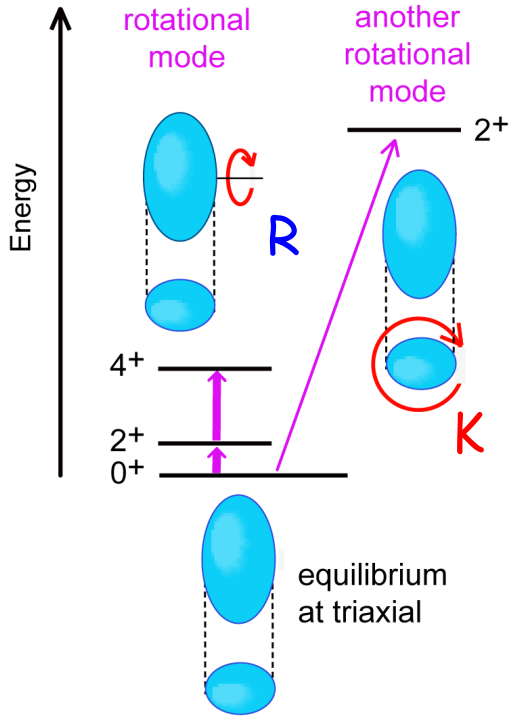

Result of MCSM calculation

c. level energies and E2 properties of ^{166}Er

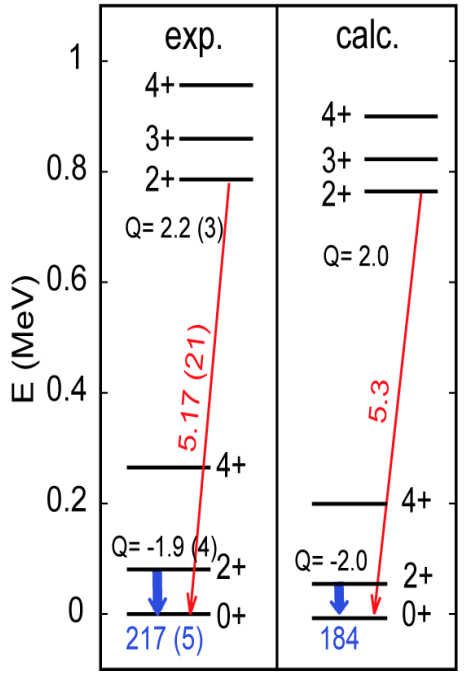

E2 quantities in W.u.

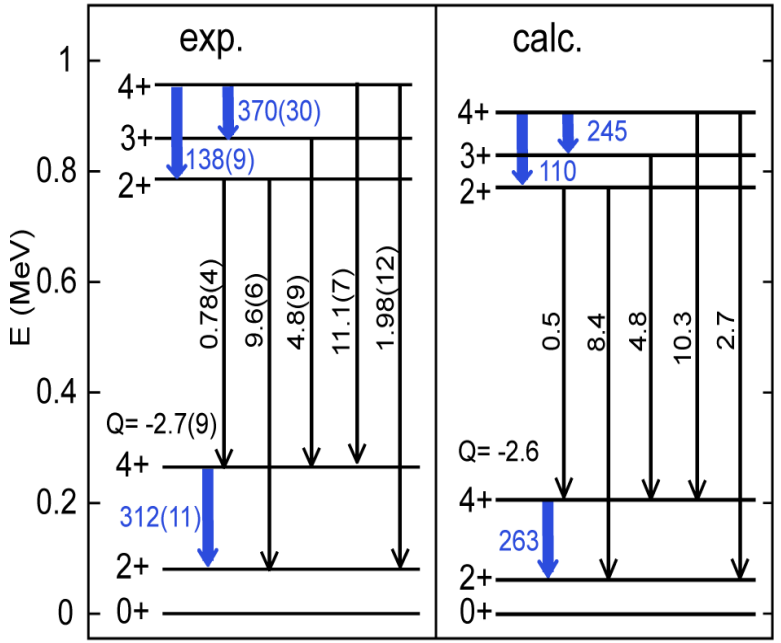

Why is the 2^+_2 level so low ?

Much higher in the Davydov model

high rigidity for R rotation
lower rigidity for K rotation
-> "stretching" lowers 2^+_2 level by ~0.5 MeV
(Rigid rotor model of Davydov fails)
The value of γ changes by ~ 1 degree.

Aage Bohr's picture

a. conventinal picture (prolate)

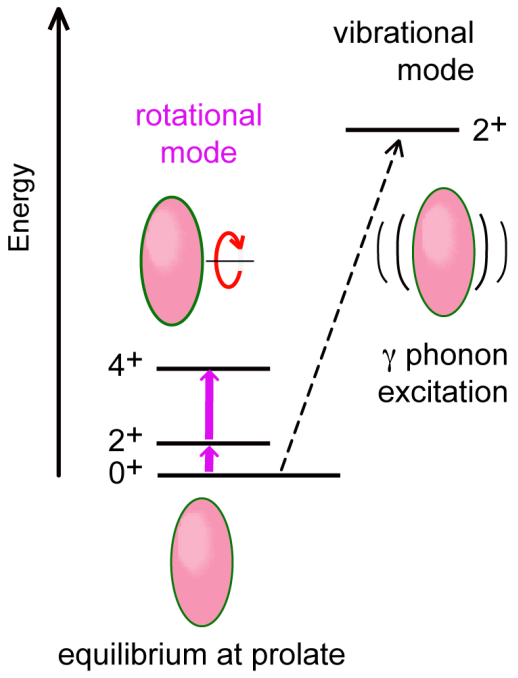

Our picture

b. present picture (triaxial)

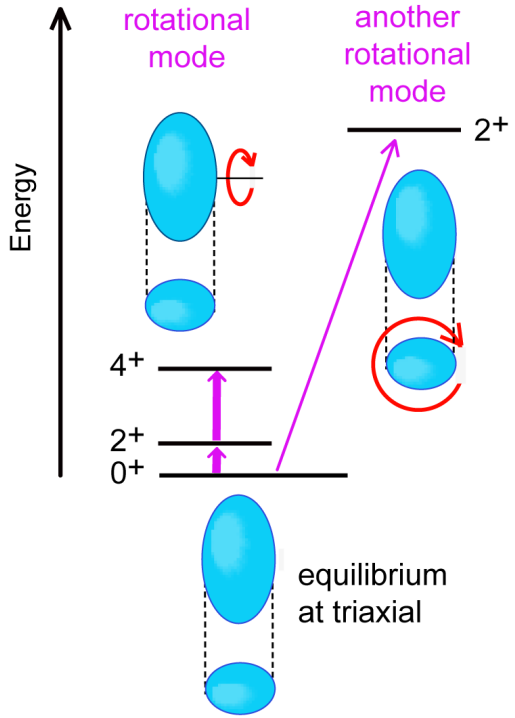

Result of MCSM calculation

c. level energies and E2 properties of ^{166}Er

E2 quantities in W.u.

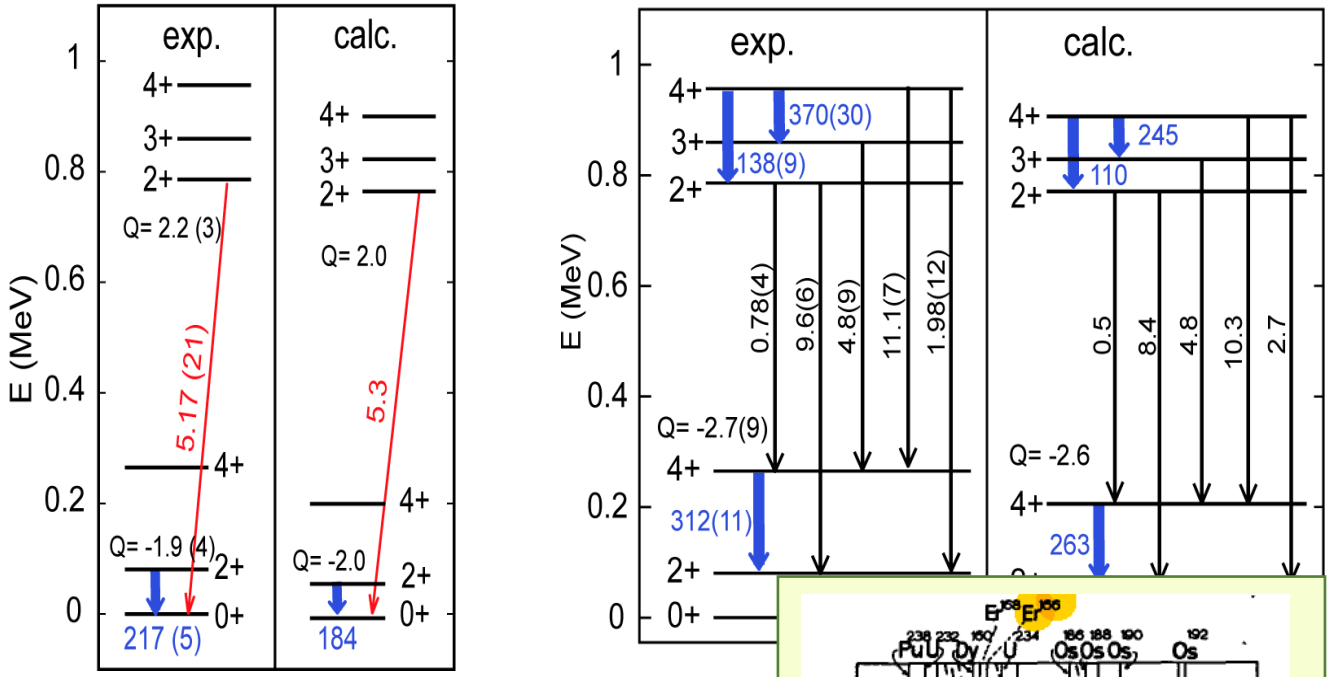

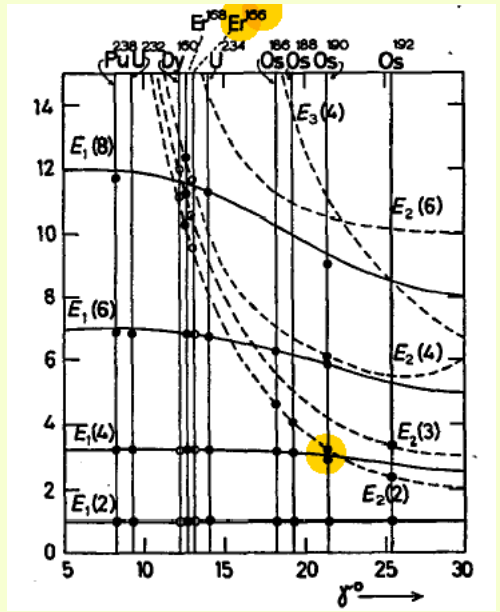

Davydov model

$2^+_2/2^+_1$ energy ratio
→ γ ~ 13 deg.

B(E2) $2^+_2/2^+_1$ ratio
→ γ ~ 9 deg.

Davydov, A.S., Filippov, G.F., Rotational states in even atomic nuclei, Nucl. Phys. **8**, 237 (1958).
Davydov, A.S., Rostovsky, V.S., Relative transition probabilities between rotational levels of non-axial nuclei. Nucl. Phys. **12**, 58 (1959).

Variations as Z and/or N changes (examples)

^{166}Er (Z=68, N=98) γ =8.4 deg

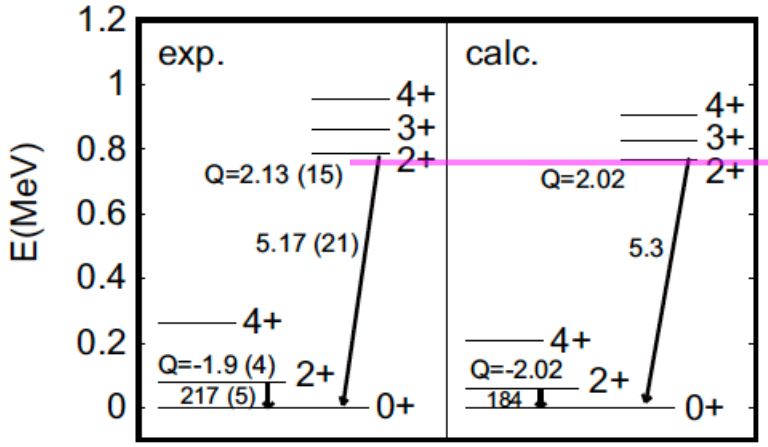

^{162}Er (Z=68, N=94)

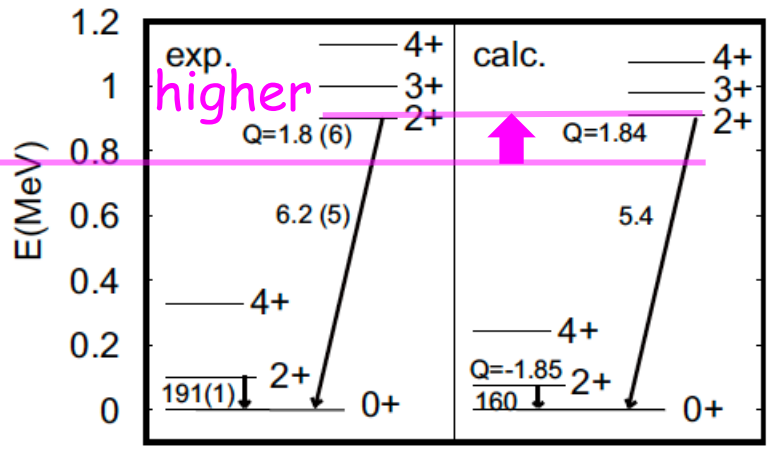

^{170}Er (not triaxial)

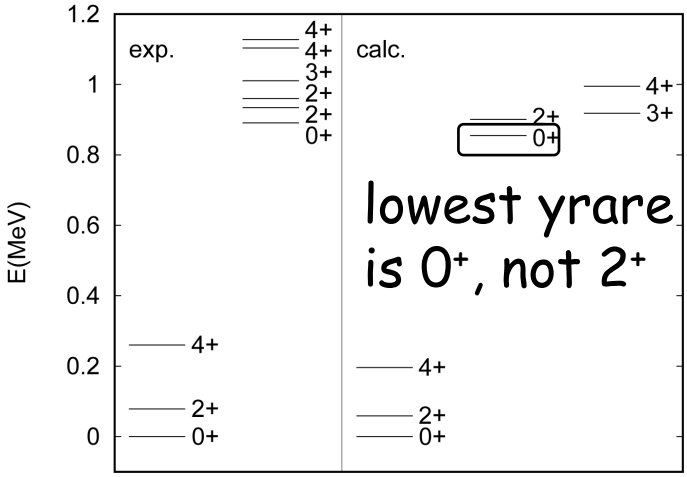

~ prolate

^{164}Dy (Z=66, N=98) γ =7.4 deg

no major change

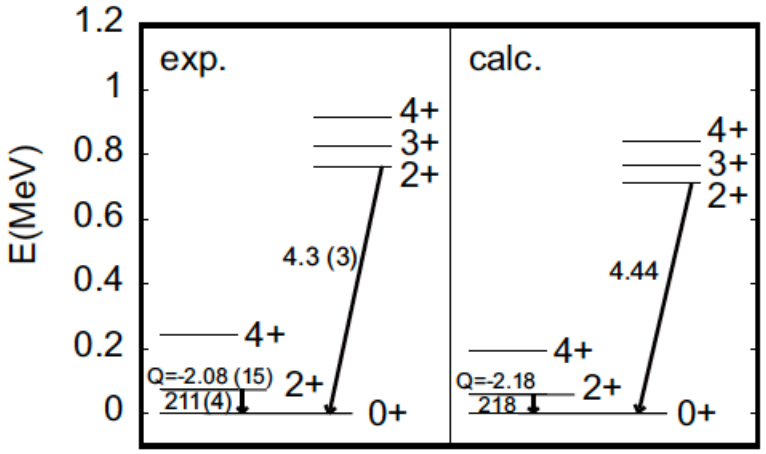

^{158}Gd (Z=64, N=94) γ =5.9 deg

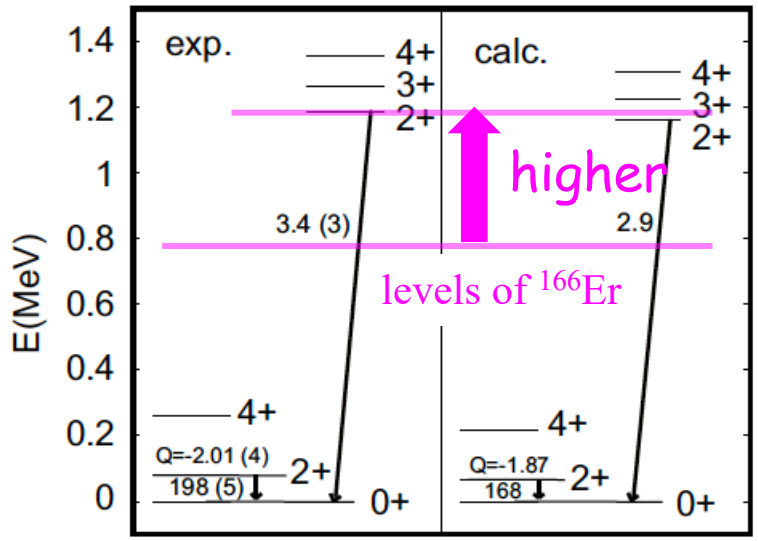

Coulex exp. showed consistent γ values

Cline et al. (1986)
Fahlander et al. (1990)
Werner et al. (2005),

for which natural interpretation is the triaxiality in the ground states.

17 triaxially strongly deformed nuclei around ^{166}Er

($Ex(2^+_2) < Ex(0^+_2)$; there can be more)

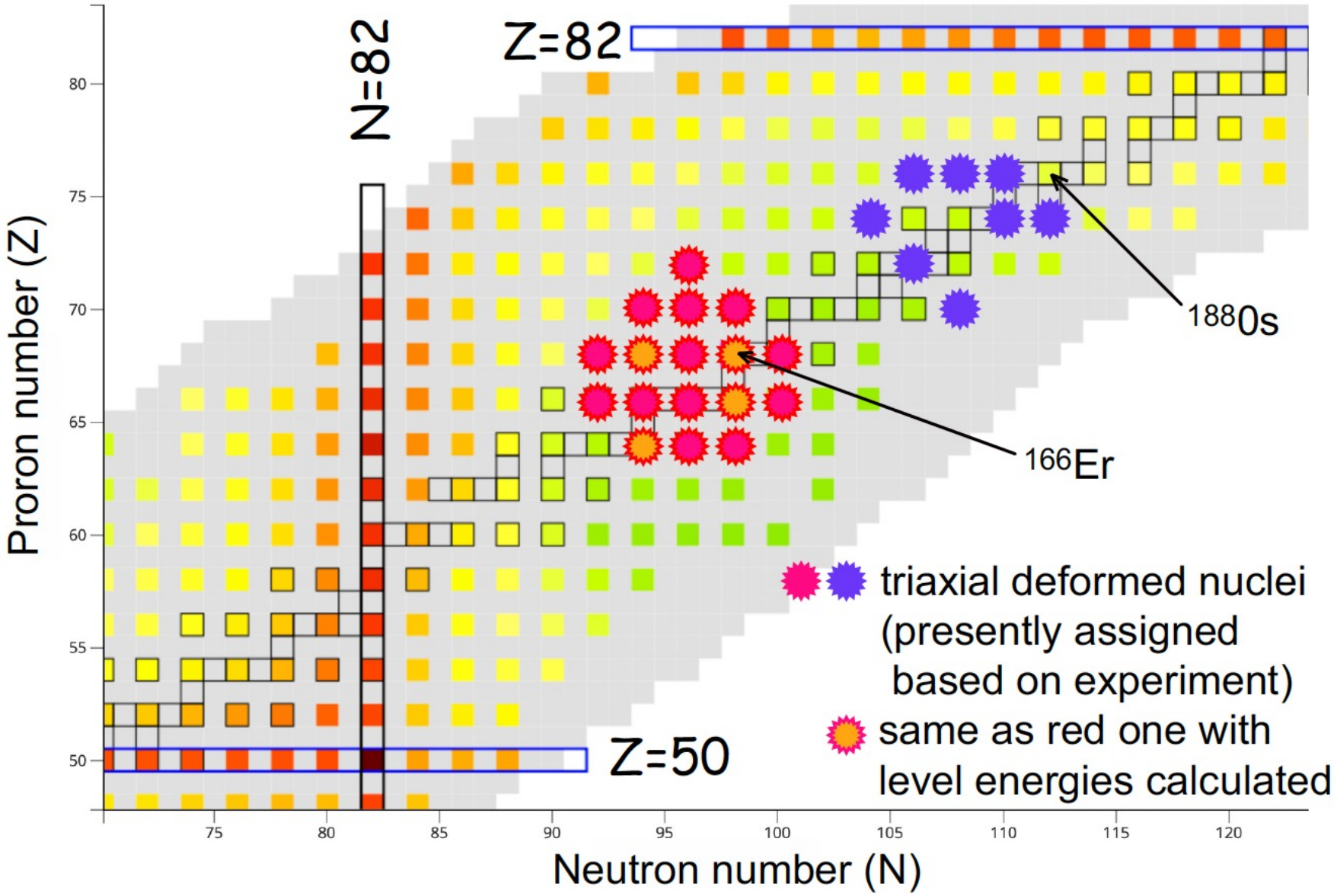

Besides existing Coulex data, could we observe their shapes by *Relativistic Heavy-Ion Collisions at LHC* ?
(*cf*: Giacalone *et al*.)

Extended scissors mode (rolling mode) is another possibility *to be studied in HIγS and RCNP.*
What about M1 excitations (γ, γ') ?

Hyper nuclei (with Λ particle) are another possibility in J-Lab and JPARC.

Global Calculations of Ground-State Axial Shape Asymmetry of Nuclei

Peter Möller,[1,*] Ragnar Bengtsson,[2] B. Gillis Carlsson,[2] Peter Olivius,[2] and Takatoshi Ichikawa[3]

Conventional view

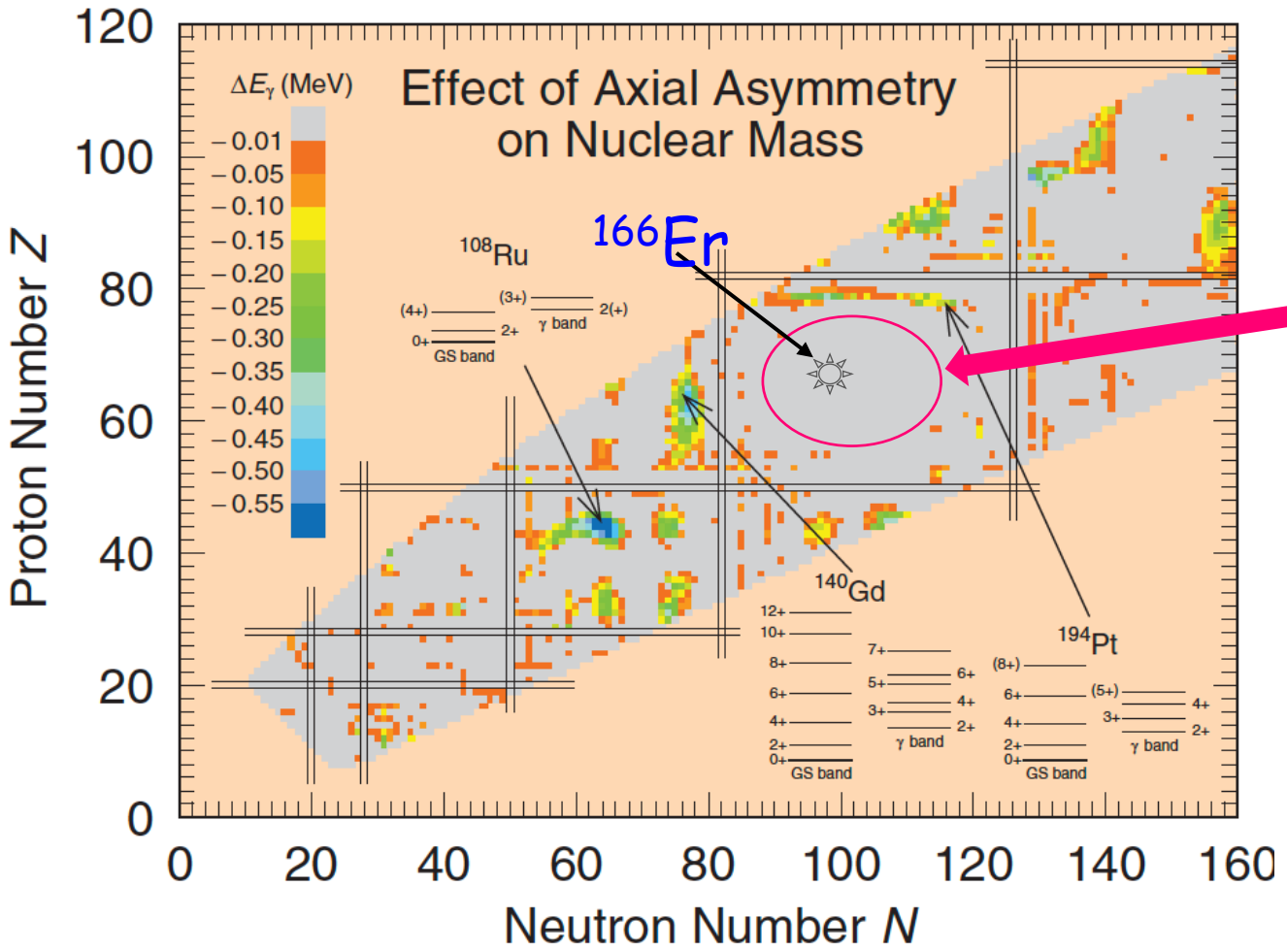

No triaxiality in the region of current interest

PES of and near the 17 triaxial deformed nuclei

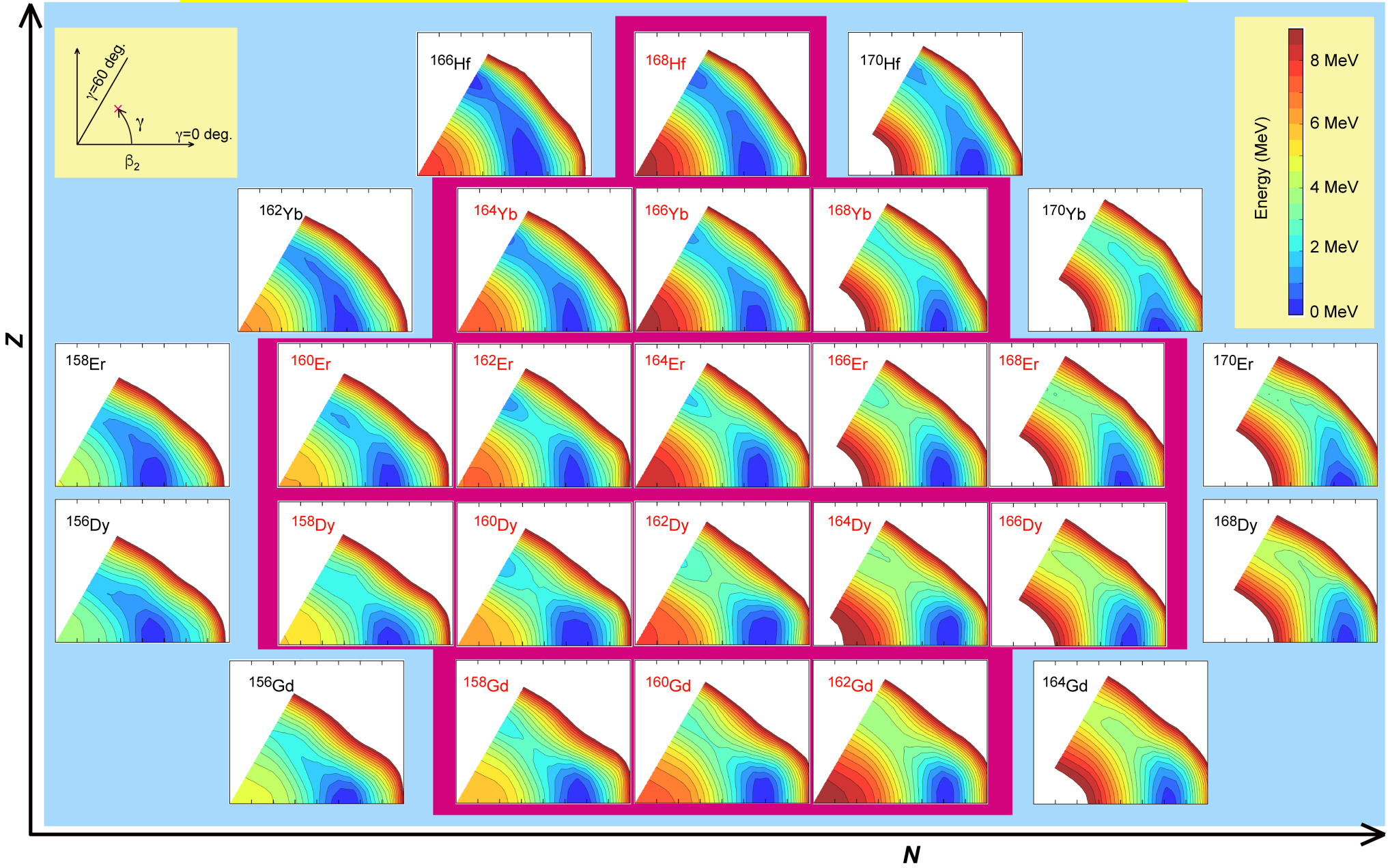

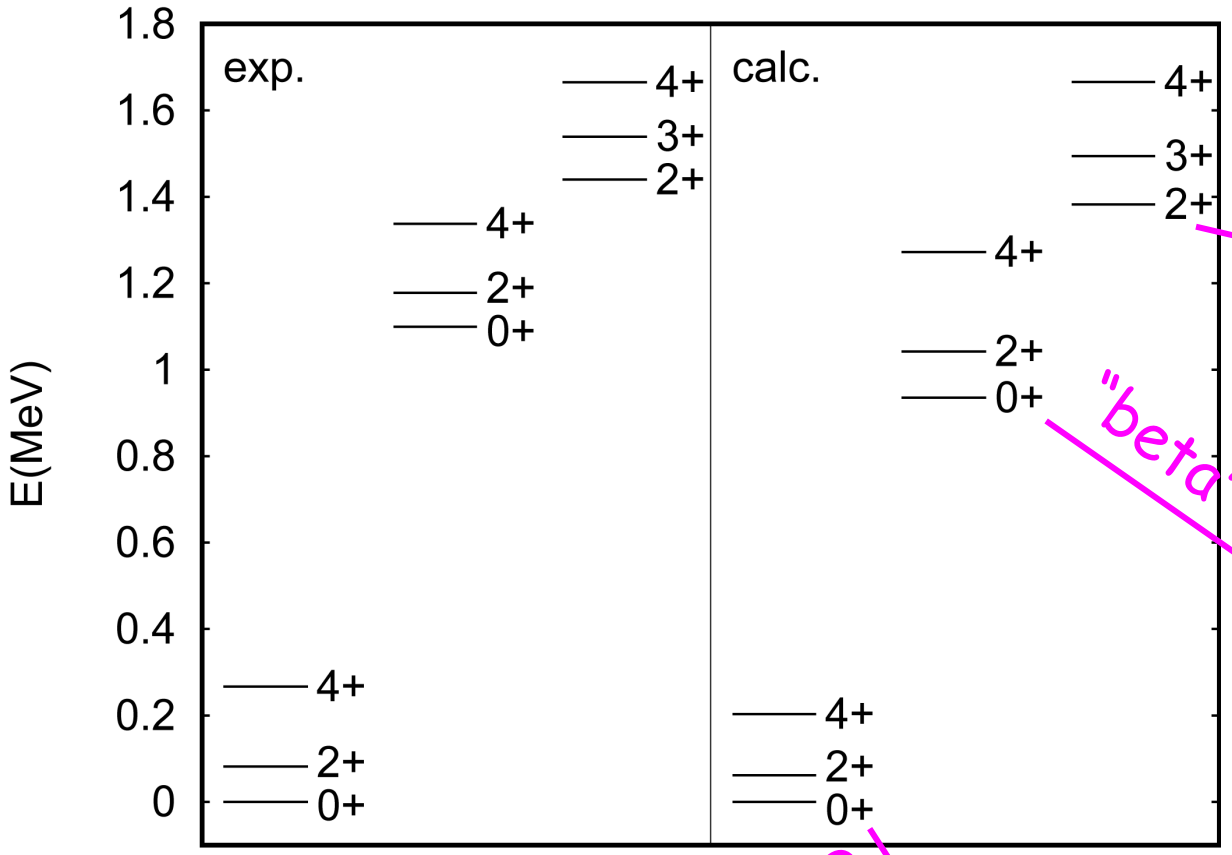

^{154}Sm

"gamma" band

"beta" band

ground band

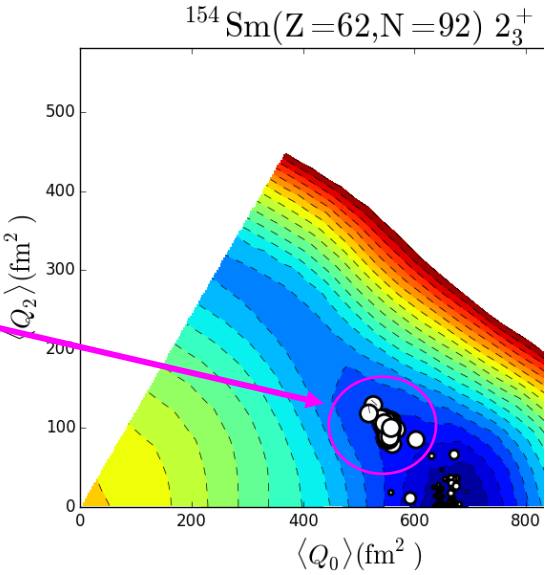

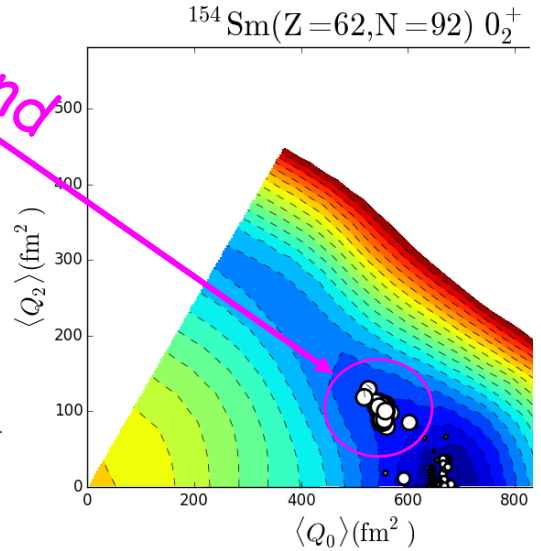

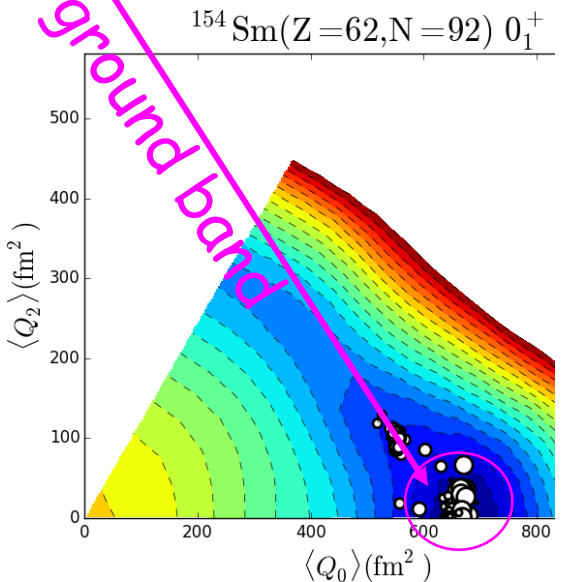

~ prolate
(γ ~ 3.3 deg)

Shape coexistence between prolate shaped band and triaxially shaped bands

$^{150\text{-}152}$Sm depict interesting patterns

Excitation energies of the lowest 2^+ states of even-even nuclei

a. Level energies of atomic nuclei with spherical and ellipsoidal shapes (examples)

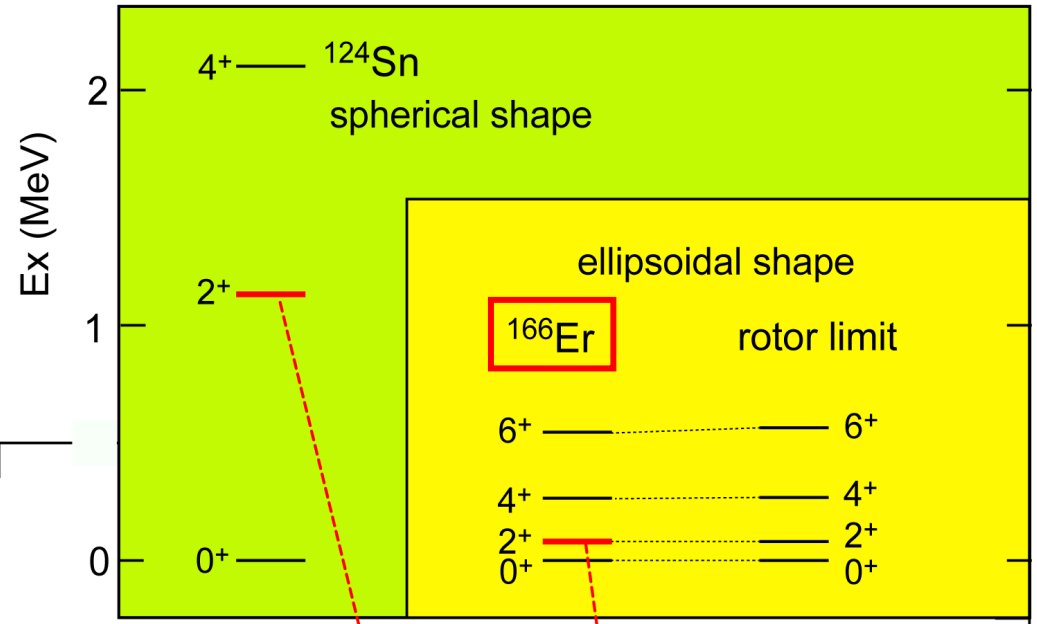

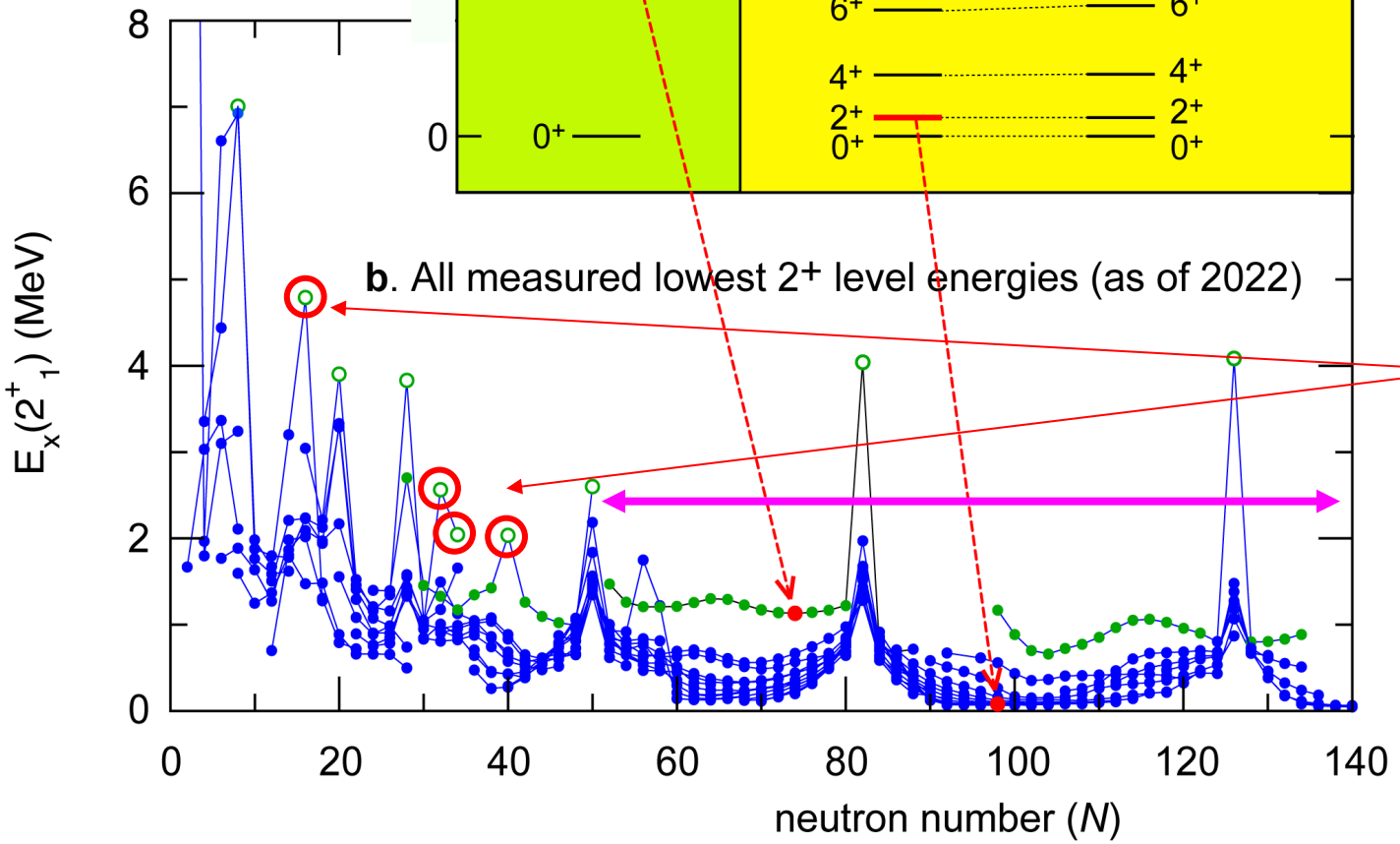

- ○ magic nuclei
- ● semi-magic nuclei
- ● other nuclei

In exotic nuclei, the shell evolution due to tensor + central monopole interactions produce new magic numbers shown by ○ (N= 16, 32, 34, 40), which are absent in Mayer-Jensen model.

Same interactions ➔ Deformed Heavy nuclei: Triaxial shapes

Summary of this part

The shell-model calculation is now feasible for rotational bands of heavy nuclei. (It is a matter of computer time; typically days, after up to weeks of waiting.)

The majority of heavy nuclei exhibit deformed shapes, which have been considered to be predominantly (axially-symmetric) prolate. Although this picture, or paradigm, is a textbook item, the same central + tensor forces as the one responsible for the shell evolution now point to triaxial shapes, in many nuclei, through a self-organization (see PRL 123, 222502 (2019)) mechanism. Triaxiality is mainly due to large-j orbitals, like $h_{11/2}$.

This may be the first case of explicit "elementary particle" effect on the nuclear shape, as one pion exchange ~ tensor force (somewhat related to Weinberg 1990).

Davydov *et al.* correctly suggested, empirically, triaxiality in many nuclei, but their rigid-rotor model is shown not to be precise enough for the excitation energies of side bands like the 2^+_2 band.

Alexander Davydov, (Ukrainian, 1912 – 1993), suggested the triaxiality of nuclear shapes and derived the features resulting from the rotation of triaxial objects. He did not present the underlying mechanism, and the rigid-rotor model may not be too good. Nevertheless, his contributions seem to be of great importance.

from Wikipedia

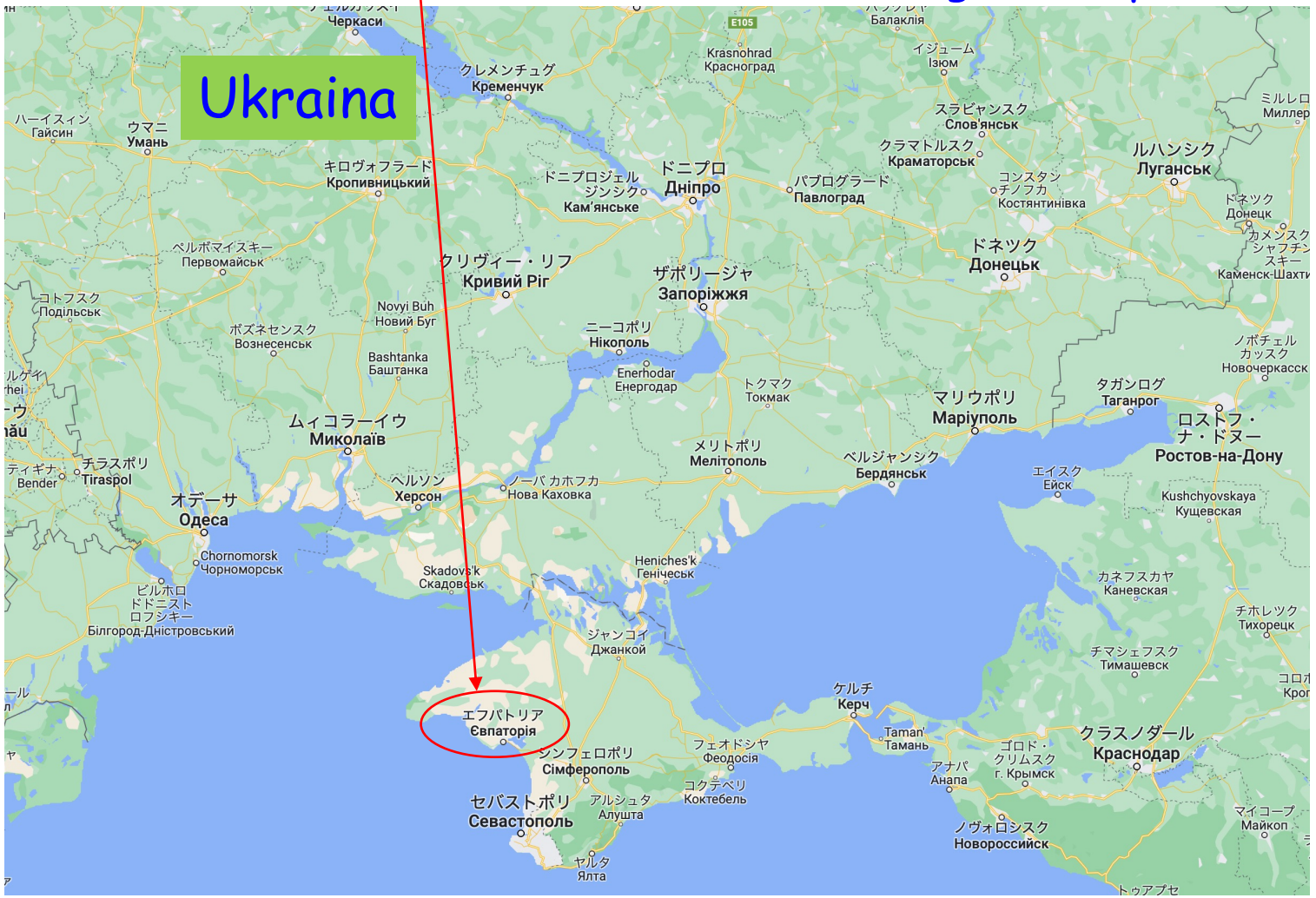

Outline

1. Basics of traditional shell model and Monte Carlo Shell Model
2. Shell evolution: from an introduction to the current landscape of magic numbers
3. Type-II Shell evolution: shape coexistence (parabola or linear or …)
4. Ellipsoidal nuclear shapes: Aage Bohr vs. Davydov
5. Shapes and driplines: who limits isotopes
6. α-clustering and nuclear matter: who likes α-cluster

Neutron driplines and its traditional view

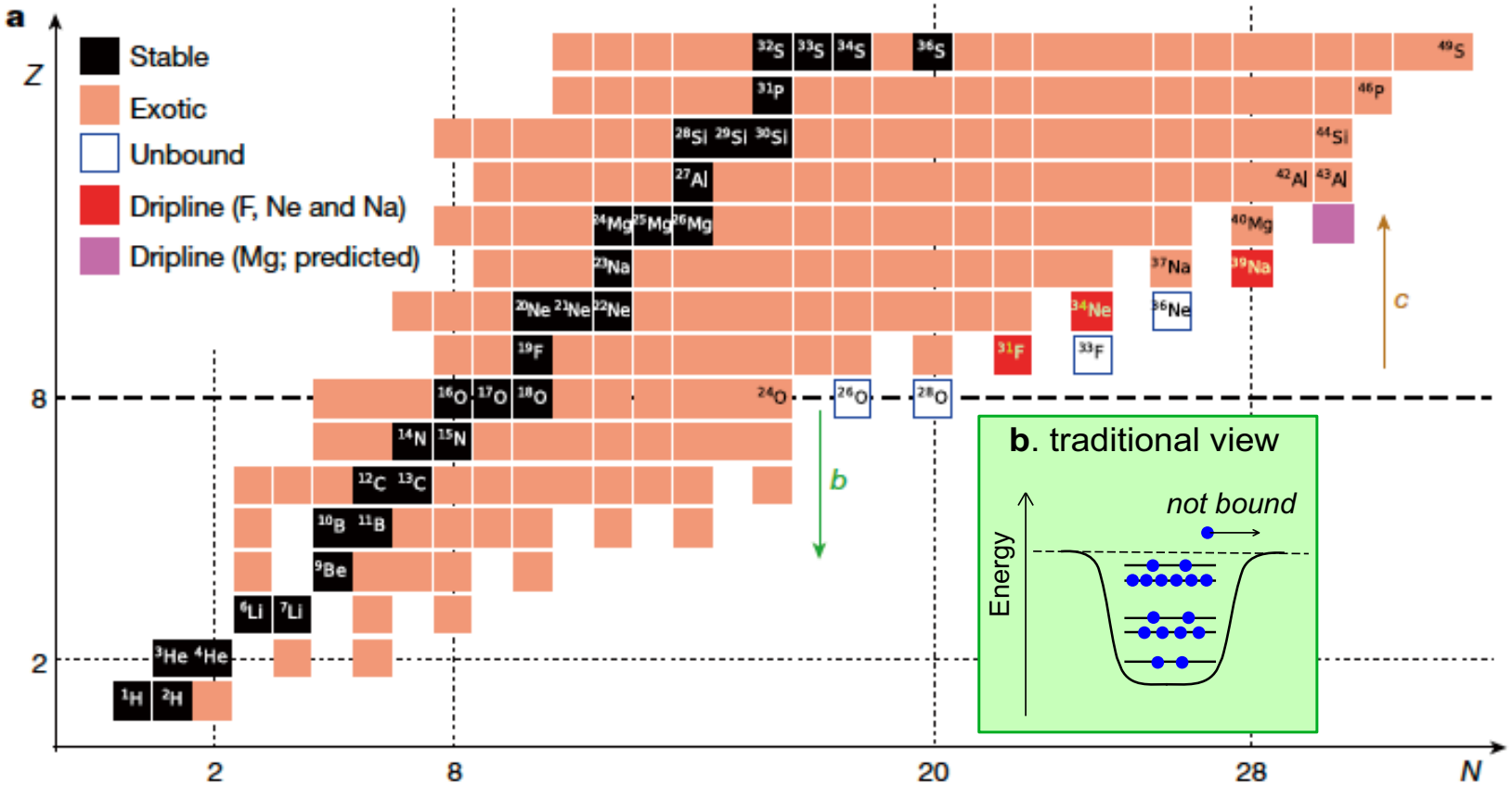

nature

Article | Published: 04 November 2020

The impact of nuclear shape on the emergence of the neutron dripline

Naofumi Tsunoda, Takaharu Otsuka ✉, Kazuo Takayanagi, Noritaka Shimizu, Toshio Suzuki, Yutaka Utsuno, Sota Yoshida & Hideki Ueno

Nature **587**, 66–71(2020) | Cite this article

A development starting from chiral EFT

EKK method* to handle consistently
two (or more) major shells
-> Effective shell-model interaction
(i) without fit of two-body m. e.,
(ii) applicable to broken magicity, or
merging two shells,
both are crucial for exotic nuclei.

*) Extended Krenciglwa-Kuo method is a magic by Takayanagi

K. Takayanagi, Nucl. Phys. A 852, 61 (2011).

N. Tsunoda, **K. Takayanagi**, M. Hjorth-Jensen, and T. Otsuka, Phys. Rev. C 89, 024313 (2014).

K. Takayanagi, Annals of Physics 350, 501 (2014).

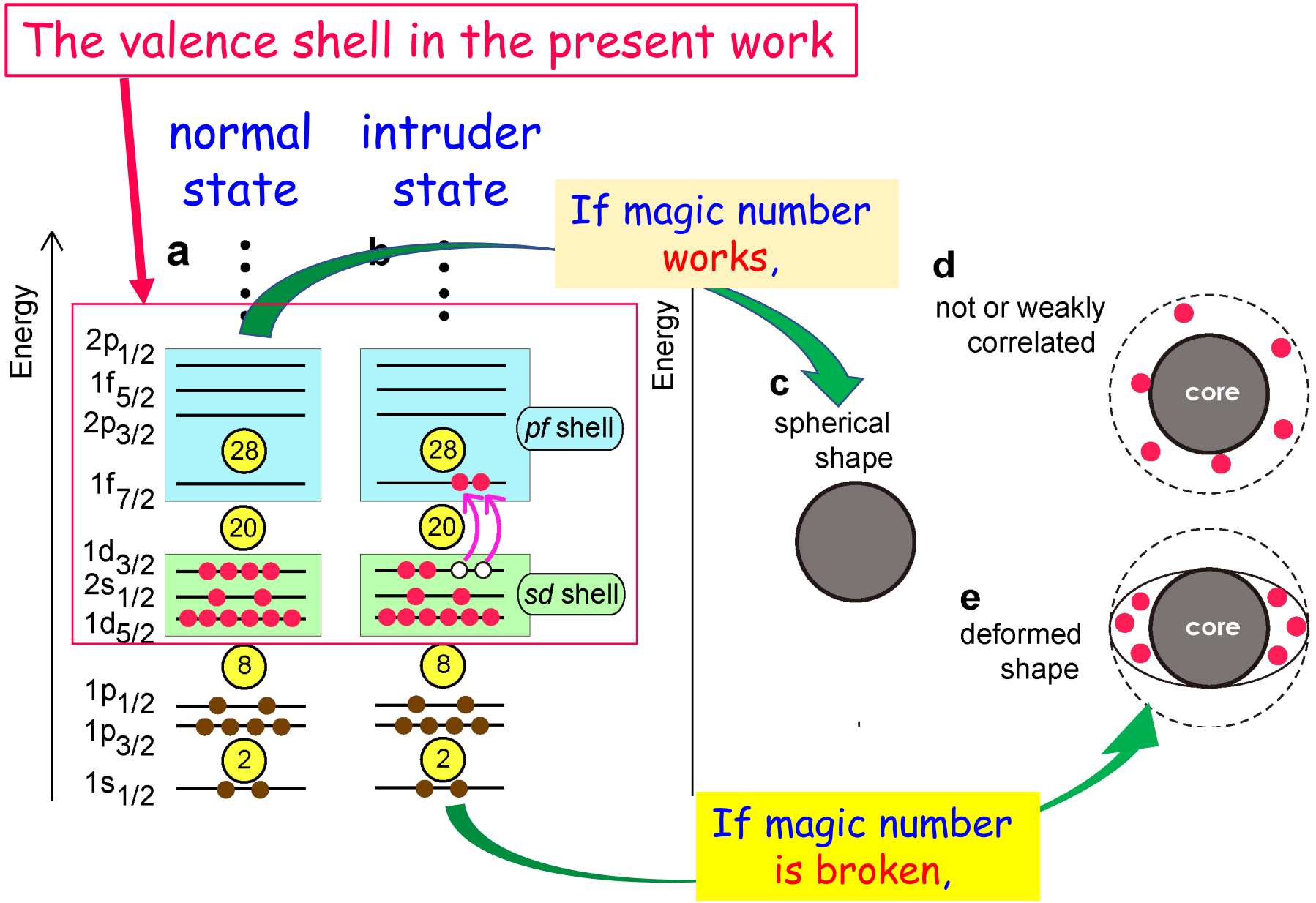
The valence shell in the present work
normal state
intruder state
a
b
Energy
2p1/2
1f5/2
2p3/2
1f7/2
1d3/2
2s1/2
1d5/2
1p1/2
1p3/2
1s1/2
28
20
8
2
pf shell
sd shell
If magic number works,
Energy
c
spherical shape
d
not or weakly correlated
core
e
deformed shape
core
If magic number is broken,

ground-state energies

Earlier (2017 PRC) work by EEdf1

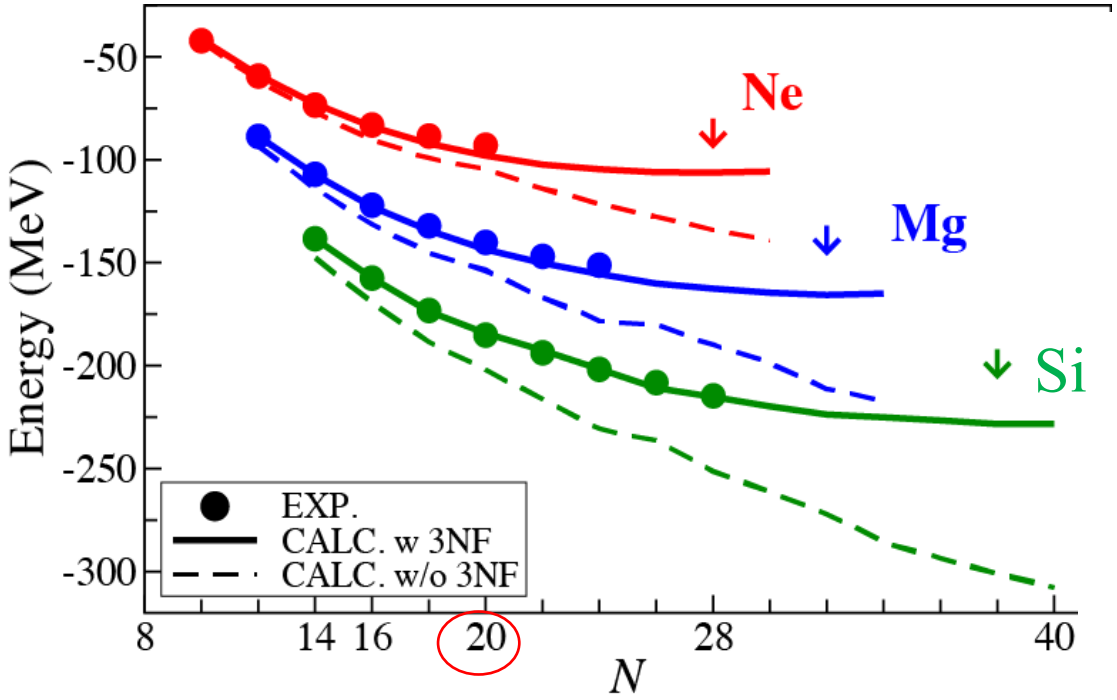

Earlier *ab initio* work on Na isotopes

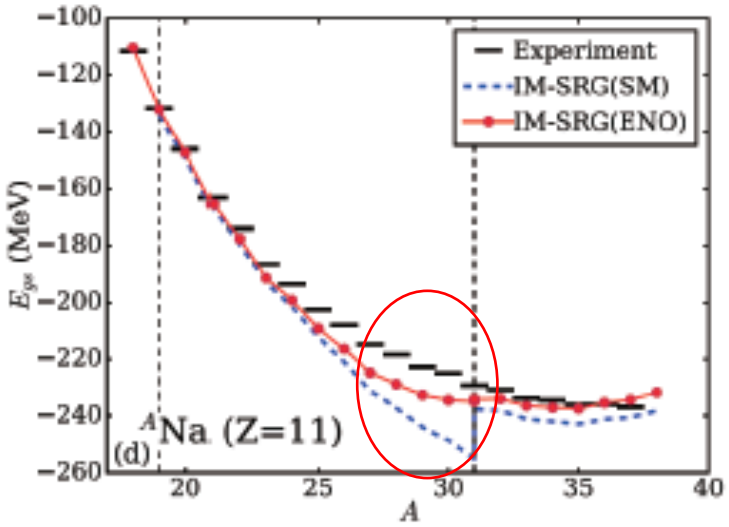

IM-SRG (SM) : core reference
IM-SRG (ENO) : ensemble reference
Stroberg et al. PRL 118, 032502 (2017)

Calculations with full sd + pf shell

PHYSICAL REVIEW C **95**, 021304(R) (2017)

Exotic neutron-rich medium-mass nuclei with realistic nuclear forces

Naofumi Tsunoda,[1] Takaharu Otsuka,[1,2,3,4] Noritaka Shimizu,[1] Morten Hjorth-Jensen,[5,6] Kazuo Takayanagi,[7] and Toshio Suzuki[8]

Ne and Mg systematics

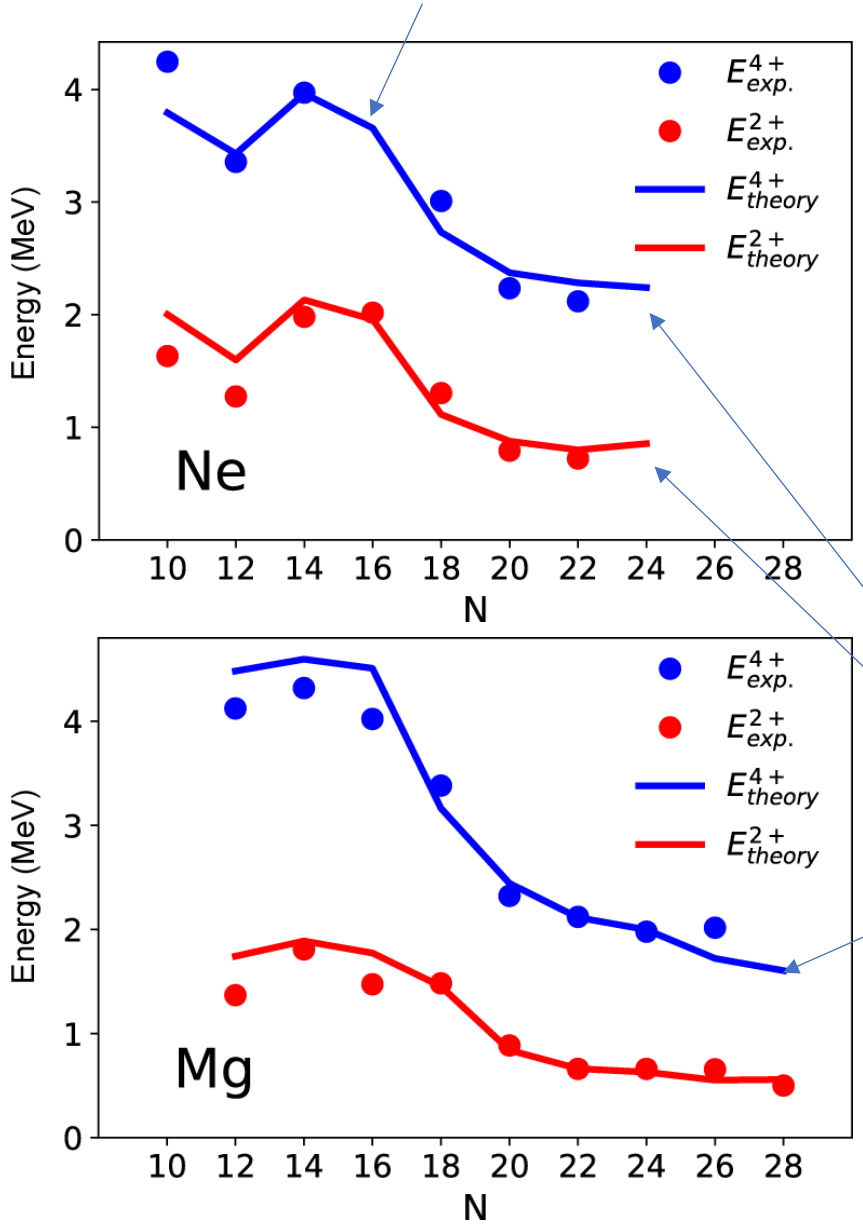

We use the EEdf1 interaction derived from the N3LO chiral EFT interaction + Fujita-Miyazawa three-nucleon force.

The EEdf1 Hamiltonian appears to be reasonable up to N~28 for Z=9-12.

Levels do not exist as bound states, because their energies are above the threshold of neutron emission.

Ground-state energy is decomposed (EEdf1 int.)

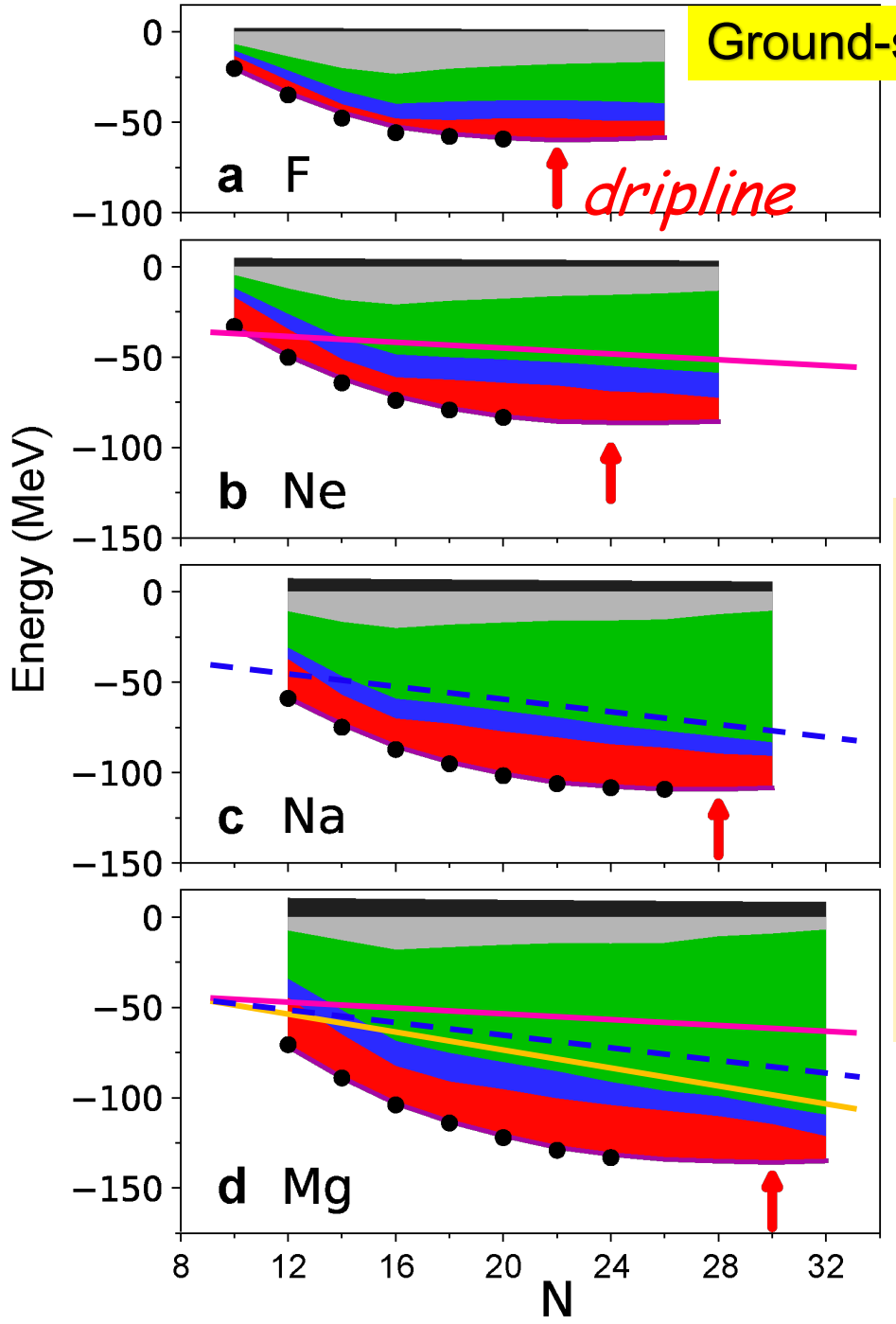

EXP.
total
Coulomb
bare SPE
monopole
pairing
rest (quadrupole *etc*)
monopole-type

The monopole effect (lower edge of green part) lowers the energy as a function of N, and its slope becomes steeper as Z because of the p-n monopole int., as shown by three lines fitted to different slopes.

The rest (~quadrupole deformation) effect (red part) varies locally.

... see next page

PHYSICAL REVIEW LETTERS **123,** 212501 (2019)

Editors' Suggestion | Featured in Physics

Location of the Neutron Dripline at Fluorine and Neon

D. S. Ahn,[1] N. Fukuda,[1] H. Geissel,[5] N. Inabe,[1] N. Iwasa,[4] T. Kubo,[1,*,†] K. Kusaka,[1] D. J. Morrissey,[6] D. Murai,[3] T. Nakamura,[2] M. Ohtake,[1] H. Otsu,[1] H. Sato,[1] B. M. Sherrill,[6] Y. Shimizu,[1] H. Suzuki,[1] H. Takeda,[1] O. B. Tarasov,[6] H. Ueno,[1] Y. Yanagisawa,[1] and K. Yoshida[1]

© T. Otsuka

PHYSICAL REVIEW LETTERS **129,** 212502 (2022)

Editors' Suggestion | Featured in Physics

Discovery of ^{39}Na

D. S. Ahn,[1,*] J. Amano,[3] H. Baba,[1] N. Fukuda,[1] H. Geissel,[5] N. Inabe,[1] S. Ishikawa,[4] N. Iwasa,[4] T. Komatsubara,[1] T. Kubo,[1,†] K. Kusaka,[1] D. J. Morrissey,[6] T. Nakamura,[2] M. Ohtake,[1] H. Otsu,[1] T. Sakakibara,[4] H. Sato,[1] B. M. Sherrill,[6] Y. Shimizu,[1] T. Sumikama,[1] H. Suzuki,[1] H. Takeda,[1] O. B. Tarasov,[6] H. Ueno,[1] Y. Yanagisawa,[1] and K. Yoshida[1]

Decomposition of the Hamiltonian

monopole part

bare SPE $\sum \epsilon_i a_i^+ a_i$

monopole $\sum_{i,j} V^{ab}_{\rm mono} a_i^+ a_j^+ a_j a_i$ $\quad V^{ab}_{\rm mono} = \sum_J \frac{(2J+1)\langle ab|V|ab\rangle_J}{2J+1}$

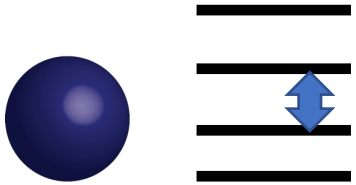

monopole: shift of SPE

multipole part

pairing J=0 nn + pp — pairing correlations

rest — quadrupole deformation, *etc*

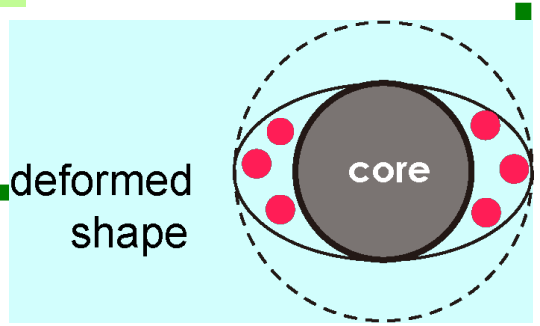

Two driving forces: an example from Mg isotopes

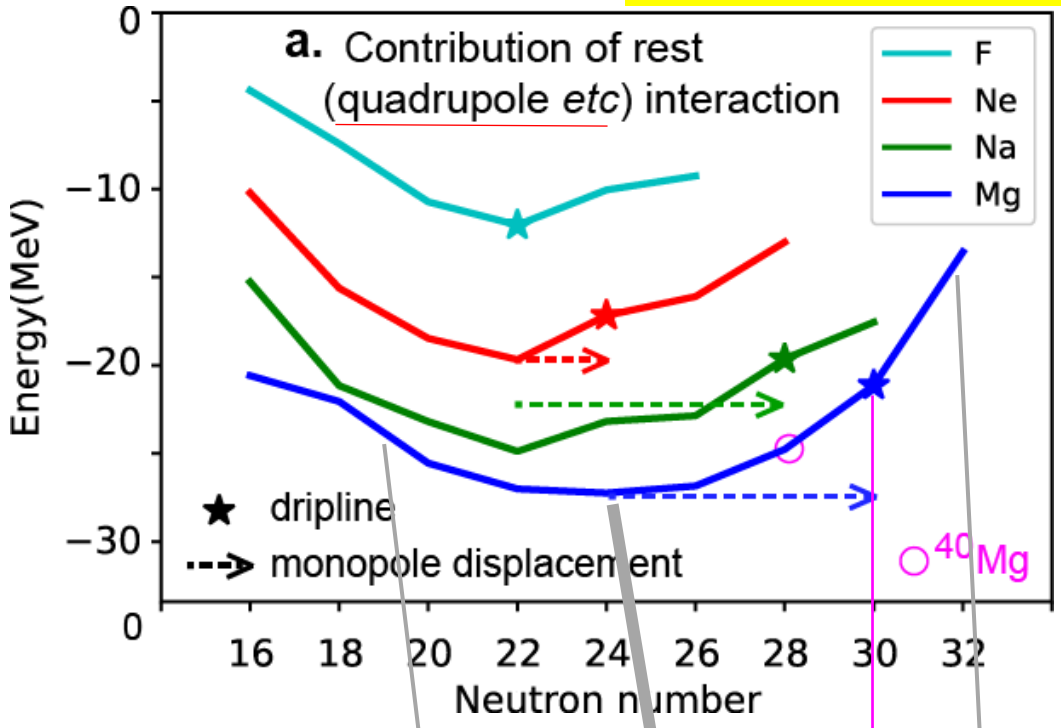

Decomposition into individual Contributions (repraise)

monopole part

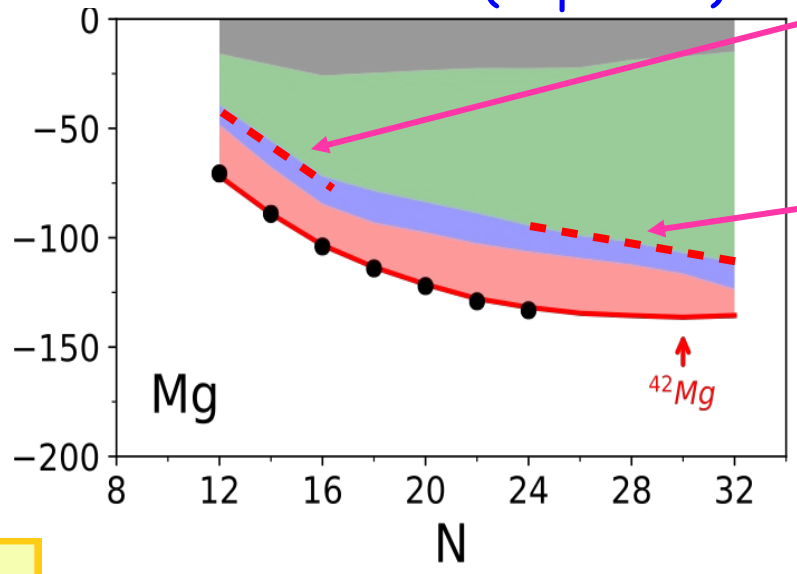

~6 MeV / neutron

~3 MeV / neutron

still substantial

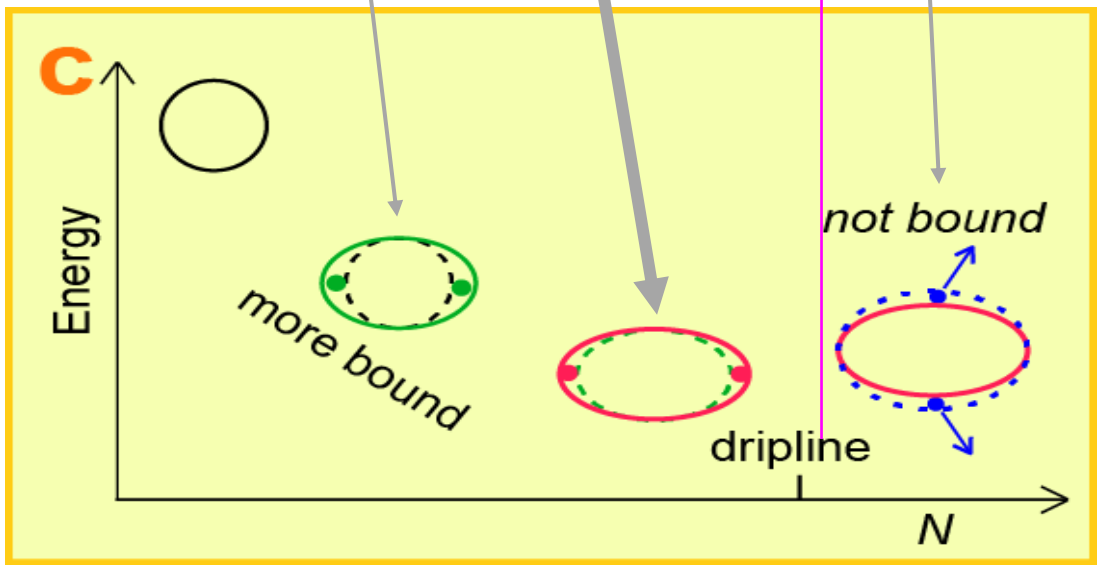

The rest (mainly deformation energy) part is saturated at *N*=24

The monopole effects compensate it, and pushes the dripline away (dashed arrows).

Dripline of F isotopes

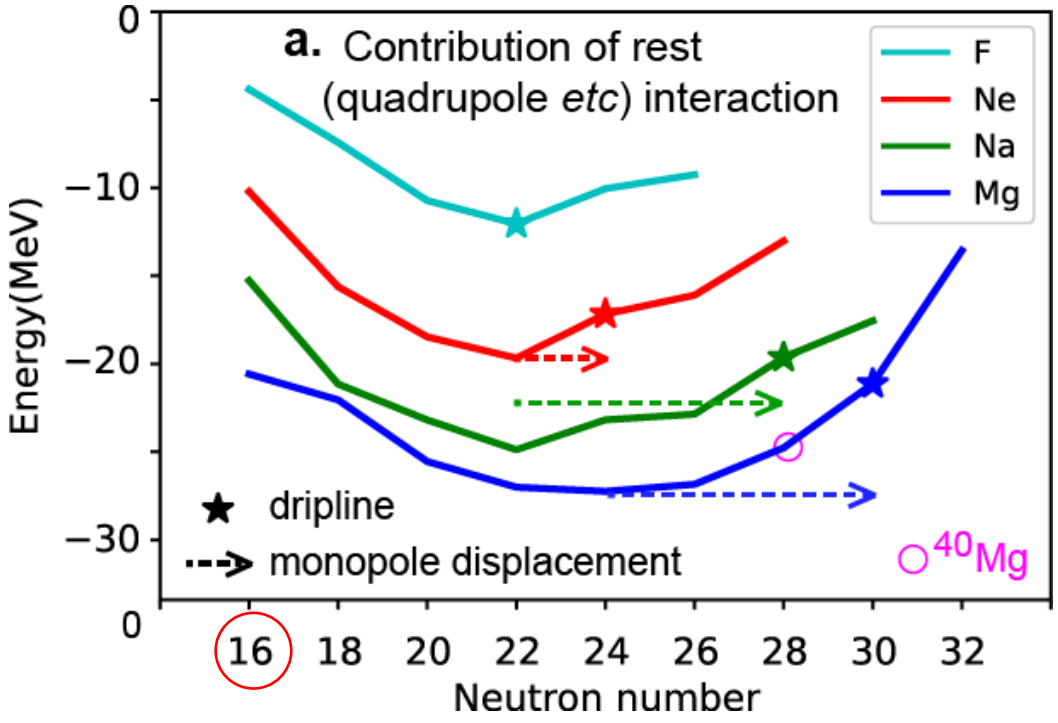

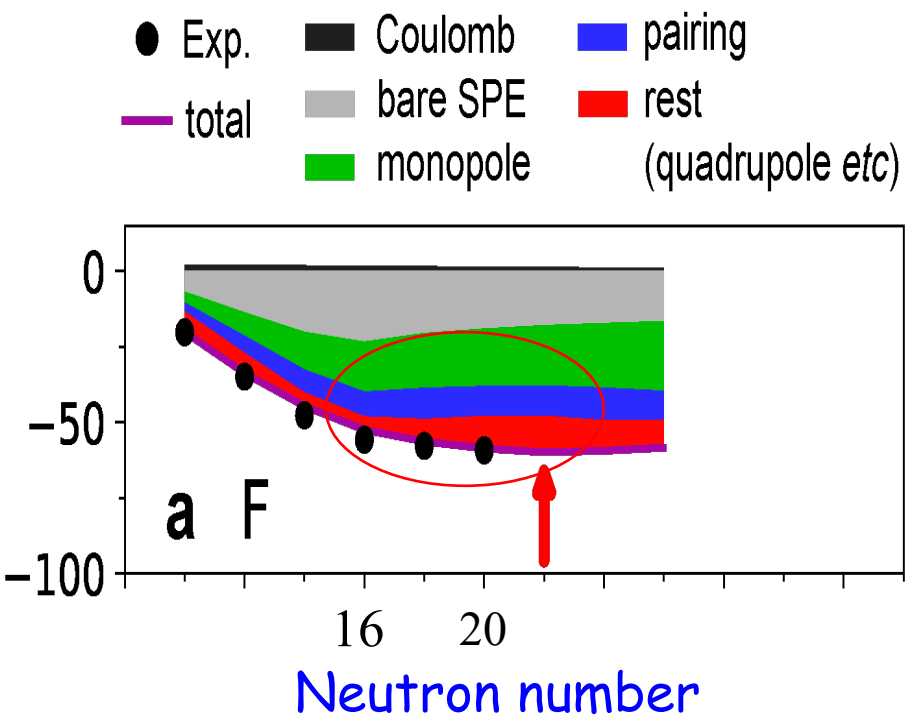

Monopole effect (edge of green part) becomes weaker for N > 16 in F isotopes. It even decreases because of high-lying d3/2 (see gray edge).

If there were no "rest" (~ quadrupole deformation) effect (red part), the dripline would be at N = 16, which is the same as oxygen isotopes.

Loose binding phenomena may be seen (?), in contrast to Ne, Na or Mg.

Summary of this section

Neutron driplines are due to two mechanisms: one has single-particle origin (b), while the other new one (c) is due to the interplay of monopole and quadrupole (deformation) energies. They may appear alternatively as Z increases.

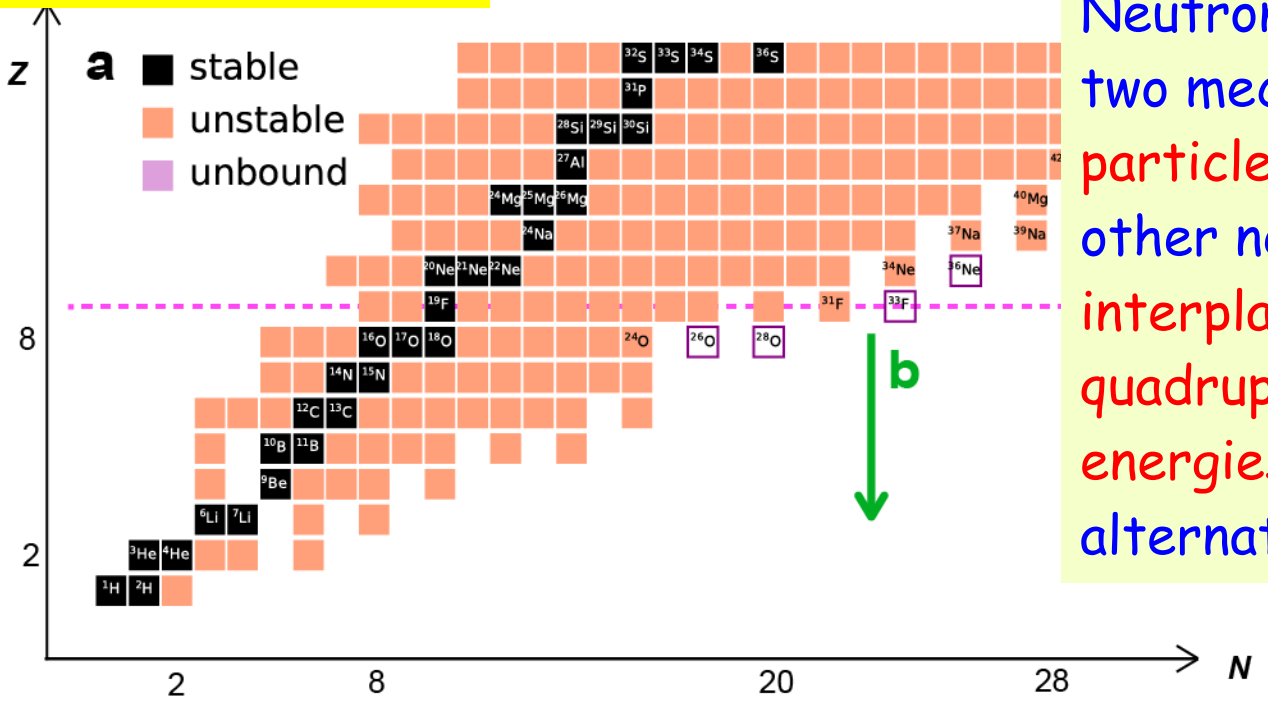

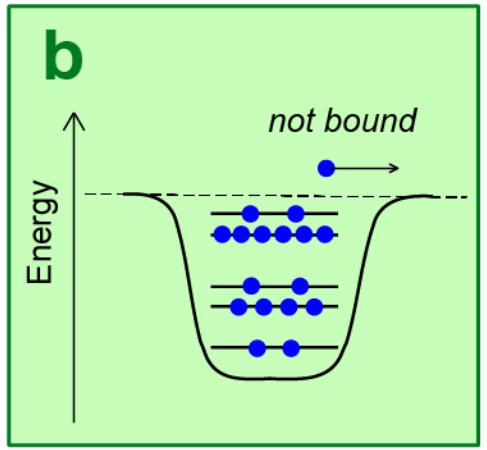

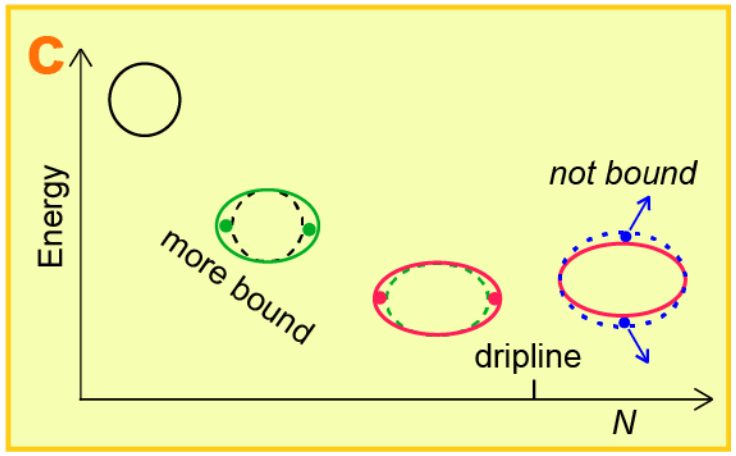

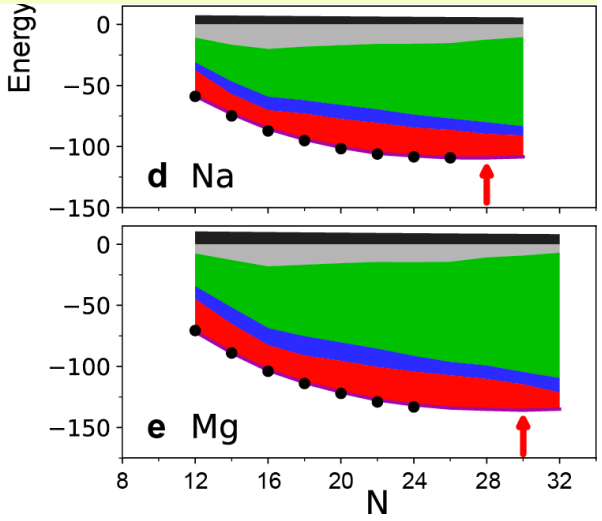

Traditional (vague) view
-> extreme: neutron halo

New view

Intermedaite case: ^{22}C
Suzuki, O, Yuan & Alahari, PLB 753, 199 (2016).

Outline

1. Basics of traditional shell model and Monte Carlo Shell Model
2. Shell evolution: from an introduction to the current landscape of magic numbers
3. Type-II Shell evolution: shape coexistence (parabola or linear or …)
4. Ellipsoidal nuclear shapes: Aage Bohr vs. Davydov
5. Shapes and driplines: who limits isotopes
6. α-clustering and nuclear matter: who likes α-cluster

Alpha clustering in atomic nuclei

- another example of novel picture -

α-Clustering in atomic nuclei from first principles with statistical learning and the Hoyle state character

T. Otsuka[1,2,3✉], T. Abe[2,4], T. Yoshida[4,5], Y. Tsunoda[4], N. Shimizu[4], N. Itagaki[6], Y. Utsuno[3,4], J. Vary[7], P. Maris[7] & H. Ueno[2]

α cluster formation - intuitive image -

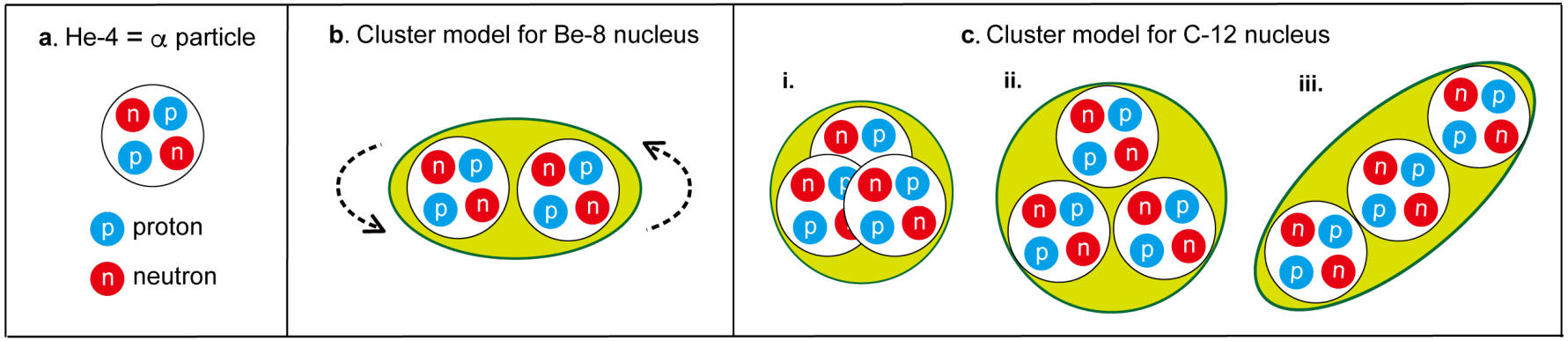

Pioneers (before 1960)

bond coupling

Wefelmeier, W. Von, Ein geometrisches Modell des Atomkerns. Z. Phys. Hadrons Nucl. 107, 332 (1937).
Wheeler J. A., Molecular Viewpoints in Nuclear Structure, Phys. Rev. **52**, 1083 (1937).
Morinaga, H., Interpretation of some of the excited states of 4n self-conjugate nuclei, Phys. Rev. C **101**, 254 (1956).

linear formation

Brink, D., Alpha-Particle Model of Light Nuclei. The Proc. Intl. School of Physics Enrico Fermi, Course, 36 (1966), p. 247.
Ikeda, K., Takigawa, N. and Horiuchi, H., The systematic structure-change into the molecule-like structures in the self-conjugate 4n nuclei. Prog. Thoer. Phys. Suppl., **E68**, 464 (1968).
Arima, A., Horiuchi, H., Kubodera, K. and Takigawa, N., Clustering in Light Nuclei, in *Advances in Nuclear Physics*, ed. by Baranger M. and Vogt E., (Springer, Boston, MA., 1973), **5**, 345.
Freer, M., Horiuchi, H., Kanada-En'yo, Y., Lee, D. and Meißner, U.-G., Microscopic clustering in light nuclei. Rev. Mod. Phys. **90**, 035004 (2018).

The snapshot state in the body-fixed frame is needed,
as this snapshot state gives the snapshot of density profile.
(*The snapshot state is nothing but the intrinsic state in most literatures.*)
(The corresponding states in the lab. frame are obtained by rotating it.)
It is difficult (or impossible) to observe it experimentally.

The clustering is one of the fundamental problems in physics, as is in this project.

Foundation from sound underlying bases

Its contemporary versions

***Ab initio* calculations on clustering aspects**

- ~~[Green's Function Monte Carlo (GFMC)]~~

  Variational Monte Carlo (VMC)

  [Wiringa et al. 2000]

- No Core Full Configuration (NCFC) :

  [Cockrel et al. 2012] *Not clustering*

- Lattice EFT : Hoyle state [Epelbaum et al. 2012]

  Initial setup

- ***ab initio No-Core* Monte Carlo Shell Model (MCSM)**

  This work -> clustering in Be and C isotopes

  its emergence and fading + Hoyle state

$^8Be(0_1^+)$

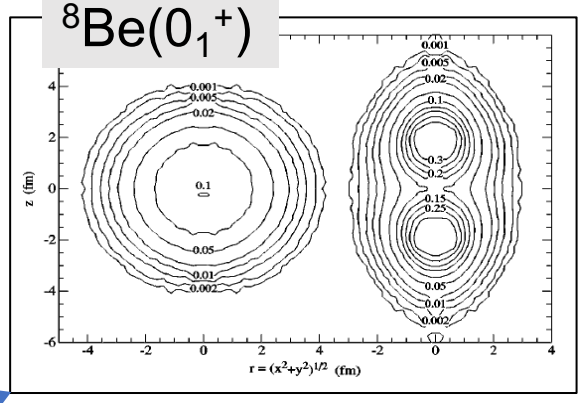

$^8Li(2_1^+)$ lab. frame density

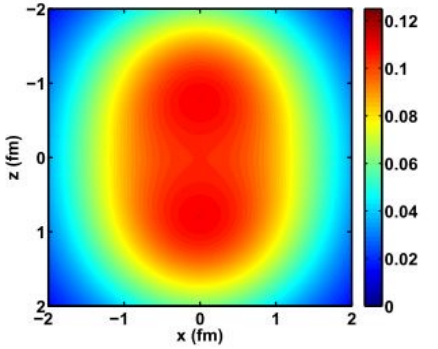

FIG. 12: (Color online) The $y = 0$ slice of the translationally-inv density for the same state is on the right. These densities were

^{12}C $(0_1^+, 2_1^+)$

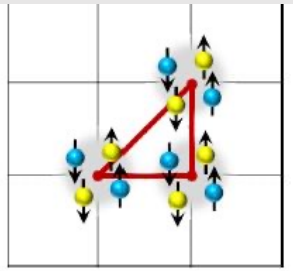

Alpha formation near the threshold energy

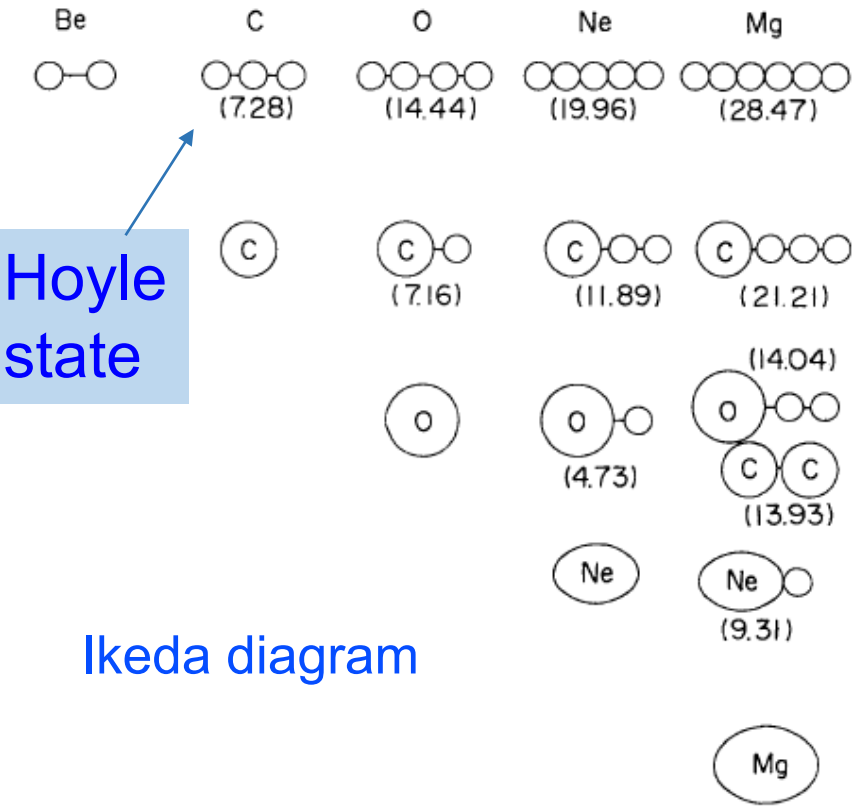

Hoyle state

Ikeda diagram

Fig. 1. Threshold energy for each decay mode. In the figure, the threshold energy for each decay mode is given in MeV. The systematics suggests the possible molecular nature around each energy. Some of the molecular states are already found and are represented in Fig. 2.

Supplement of the Progress of Theoretical Physics, Extra Number, 1968

The Systematic Structure-Change into the Molecule-like Structures in the Self-Conjugate 4*n* Nuclei

Kiyomi IKEDA,*) Noboru TAKIGAWA and Hisashi HORIUCHI

The alpha clustering is considered to occur near the threshold energy, as a complementary binding mechanism.
This is a nice idea, and sounds plausible.

This has been a strong guiding principle for half a century.
We investigate whether this principle dominates the alpha clustering or not.

More interestingly, the clustering seems to be 0% or 100% in the argument based on the threshold effect, like a phase transition.

How to calculate ?

ab initio No-Core Monte Carlo Shell Model

(MCSM)

No inert core, *or* all nucleons are activated

Nucleon-nucleon interactions are fixed prior to this study, based on fundamental approaches such as the chiral Effective Field Theory of QCD.

Single-particle states included

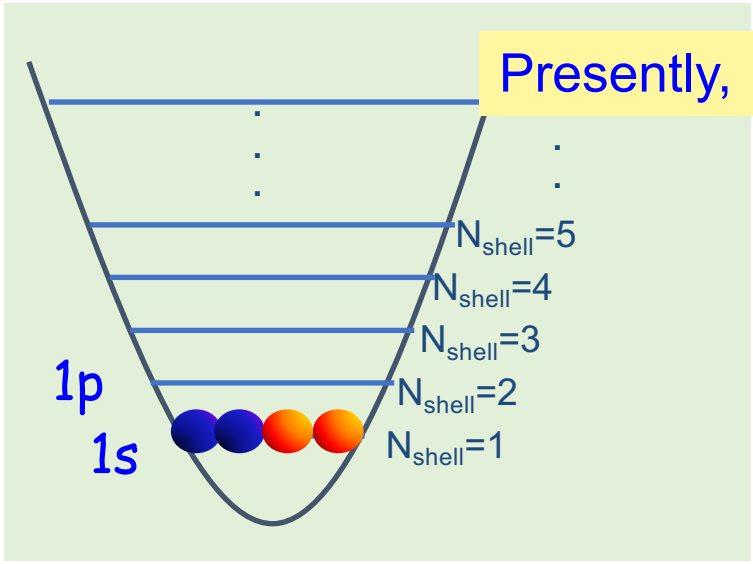

Solve the Schrodinger equation

$$H\Psi = E\Psi$$

E : eigenenergy

Ψ : eigenstate

Nucleon-Nucleon interaction + kinetic energy

Be : JISP16 fitted to *NN* scattering + fine tuning

Shirokov, A. M., Vary, J. P., Mazur, A. I. and Weber, T. A., Realistic nuclear Hamiltonian: Ab exitu approach. Phys. Lett. B **644**, 33 (2007).

C : Daejeon16 based on chiral EFT with SRG + fine tuning

Shirokov, A. M., Shin, I. J., Kim, Y., Sosonkina, M., Maris P. and Vary, J. P., N3LO *NN* interaction adjusted to light nuclei in *ab exitu* approach. Phys. Lett. B **761**, 87 (2016).

Machleidt, R. & Entem, D. R., Chiral effective field theory and nuclear forces, Phys. Rep. **503**, 1 (2011).

The interactions are fixed prior to the present calculation.

Why do we need the intrinsic density ?
-- in the case of MCSM eigenstate --

$$|\Phi\rangle = \sum_{i=1}^{N_{basis}} c_i |\Phi_i\rangle =$$ c_1 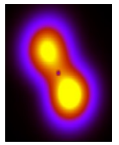 + c_2 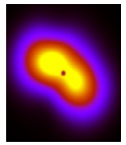 + c_3 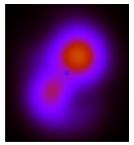 + c_4 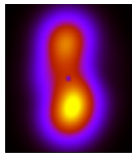 + ...

Angular-momentum projection

$$|\Psi\rangle = \sum_{i=1}^{N_{basis}} c_i P^J P^\pi |\Phi_i\rangle$$

We need something like this.

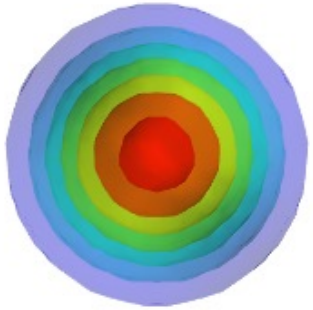

^{8}Be 0^+ ground state

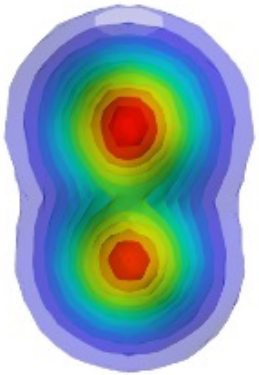

Laboratory frame

"Intrinsic" (body-fixed) frame

MCSM eigenstate :

$$\left|\Psi(D)\right\rangle = \sum_{n=1}^{N_B} c_i P^{J,\Pi} \left|\phi(D^{(n)})\right\rangle$$

Deformed Slater determinant with three axes of ellipsoid

For J^π projected states, individual orientations are not relevant.

$$\left|\Psi_{B.A.}(D)\right\rangle = \Big| c_1 + c_2 + c_3 + \cdots + c_{98} + c_{99} + c_{100} \Big\rangle$$

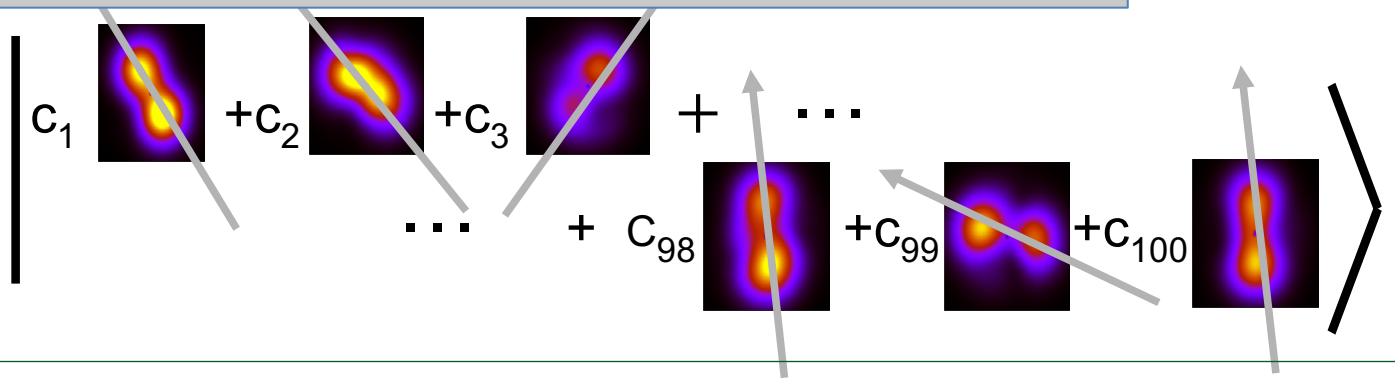

For "intrinsic state", all basis states are aligned so that three axes of the ellipsoid are placed on the given directions, e.g. the longest one on the z axis.

$$\left|\Psi_{\text{intr.}}(D)\right\rangle = \Big| c_1 + c_2 + c_3 + \cdots + c_{98} + c_{99} + c_{100} \Big\rangle$$

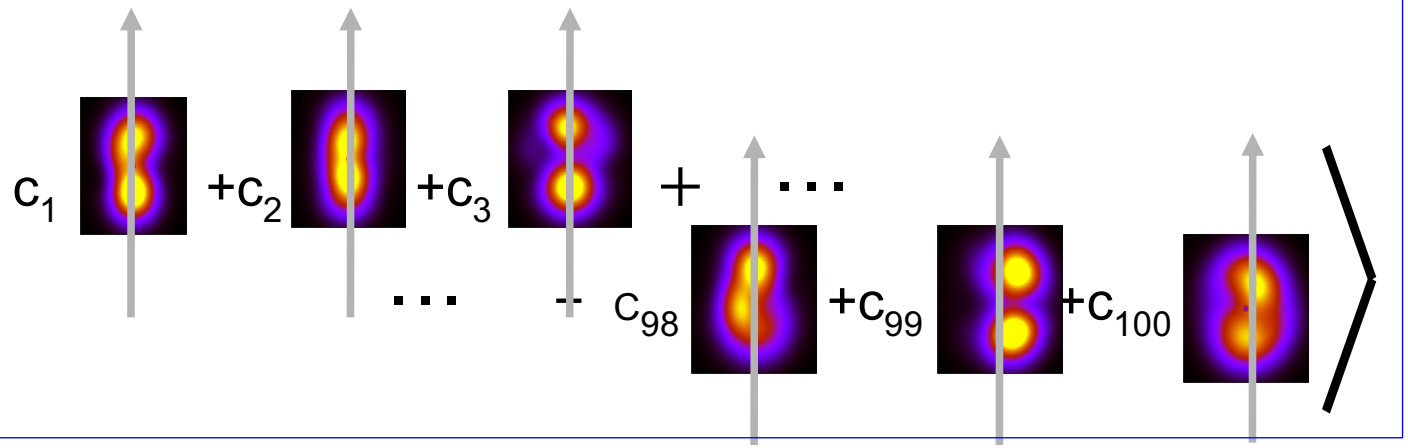

Snapshot of density profile

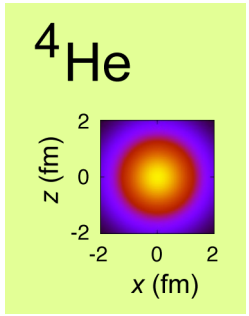

Laboratory-frame

Body-fixed (intrinsic) frame

Q aligned superposed state

^{8}Be

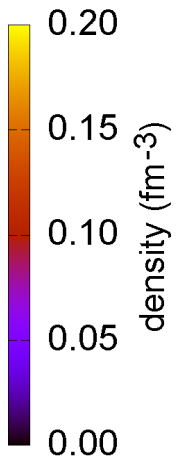

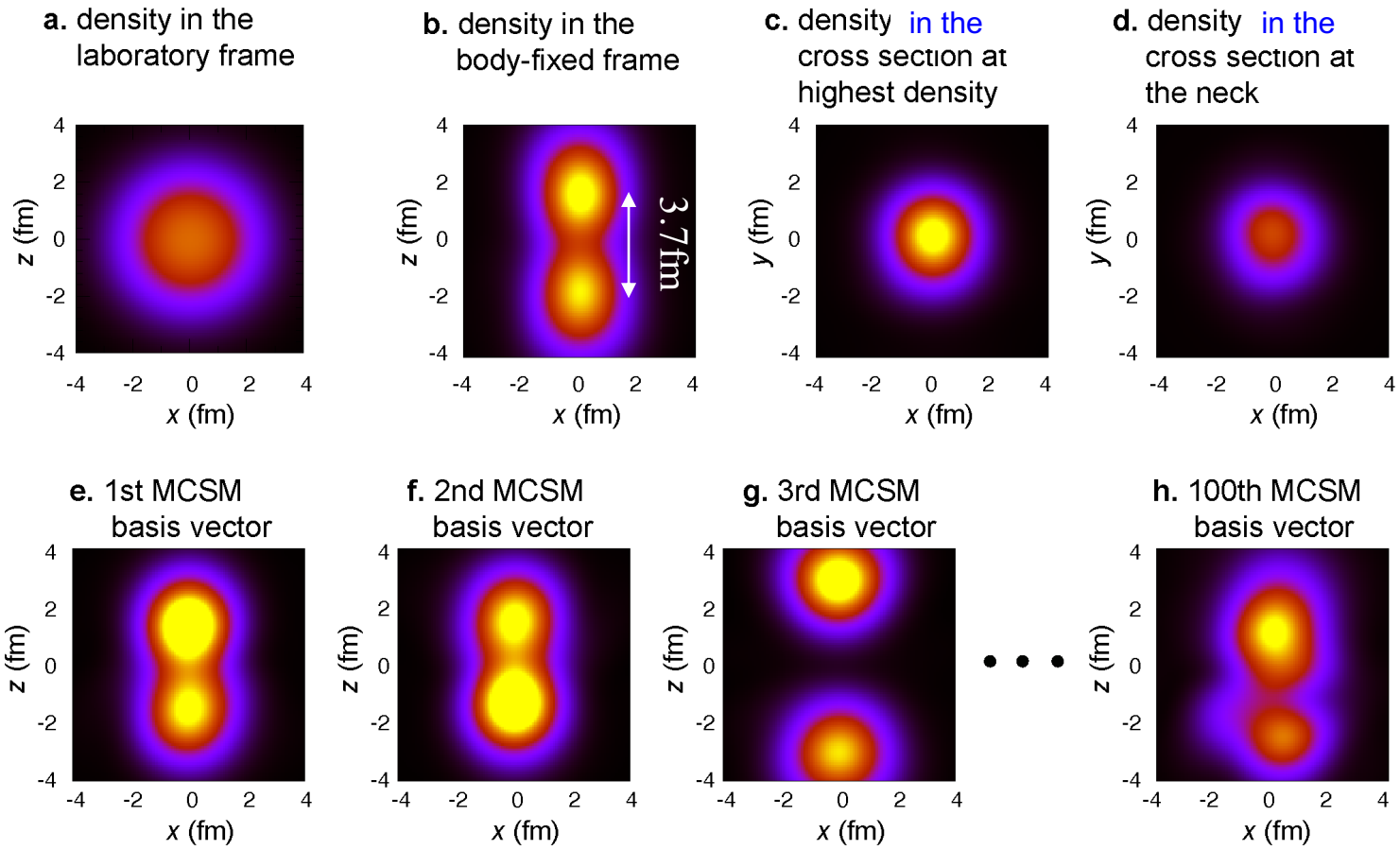

Alignment of MCSM basis vectors (Q aligned)

T-plot analysis of 0+ states applied to Be isotopes

a.

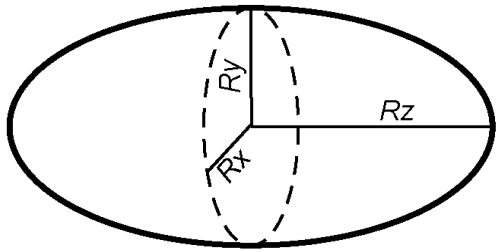

$$Rz = \{1 + 0.63\,\beta_2\,\cos(\gamma)\}\,R_0$$
$$Ry = \{1 + 0.63\,\beta_2\,\sin(\gamma - 30^\circ)\}\,R_0$$
$$Rx = \{1 - 0.63\,\beta_2\,\cos(60^\circ - \gamma)\}\,R_0$$

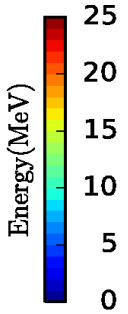

T-plot

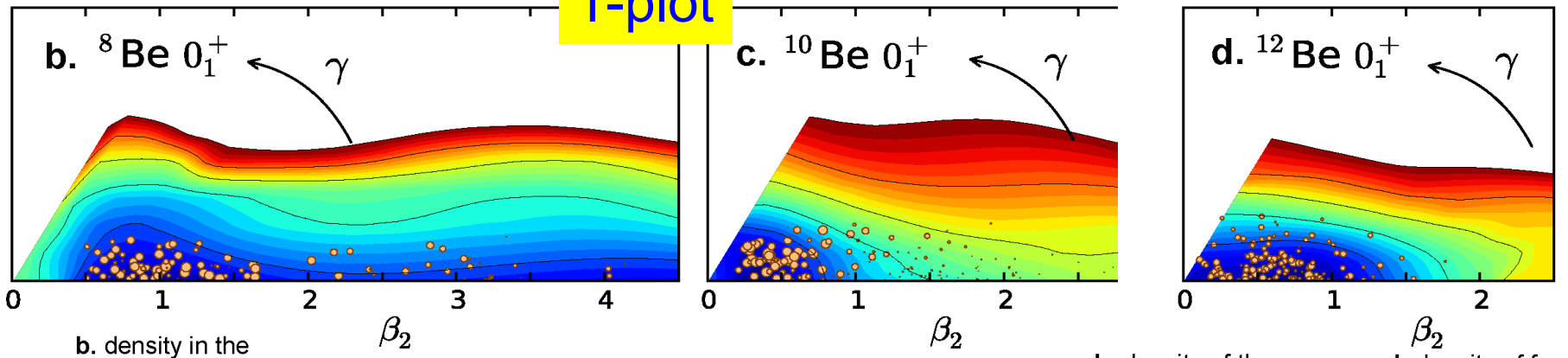

b. density in the body-fixed frame

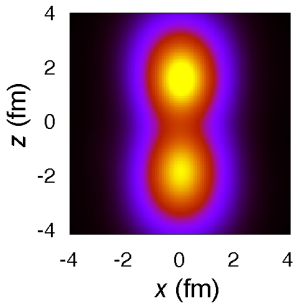

^{8}Be

i. density of the α cluster part (twice proton density)

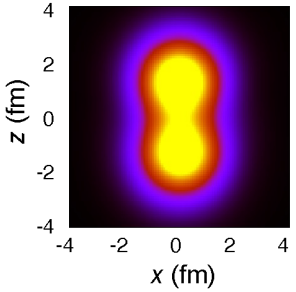

j. density of two excess neutrons

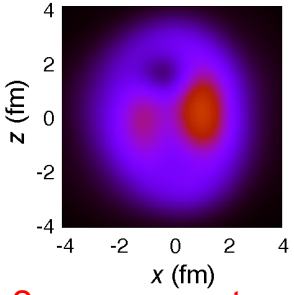

2 excess neutrons

^{10}Be

k. density of the α cluster part (twice proton density)

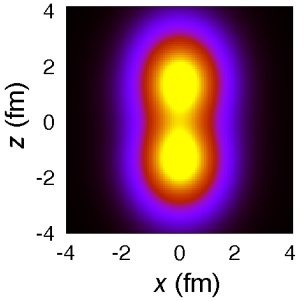

l. density of four excess neutrons

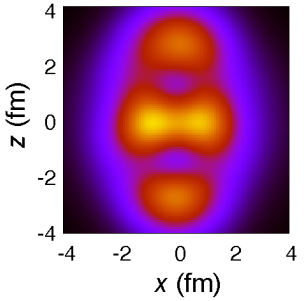

4 excess neutrons

^{12}Be

Energy level & transition strength of ^{12}C

ab initio no-core MCSM + Daejeon 16 interaction (Shirokov et al.)
based on chiral EFT (Machleidt-Entem, 2011)

charges protons 1e
neutrons 0e

correlation effects are explicitly treated
(no medium correction needed)

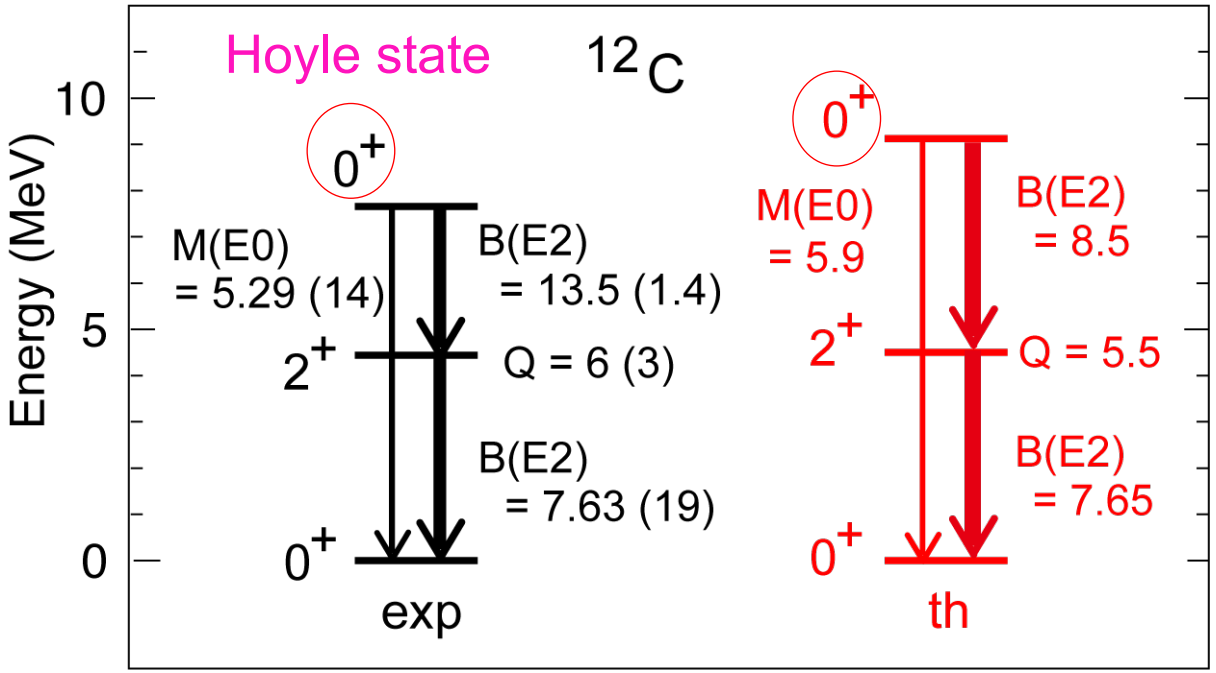

convergence pattern as
functions of energy variance

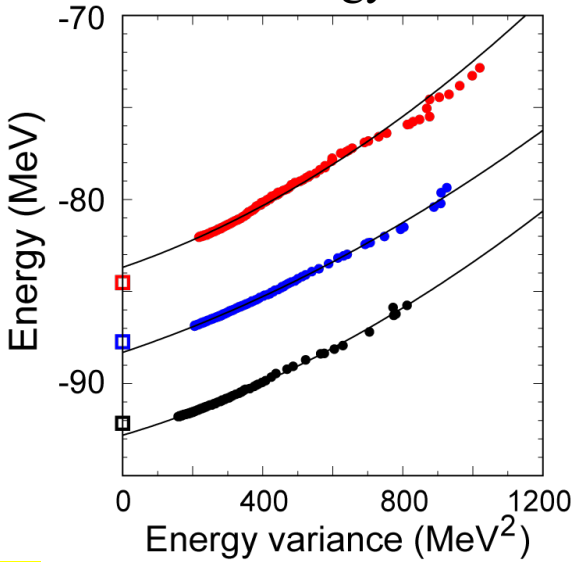

Strong deformation (β_2~0.6, oblate) in the 0^+_1 and 2^+_1 states can now be described from *first principles*.

Stringent test for the Daejeon 16 interaction and the present No-Core MCSM.

Hoyle state of ^{12}C Ex = 7.65 MeV

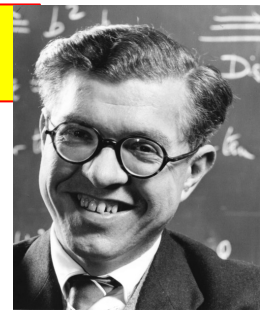

ON NUCLEAR REACTIONS OCCURRING IN VERY HOT STARS. I. THE SYNTHESIS OF ELEMENTS FROM CARBON TO NICKEL

F. HOYLE*
MOUNT WILSON AND PALOMAR OBSERVATORIES
CARNEGIE INSTITUTION OF WASHINGTON
CALIFORNIA INSTITUTE OF TECHNOLOGY
Received December 22, 1953

$A_0 = 4$, $Z_0 = 2$, and $A_1 = 8$, $Z_1 = 4$, in the formulae of the previous section. The important energy level of the C^{12} nucleus in the present problem is one very recently identified by Dunbar, Pixley, Wenzel, and Whaling (1953). This level occurs at about 7.68 mev above ground level, which corresponds to a value of E_R of about 0.31 mev. (It will

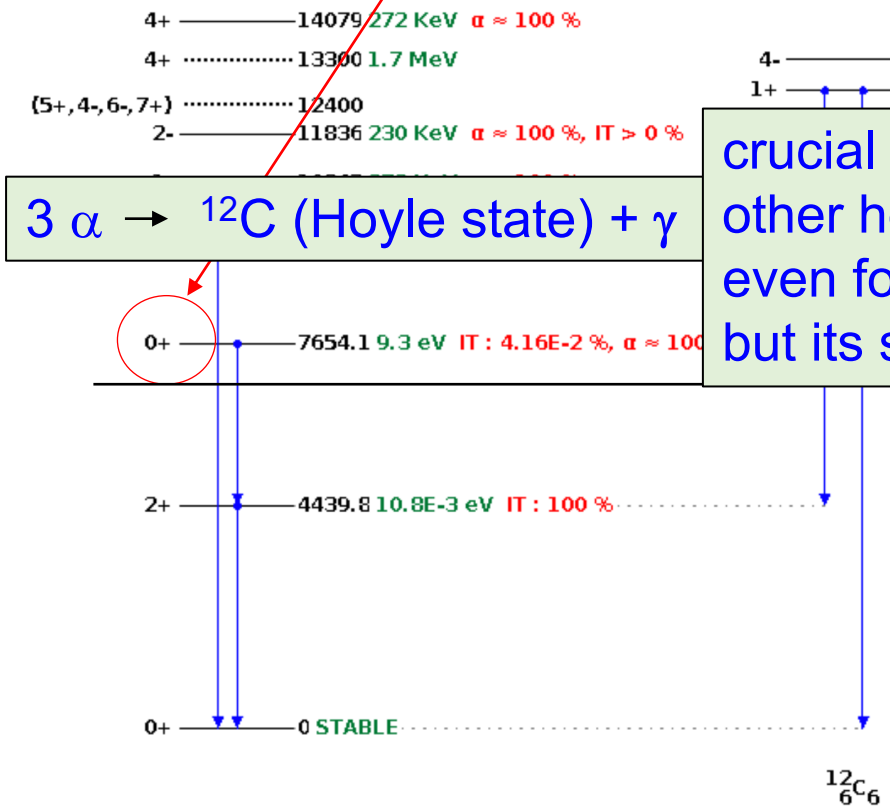

3 α → ^{12}C (Hoyle state) + γ

crucial for the syntheses of carbon and other heavier elements in stars and even for the birth of the life like us, but its structure remains unknown

α threshold

Nucleon densities in the body-fixed frame

after proper orthogonalization

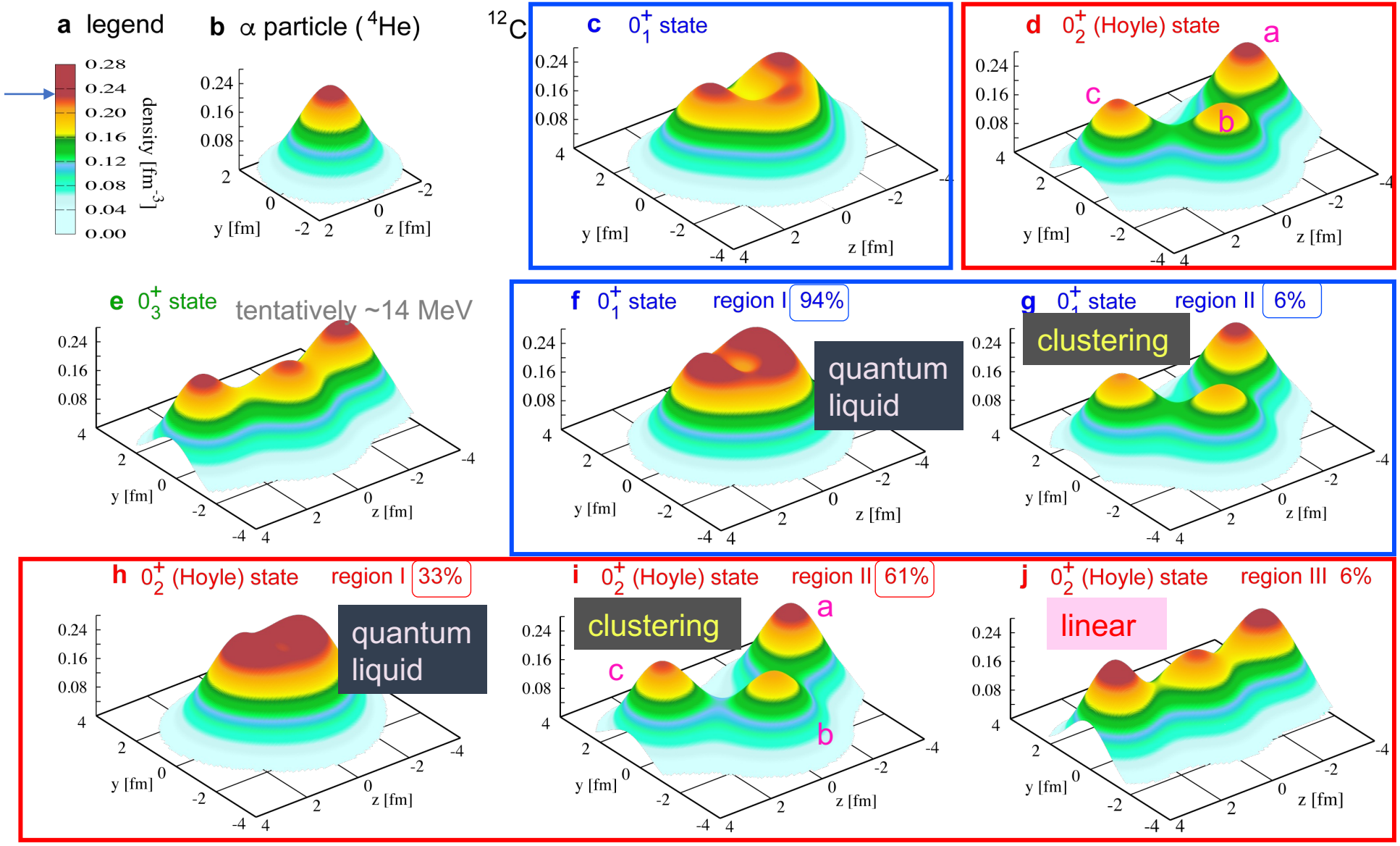

^{12}C : MCSM basis vectors classified by quadrupole shapes (*T plot by Tsunoda*)

T plot circles are spread in the case of ^{12}C. A characteristic feature.

Unique structures appear at low excitation energies … different from other nuclei

PES is divided into three
- I $\beta_2 < 0.7$, oblate basin in the PES
- II triaxial
- III very prolate

β_2=0.7, γ=6 deg ➔ basis vectors decomposed into regions I, II and III

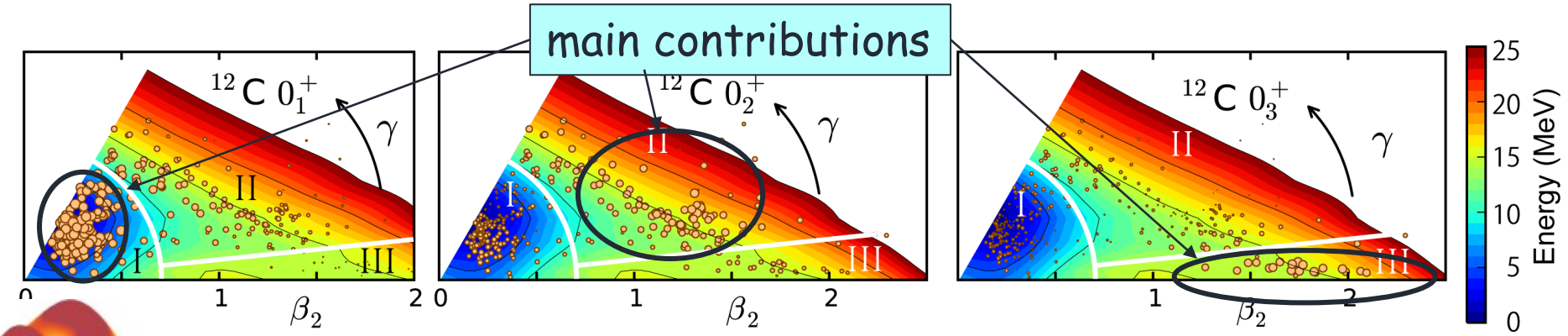

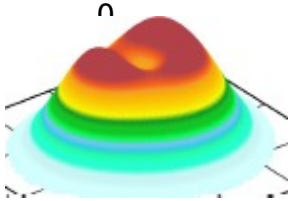

oblate (pancake)

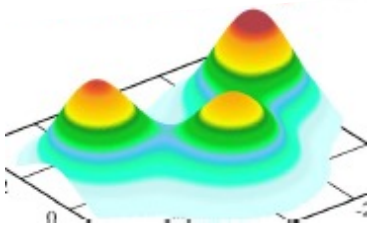

Hoyle state

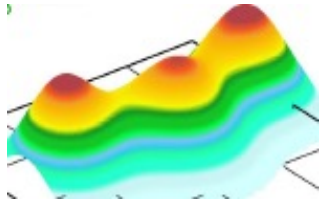

prolate (football)

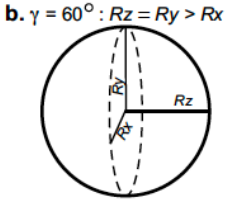

Rz : Ry : Rx = 2 : 2 : 1

Rz : Ry : Rx = 5 : 1 : 1

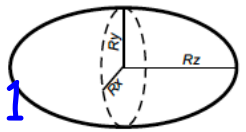

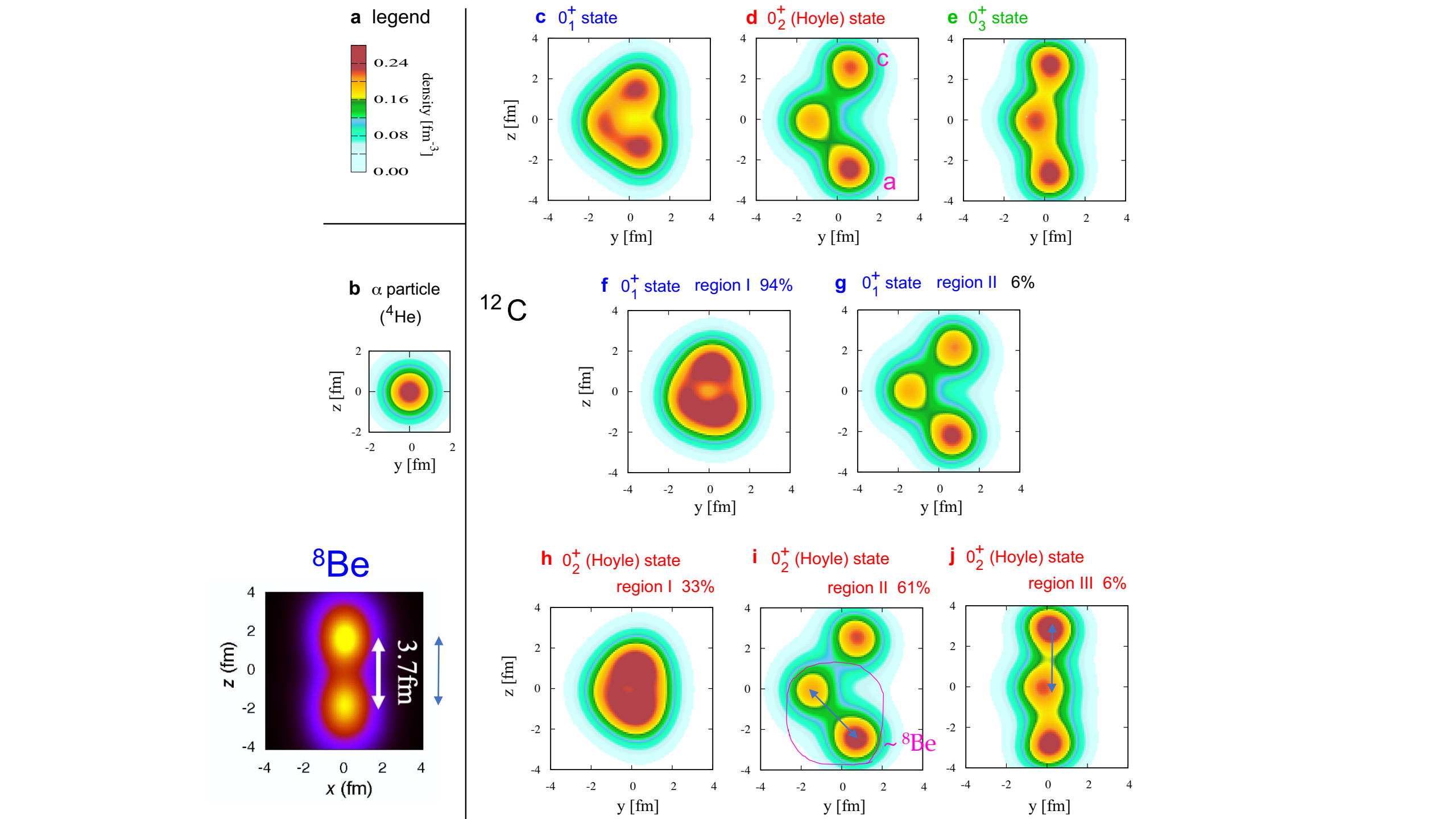
a legend
0.24
0.16
0.08
0.00
density [fm^{-3}]
b α particle
(^{4}He)
z [fm]
y [fm]
^{12}C
c 0_1^+ state
d 0_2^+ (Hoyle) state
e 0_3^+ state
c
a
f 0_1^+ state region I 94%
g 0_1^+ state region II 6%
^{8}Be
3.7fm
z (fm)
x (fm)
h 0_2^+ (Hoyle) state
region I 33%
i 0_2^+ (Hoyle) state
region II 61%
~ ^{8}Be
j 0_2^+ (Hoyle) state
region III 6%

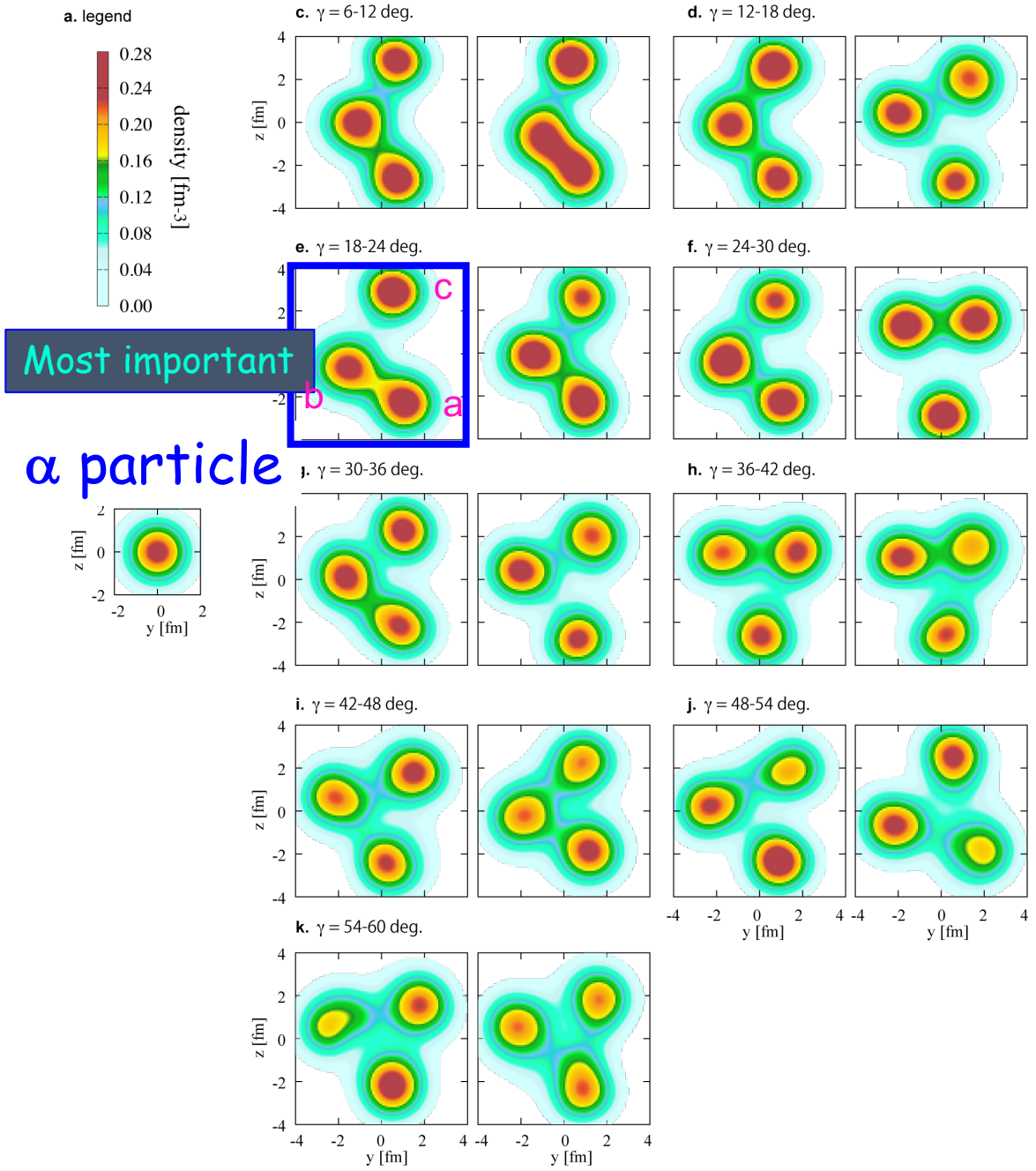

Most important

α particle

density profiles of major MCSM basis vectors (Slater determinants) in region II, generated by the interaction.

Triangle configurations with three α clusters are favored (compare to single α)

Fluctuations within such configurations

From ^{8}Be to ^{12}C, and the crossover in the ground & Hoyle states of ^{12}C

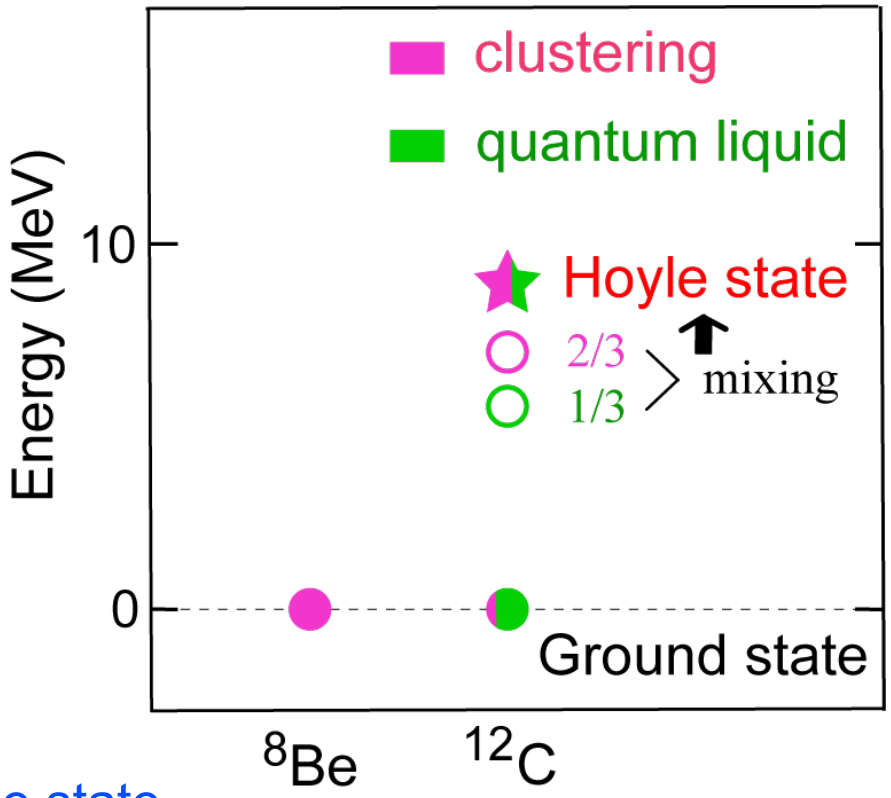

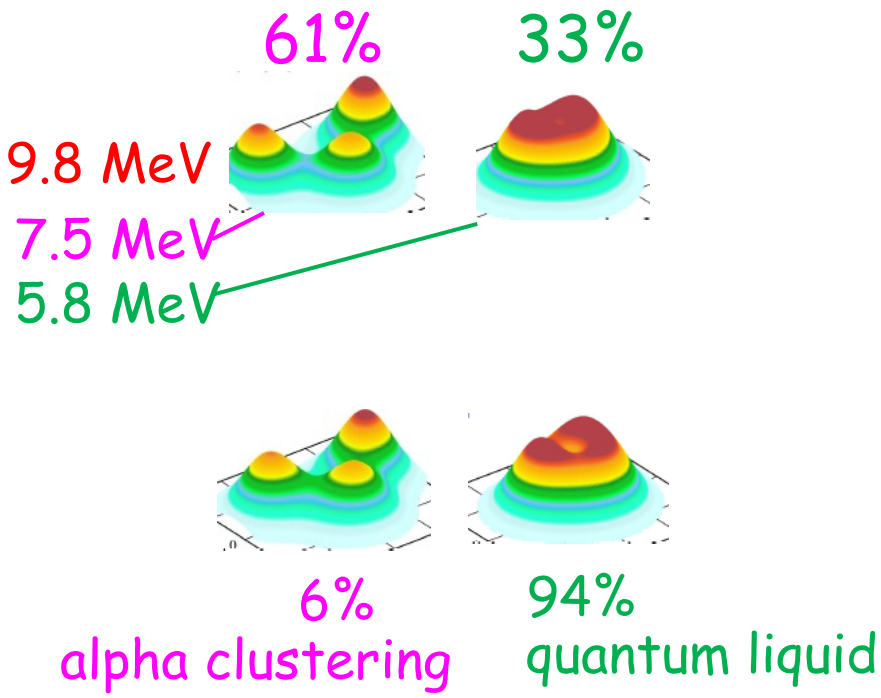

Hoyle state

The mixing occurs also due to the orthogonality to the ground state.

The mixing pushes the Hoyle state upwards by ~3 MeV (repulsive effect).

The present mixing seems to be consistent with the BEC (THSR) model.

Ground state :

the mixing matrix element is ~ -3 MeV (attractive effect) with 6% (ampl. ~ 0.24) alpha clustering. →alpha decay, alpha knockout

A completely different analysis (no physics, data science)

classification of MCSM basis vectors by the cluster analysis of through unsupervised statistical learning

distance : $D(i,j) = 1 - |(\phi_i, \phi_j)|^2$ for basis vectors ϕ_i and ϕ_j

where parenthesis means a scalar product (overlap integral) with the $J^\pi = 0^+$ projection

connect basis vectors from the shortest distance to longer up to the threshold

independent confirmation of the validity of the region decomposition

h. Dendrogram for ^{12}C (cluster analysis through unsupervised statistical learning)

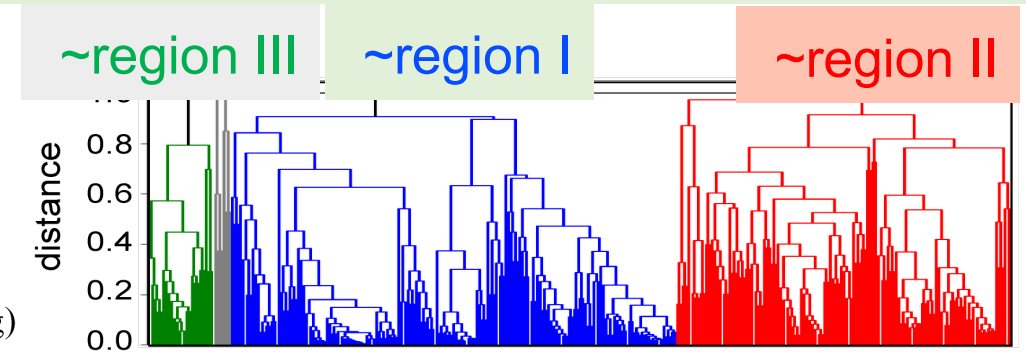

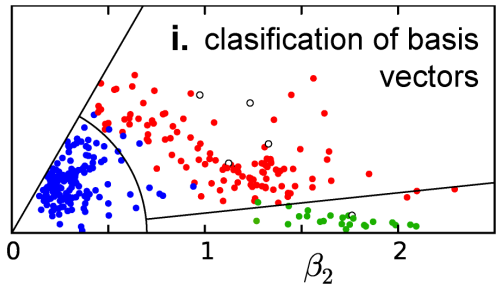

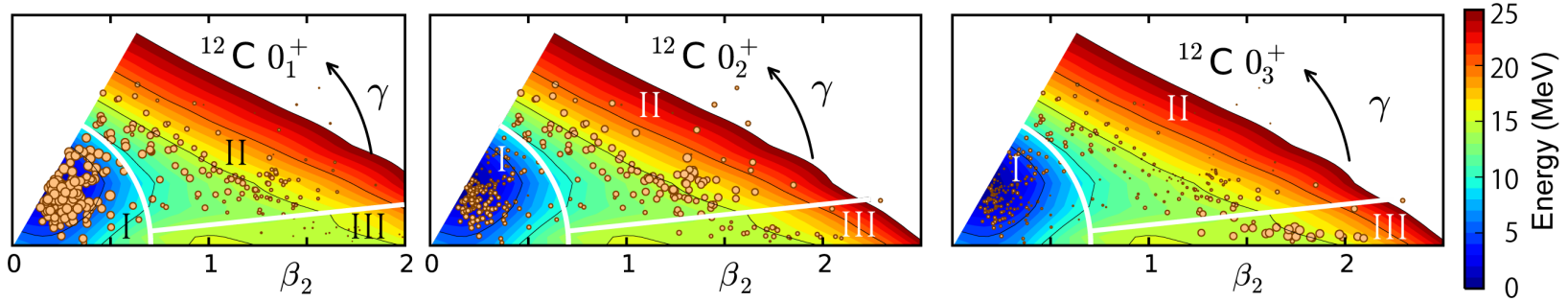

Summary of the clustering part

α clustering from first principles without any assumption

Perfect oblate rotational band from first principles in ^{12}C

Nuclear forces favor both quantum liquid and alpha cluster

Transition between them is not a phase transition but a crossover

Alpha cluster emerges without threshold effect (←→Ikeda diagram) even in the well-bound ground state of ^{12}C. → knockout of "pre-formed" alpha particle

13, 2234 (2022) *open access*

α-Clustering in atomic nuclei from first principles with statistical learning and the Hoyle state character

T. Otsuka[1,2,3✉], T. Abe[2,4], T. Yoshida[4,5], Y. Tsunoda[4], N. Shimizu[4], N. Itagaki[6], Y. Utsuno[3,4], J. Vary[7], P. Maris[7] & H. Ueno[2]

E N D

Thank you for your attention for three hours with 124 slides